

Theses and dissertations

1-1-2011

An Investigation Of The Performance Of District Heating Substations Using Computer Simulation

Edmund Wong
Ryerson University

Follow this and additional works at: <http://digitalcommons.ryerson.ca/dissertations>



Part of the [Heat Transfer, Combustion Commons](#)

Recommended Citation

Wong, Edmund, "An Investigation Of The Performance Of District Heating Substations Using Computer Simulation" (2011). *Theses and dissertations*. Paper 1638.

AN INVESTIGATION OF THE PERFORMANCE OF DISTRICT HEATING SUBSTATIONS USING COMPUTER SIMULATION

by

Edmund Wong

B.A.Sc., University of Waterloo, June 2008

A thesis
presented to Ryerson University

in partial fulfillment of the
requirements for the degree of
Master of Applied Science
in the Program of
Building Science

Toronto, Ontario, Canada, 2011

© Edmund Siu Wing Wong – 2011

Author's Declaration

I hereby declare that I am the sole author of this thesis or dissertation.

I authorize Ryerson University to lend this thesis or dissertation to other institutions or individuals for the purpose of scholarly research.

I further authorize Ryerson University to reproduce this thesis or dissertation by photocopying or by other means, in total or in part, at the request of other institutions or individuals for the purpose of scholarly research.

An Investigation of the Performance of District Heating Substations using Computer Simulation

Master of Applied Science, 2011

Edmund Siu Wing Wong

Building Science

Ryerson University

Abstract

Low primary temperature drop across district heating substations is an undesirable phenomenon observed in the district heating industry. Professionals in the industry have argued that this is caused by inappropriate sizing and controls of district heating substations. The thesis aims to investigate the impact of design and operation parameters on the performance of district heating substations, so that building designers and engineers can potentially better design and operate new and existing district heating substations. The thesis shows that, by developing and using a physical model as a computational tool for sensitivity analysis, different design and operation parameters can be evaluated. This generates insights for energy conserving control strategies to be developed. A preliminary control strategy was proposed for district heating substations, and simulation results show energy saving potentials.

Acknowledgement

This thesis could not have been completed without the help and support from many kind and extraordinary individuals.

I want to express my gratitude to Dr. Zaiyi Liao, my graduate supervisor and mentor, for your dedicated support, inspirations and criticisms throughout this thesis study and my academic career at Ryerson. Without your guidance, little would have been achieved. To Dr. Russell Richman, for your professional advice and kind support as part of the thesis supervising committee. To Dr. Mark Gorgolewski, for sharing your knowledge and passions in building science and in the area of sustainability, which has inspired me greatly during my academic career at Ryerson. To Dr. Alan Fung and Dr. Hua Ge, for your valuable comments and advice on this thesis.

I would also like to thank my parents, Danny and Judy, for their unconditional supports and being so understanding during the time spent on my research.

Finally, I would like to thank my lab colleagues, Ringo Ng and Surinder Jassar, who have been a great group to work and share ideas with.

Table of Contents

Author's Declaration	ii
Abstract.....	iii
Acknowledgement	iv
Table of Contents.....	v
List of Tables	viii
List of Figures	x
Nomenclature	xiv
1. Introduction	1
1.1 Background.....	1
1.2 Research Objective.....	3
1.3 Methodologies	5
1.4 Thesis Outline.....	6
2. Overview of District Heating Systems.....	8
2.1 Introduction.....	8
2.2 Background of District Heating Systems	8
2.2.1 Centralized Production Plant	9
2.2.2 Distribution Network	11
2.2.3 District Heating Substation and Building Heating System.....	13
2.3 Potential Benefits of District Heating Systems	15
2.4 District Heating Systems in Canada.....	17
2.5 Practical Problems.....	19

2.6 Concluding Remarks.....	21
3. Development of a Dynamic Physical Model	22
3.1 Introduction.....	22
3.2 Approach for Developing a Physical Model for a District Heating Substation	22
3.3 Physical Modelling of a Dynamic System using Lumped-Capacitance Method	25
3.3.1 Physical Modelling of a Dynamic System – Heat Transfer across Building Envelope	
.....	27
3.3.2 Physical Modelling of a Dynamic System – Hot Water Radiator	31
3.3.3 Physical Modelling of a Dynamic System – Heat Exchanger	33
3.3.4 Physical Modelling of a Dynamic System – Interior Room	37
3.3.5 Thermostatic Radiator Valve	40
3.3.6 Controller at a District Heating Substation.....	41
3.4 Integrated Model	42
3.5 Model Parameters.....	43
3.6 Concluding Remarks.....	48
4. Simulation for a Canadian Residential House connected to District Heating	50
4.1 Introduction.....	50
4.2 Methods of Performance Evaluation	52
4.3 Simulation Results and Discussions	56
4.3.1 Impact of Ratio of Capacity-to-Load	59
4.3.2 Impact of Climatic Locations.....	68
4.3.3 Impact of Primary Water Supply Modes	73

4.4 Concluding Remarks.....	79
5. Improving the Performance of District Heating Substation	82
5.1 Introduction.....	82
5.2 Previous Researches.....	82
5.3 Theory.....	85
5.4 Proposed Control Scheme.....	88
5.5 Simulation Results and Discussion	91
5.6 Limitations	97
5.7 Concluding Remarks.....	98
6. Conclusions and Future Studies.....	99
6.1 Conclusions.....	99
6.2 Future Studies	100
Appendix – Calculating Design Load using ASHRAE guidelines	102
References	110

List of Tables

Table 1: Examples of existing district heating systems in Canada [Arkay & Blais, 1995]	19
Table 2: Residential building type by share in Canada [NRCan, 2008].....	44
Table 3: Residential building type by quantities in Canada [NRCan, 2008].....	44
Table 4: Residential single detached secondary energy use by end-use [NRCan, 2008]	45
Table 5: Building dimension of the simulation model house	45
Table 6: Properties of building materials.....	46
Table 7: Heat exchanger design specifications for Toronto, Montreal and Vancouver	48
Table 8: Simulation case parameters.....	52
Table 9: Simulation results for high load period from January to April	58
Table 10: Simulation results for low load period from April to May	59
Table 11: Mean primary temperature drop, primary return temperature, primary and secondary flow rate during high load period with different primary supply modes.....	92
Table 12: Design data for the model house for three Canadian metropolitan cities.....	103
Table 13: Thermal resistance of the building envelope	103
Table 14: Design heat losses (Q_{es}) across different building surfaces, in [W]	104
Table 15: The design infiltration and required ventilation flow rate, and the combined infiltration/ventilation design heat load for the model house.....	106
Table 16: A summary of the model house total design heating load.....	107

Table 17: Heat exchanger design specifications for Toronto, Montreal and Vancouver..... 109

List of Figures

Figure 1: A simplified diagram showing the main parts of a district heating system	9
Figure 2: A simplified CHP process based on the Rankine cycle.....	10
Figure 3: A primary supply temperature curve based on outdoor temperature [Euroheat & Power, 2008].....	12
Figure 4: A simplified diagram of a district heating substation connected to a radiator.....	14
Figure 5: Primary and secondary supply temperature curve based on outdoor temperature [Euroheat & Power, 2008; Gustafsson et al., 2010]	15
Figure 6: Average primary resource factors by heating systems based on data from 32 European nations	16
Figure 7: A simplified system schematic of the Drake Landing Solar Community Project [Sibbitt et al., 2007]	18
Figure 8: Heat balancing on the first half of the inner layer of a wall envelope	28
Figure 9: Heat balancing on the second inner node of a wall envelope	29
Figure 10: Heat balancing on the outer node of a wall envelope	30
Figure 11: The wall model developed in Matlab Simulink showing the inter-connections between temperature nodes.....	31
Figure 12: The radiator model created in Matlab Simulink environment.....	33
Figure 13: A graphical representation of a multi-stage heat exchangers	35
Figure 14: Heat exchanger model in Matlab Simulink environment [Gustafsson et al., 2008] ...	37
Figure 15: A sketch of heat transfer dynamics within a zone [Xu et al., 2008]	38

Figure 16: The interior room model developed in Matlab Simulink environment	39
Figure 17: Thermostatic radiator valve model in Matlab Simulink environment	41
Figure 18: A PI-controller created in Matlab Simulink environment.....	42
Figure 19: A diagram showing the overall structure of the integrated simulation model.....	43
Figure 20: Simulated indoor temperature with different RCL for Toronto during high heating load period with primary supply mode A (top), primary supply mode B (middle) and primary supply mode C (bottom)	62
Figure 21: Simulated indoor temperature with different RCL for Montreal during high heating load period with primary supply mode A (top), primary supply mode B (middle) and primary supply mode C (bottom)	63
Figure 22: Simulated indoor temperature with different RCL for Vancouver during high heating load period with primary supply mode A (top), primary supply mode B (middle) and primary supply mode C (bottom)	64
Figure 23: Simulated instantaneous heat transfer rate with different RCL during high heating load period with primary supply mode C for Toronto (top), Montreal (middle) and Vancouver (bottom)	65
Figure 24: Simulated primary water temperature drop with different RCL during high heating load period with primary supply mode A for Toronto (top), Montreal (middle) and Vancouver (bottom)	66
Figure 25: Simulated primary water temperature drop with different RCL during low heating load period with primary supply mode A for Toronto (top), Montreal (middle) and Vancouver (bottom)	67
Figure 26: Plot of outdoor temperature for Toronto, Montreal and Vancouver	69

Figure 27: Plot of secondary temperature set-point for hot water radiator	69
Figure 28: Simulated secondary flow rate at different RCL for Vancouver during high load period with primary supply mode A (top), primary supply mode B (middle), and primary supply mode C (bottom).....	70
Figure 29: Radiator system control curve based on outdoor temperature	71
Figure 30: Simulation of indoor temperature for a heating system with a RCL of 0.7 in Vancouver	72
Figure 31: simulation of primary mass flow rate for a heating system with a RCL of 0.7 in Vancouver	73
Figure 32: simulation of primary return temperature for a heating system with a RCL of 0.7 in Vancouver	73
Figure 33: Simulated indoor temperature with different primary supply modes at RCL of 1.0 during high heating load period for Toronto (top), Montreal (middle) and Vancouver (bottom)	76
Figure 34: Simulated indoor temperature with different primary supply modes at RCL of 0.7 during high heating load period for Toronto (top), Montreal (middle) and Vancouver (bottom)	77
Figure 35: Simulated heating demand and instantaneous heat transfer rate with RCL of 1.0 and 0.7 with primary supply mode C for Toronto (top), Montreal (middle) and Vancouver (bottom)	78
Figure 36: A plot of primary water supply temperature for Vancouver with supply mode A and C	79
Figure 37: A plot of primary water flow rate for Vancouver with supply mode A and C.....	79

Figure 38: Operation curves of the secondary loop – hydronic radiator system.....	87
Figure 39: Simulated secondary flow rate and design secondary flow rate for a residential house connected to district heating in Toronto.....	88
Figure 40: Conventional control scheme of district heating substation and secondary loop.....	89
Figure 41: Diagram of the new proposed control scheme	90
Figure 42: Control logic of the flow control actuator	91
Figure 43: Simulated Primary Temperature Drop with Conventional and New Control Scheme with Primary Supply Mode A (top), Primary Supply Mode B (middle) and Primary Supply Mode C (bottom).....	94
Figure 44: Simulated Secondary Flow Rate with Conventional and New Control Scheme with Primary Supply Mode A (top), Primary Supply Mode B (middle) and Primary Supply Mode C (bottom).....	95
Figure 45: Simulated Indoor Temperature with Conventional and New Control Scheme with Primary Supply Mode A (top), Primary Supply Mode B (middle) and Primary Supply Mode C (bottom)	96

Nomenclature

A	area (m^2)
A_{cf}	building conditioned floor area (m^2)
A_L	building effective leakage area (m^2)
A_{es}	building exposed surface area (m^2)
A_{ul}	unit leakage area (cm^2/m^2)
ACH	air exchange per hour (change/hr)
Cp	heat capacity ($\text{J}/\text{kg}\cdot\text{K}$)
C_s	air sensible heat factor $\text{W}/(\text{L}\cdot\text{s}\cdot\text{K})$
F_p	heat loss coefficient per foot of perimeter ($\text{W}/\text{m}\cdot\text{K}$)
h_c	convective heat transfer coefficient ($\frac{\text{W}}{\text{m}^2\cdot\text{K}}$)
h_r	radiative heat transfer constant ($\frac{\text{W}}{\text{m}^2\cdot\text{K}}$)
h_h	heat transfer coefficient of water from the primary loop ($\text{W}/\text{m}^2\cdot\text{K}$)
h_c	heat transfer coefficient of water from the secondary loop ($\text{W}/\text{m}^2\cdot\text{K}$)
IDF	infiltration driving force, ($\text{L}/\text{s}\cdot\text{cm}$)
K_{vs}	valve characteristic coefficient (m^3/h)
k	thermal conductivity ($\frac{\text{W}}{\text{m}\cdot\text{K}}$)
L	thickness of conductive material (m)
\dot{m}_p	primary water flow rate (kg/s)
\dot{m}_s	secondary water flow rate (kg/s)
\dot{m}_h	mass flow rate of water at the primary loop (kg/s)
\dot{m}_c	mass flow rate of water at the secondary loop (kg/s)

P	pressure (Pa)
p	perimeter (m)
q	heat transfer rate (W)
q_{cd}	thermal conduction transfer rate (W)
q_{cv}	thermal convective transfer rate (W)
q_r	radiative transfer rate (W)
$q_{transfer}$	heat transfer rate from the water to the indoor environment (J/s)
q_{water}	net heat transfer rate from water flowing in and out of the radiator (J/s)
$q_{accumulation}$	accumulation rate of heat in the radiator (J/s)
q_{pe}	heat loss through perimeter (W)
Q	volumetric flow rate (L/s)
Q_i	air volumetric flow rate via infiltration (L/s)
Q_{sup}	total ventilation supply airflow rate (L/s)
Q_{exh}	total ventilation exhaust airflow rate (L/s)
Q_v	required ventilation flow rate (L/s)
q_{es}	heat loss across the exterior surface (W)
R_{SI}	R-value in metric system – a measure thermal resistance ($m^2 \cdot K/W$)
$R_{IMPERIAL}$	R-value in imperial system – a measure thermal resistance ($hr \cdot ^\circ F \cdot ft/BTU$)
t	time (s)
T	Temperature ($^\circ C$ or K)
T_{in}	indoor temperature ($^\circ C$)
$T_{c,in}$	water temperature entering the heat exchanger from the secondary loop ($^\circ C$)

$T_{c,out}$	water temperature exiting the heat exchanger to the secondary loop ($^{\circ}\text{C}$)
$T_{h,in}$	water temperature entering the heat exchanger from the primary loop ($^{\circ}\text{C}$)
$T_{h,out}$	water temperature exiting the heat exchanger to the primary loop ($^{\circ}\text{C}$)
T_{ps}	primary water supply temperature ($^{\circ}\text{C}$)
T_{pr}	primary water return temperature ($^{\circ}\text{C}$)
$T_{rad,in}$	water temperature entering the radiator ($^{\circ}\text{C}$)
$T_{rad,out}$	water temperature exiting the radiator ($^{\circ}\text{C}$)
T_s	surface temperature ($^{\circ}\text{C}$)
T_w	heat transfer wall surface temperature of heat exchanger ($^{\circ}\text{C}$)
T_{∞}	temperature of fluid at a distance far enough from the surface not to be affected by its temperature ($^{\circ}\text{C}$)
V	volume (m^3)
θ	log mean temperature difference
ϵ	thermal emittance
σ	Stefan-Boltzmann constant at 5.67×10^{-8} ($\frac{\text{W}}{\text{m} \cdot \text{K}^4}$)
ρ	density (kg/m^3)

1. Introduction

This thesis is concerned with the investigation of the impact of design and operation parameters on the performance of district heating substations. It aims to generate knowledge for building designers and engineers to better understand and evaluate the performance of district heating substations under different conditions, so that the performance of new and existing district heating substations can be enhanced by better design and operation.

1.1 Background

The operation of residential and commercial buildings accounts for approximately 30% of the total energy consumption in Canada, and 56% of that energy is used for space heating [Natural Resource Canada (NRCan), 2008]. Residential and commercial buildings also account for 28% of total greenhouse gas emissions [NRCan, 2008]. As concerns for climate change continue to grow, a strong emphasis has been placed across the globe to reduce energy consumption and greenhouse gas emissions of buildings. Improving the energy efficiency of building heating systems can contribute to the global effort in energy conservation and reduction in greenhouse gas emission.

Case studies have shown that adopting district energy systems can potentially achieve a wide range of social, economic, and environmental benefits [Sibbitt et al., 2007; Gabrielaitiene, Bohn, & Sundén, 2007; Hu, Zhou, Wang, & Neumaier, 2005; NRCan, 2004; Nijjar, Fung, Hughes, & Taherian, 2009]. International Energy Association (1998) and Euroheat & Power (2005) have also promoted district heating as a sustainable energy system that can aid

nations to effectively reduce global fossil fuel consumption and greenhouse gas emissions. In Canada, interests in district heating systems are growing, and low-density communities are starting to adopt district heating systems to replace conventional on-site heating systems. Examples of low-density communities in Canada that have adopted district heating systems include, but not limited to, the Drake Landing community, Markham downtown and the Band Council of Ouje-Bougoumou.

To harness the potential benefits for adopting district heating systems, it is essential that district heating substations are designed and operated effectively. Ineffective design and operation of district heating substations lead to poor energy performance and uncomfortable indoor environments. Poor energy performance is reflected by a low primary temperature drop across district heating substations. Low primary temperature drop across district heating substations is detrimental to the overall performance of a district heating system, and is undesirable to both the district heating suppliers and end-users.

Professionals in the district heating industry have questioned that low primary temperature drop is potentially caused by inappropriate design and control of district heating substations. The challenge is that the interactions between district heating substations and hydronic heating systems are complex. It is difficult for building designers and engineers to evaluate the impact of design and operation parameters on the performance of district heating substations. The challenge is further enhanced when novel and innovative building service and control systems are involved. Without the use of a computer simulation model, it is difficult to evaluate the performance of district heating substations in professional practises.

Reducing primary temperature drop across district heating substations is a research problem addressed in literature [Gustafsson, Delsing, & van Deventer, 2010; Li & Zaheeruddin, 2007; Xu, Hung, Fu, & Di, 2011; Zhao, Bohn, & Ravn, 1995; Zsebik & Siku, 2011]. Gustafsson et al. (2010) proposed a control strategy of secondary supply temperature based on primary supply temperature. Li and Zaheeruddin (2007) proposed six hybrid fuzzy logic control strategies to regulate fuel firing rate, water flow rate or water temperature in a district heating system. Xu et al. (2011) suggested daily and hourly adjustment of supply water temperature according to the flow performance of the distribution network. Zhao, Bohn, & Ravn (1995) investigated the time delay and thermal storage in distribution network to optimize the performance of a district heating system. Zsebik and Siku (2001) investigated the connection types of heat exchangers in a substation and their effect on primary return temperature.

Despite a rigorous literature review, the question of how the design of a district heating substation affects its energy performance remains unanswered. This thesis focuses on investigating the positive or negative impacts of over- and under-sizing of heating equipment on the performance of a district heating substation under different climatic and operating conditions.

1.2 Research Objective

The research objective of this thesis is to investigate the thermodynamic interactions between a district heating substation and a heating system within a building under different design and operation parameters. It aims to generate new knowledge for building designers

and engineers to better design and operate district heating substations, and in turn improves the energy performance of district heating systems. This is done by three steps:

- (1) developing a physical model of a district heating substation connected to a hydronic heating system
- (2) investigating the impact of sizing of heating devices on the performance of a district heating substation under different climate and operating conditions, and
- (3) devising a new control strategy for district heating substations.

A physical model for a district heating substation and a heating system is developed.

The physical model serves as a computational tool that can enable building designers and engineers to investigate the thermodynamic interactions between heating equipment.

A simulation study is conducted to investigate the impact of sizing on the performance of a district heating substation under different climate and operating conditions. Indoor temperature and primary return temperature are considered as the main variables to assess performance. The positive and negative impacts of over- and under-sizing are discussed, and a solution is presented to remediate the ineffective performance caused by an under-size system.

A new, preliminary control strategy is proposed to further enhance the energy performance of district heating substations. The performance between the proposed and conventional control strategies are compared using the simulation model. Simulation results show that the new control strategy has the potentials to increase primary water temperature drop. The successful development of the proposed control strategy can be applied to district

heating substations, and potentially improve the overall energy performance of district heating systems.

1.3 Methodologies

The mechanical equipment within a district heating substation and a residential building are individually modelled based on first-principle heat and mass transfer equations. The physical modelling of different mechanical equipment are then joined together to generate an integrated model. Matlab Simulink is used as the computational platform to implement the simulation model. The simulation model allows the users to overcome the barrier of complex thermodynamic interactions between heating equipment. It can also be used to evaluate the control strategy proposed.

After the simulation model is developed, sensitivity analysis is conducted to evaluate the impact of sizing under different primary supply conditions and Canadian climates. Toronto, Vancouver, and Montreal were chosen as the locations for the simulation study as they represent the three biggest and most populated cities in Canada. Canadian Weather for Energy Calculations (CWEC) climatic data for the nearest weather stations is used. The building and heating equipment design conditions, such as envelope structure and equipment sizing are chosen according to literature and design guidelines to best reflect the residential homes in Canada.

1.4 Thesis Outline

This thesis begins with introduction, where the research problem is presented and the research objective and methodologies are described. The remaining of this thesis is organized into 4 chapters as below:

Chapter 2 is a background review of district heating systems. It introduces the fundamentals of district heating, type of equipment involved and some modern district heating systems. Practical problems experienced in the district heating industry are also elaborated.

Chapter 3 describes the modelling approach, the theory behind development of the simulation model, and the governing fundamental heat transfer equations. Assumptions are listed out and the design and operation parameters are explained. Design load is calculated based on ASHRAE guidelines.

Chapter 4 presents the simulation results of a district heating substation connected to a single-detached residential house. Simulations were performed using five different ratio of capacity-to-load, three different locations and three different primary water supply schemes. The impact of different design parameters on primary water return temperature and indoor temperature is investigated. A method to remediate an under-sized heating system is also presented.

In chapter 5, a new control strategy which aims to increase the primary water temperature drop across district heating substations is proposed. The performance of the new control strategy is simulated and compared with the conventional control method. The simulation was performed using three different locations and three different primary water

supply schemes. Potential benefits and limitations of the proposed control strategy are discussed.

Chapter 6 concludes this thesis and points out the future work.

2. Overview of District Heating Systems

2.1 Introduction

The application of district heating systems had been limited to high density communities. But over the past decades, there has been significant technological advancement in district heating systems. The applicability of district heating systems has been extended from urban to rural settings. New district heating systems can incorporate the usage of renewable resources and energy conservation measures, making district heating an effective energy system that can potentially reduce the dependence of fossil fuels and greenhouse gas emissions [Joagoda, R. Lonseth, A. Lonseth, & Jackman, 2011]. The upcoming sections present the fundamentals of district heating systems, their potential benefits, existing district heating systems in Canada and practice problems observed in district heating systems.

2.2 Background of District Heating Systems

District heating system distributes heat generated at a centralized location for heating requirements in buildings such as space heating and domestic hot water supply (DHWS). There are many existing district heating systems around the world. The exact operation mode of each district heating system varies, but there exists some general similarities. A district heating system can be divided into three main parts: (1) the centralized production plant, (2) the distribution network, and (3) the consumers. Figure 1 depicts the main parts of a district heating system in a simplified diagram.

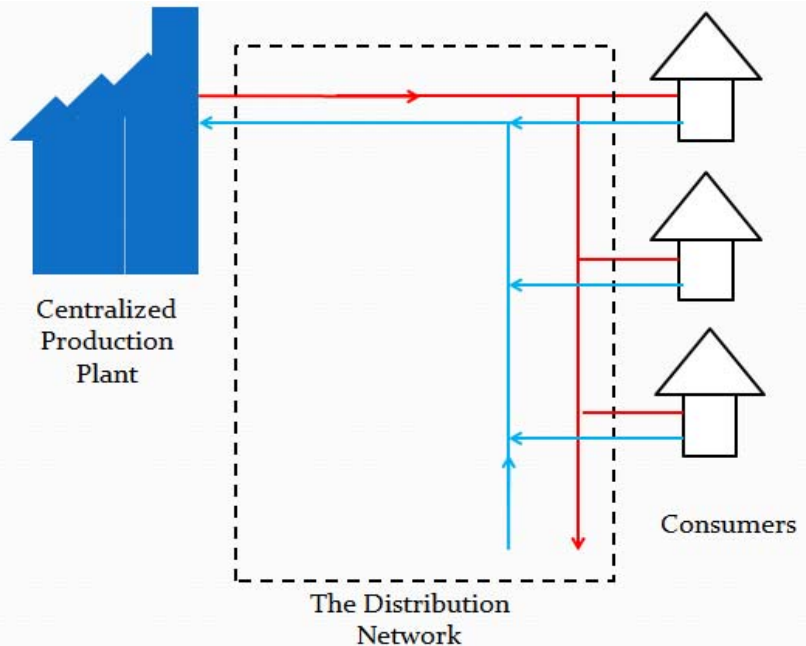


Figure 1: A simplified diagram showing the main parts of a district heating system

2.2.1 Centralized Production Plant

A centralized production plant generates thermal energy by burning combustible materials such as natural gas, oil and coal. Other fuel sources have also been used in district heating systems such as biomass, solar energy, and geothermal energy. Regardless of the fuel source used, all centralized production plants generate and transfer heat to a circulation medium for distribution. The circulation medium used for district heating is commonly hot water or steam [Arkay & Blais, 1995].

Typically, the centralized production plant generates only thermal energy. However, many modern district heating systems can generate both electricity and thermal energy at the same time. This is known as Combined Heat and Power, and is often abbreviated as CHP. CHP utilizes the waste heat from electricity production process for district heating. Figure 2 depicts a simplified CHP process based on the Rankine cycle [Smith, Van Ness, & Abbott, 2005]. Water

is heated at the boiler to generate high pressure steam. The high pressure steam passes across the turbine for electricity generation, and its pressure is decreased. Then, the heat in the low pressure steam is extracted by the condenser, which is connected to a district heating network. The low pressure steam becomes liquid after passing through the condenser and is pumped back into the boiler, and the process repeats.

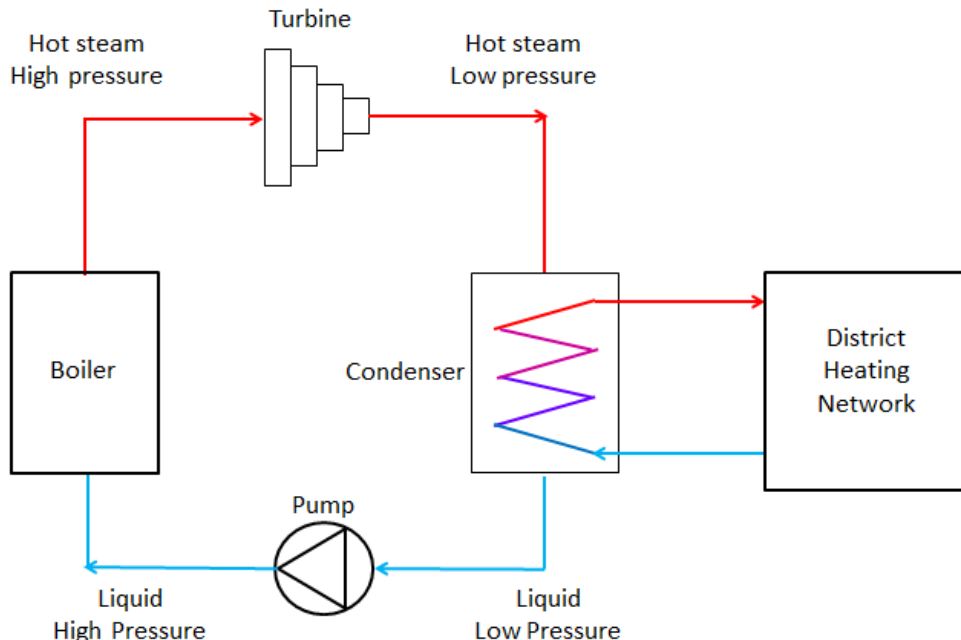


Figure 2: A simplified CHP process based on the Rankine cycle

Other than using combustible fuel, solar and geothermal energy can be used as fuel sources in district heating systems. Example of a solar district heating system is presented in Section 2.4. Solar energy and geothermal energy are considered as renewable energy. They can reduce the dependence of fossil fuels and reduce greenhouse gases emissions. Kyoto protocol, signed by 37 countries, has forced governments to curtail emissions of greenhouse gas. This caused many countries to introduce incentive programs to convert their energy

sources from fossil fuels to renewable energy sources [Jagoda et al., 2011], increasing interests in solar and geothermal district heating systems.

2.2.2 Distribution Network

In a district heating system, the distribution network is a circulation loop of below-grade, insulated pipes where hot water or steam is transported from the centralized plant to the consumers. Modern district heating systems use a closed distribution loop, where water is returned to the centralized plant after passing through the distribution network. The distribution network is also known as the primary loop. As a result, the water or steam that is supplied to consumers is called the primary supply, and the water that is returned to the centralized plant is called the primary return.

There are losses of thermal energy at the distribution network, and this is due to the temperature gradient between the circulation medium and the ground. A higher temperature in the circulation medium will increase the distribution losses. Therefore, it is advantageous to maintain the primary supply at a reasonable low temperature. The distribution losses of a steam-based district heating system are usually higher than a water-based system. This is one reason why water-based systems are more advantageous than steam-based systems.

Water-based systems are also more advantageous than steam-based systems when district heating is used in tandem with CHP. In CHP, production of steam pressure at over 150 psi or above reduces the efficiency of electricity production by 50%, whereas the production of hot water reduces efficiency by less than 10% [Arkay & Blais, 1995]. A disadvantage of using liquid as a circulation medium is that pumps are required in the distribution network.

The primary supply temperature is different among existing district heating systems. For example, the district heating system in downtown Toronto supplies saturated steam to its customers at 200°C all-year round, whereas the Drake Landing solar district heating system supplies hot water with its temperature varies between 40 to 50°C. Many district heating systems vary the primary supply temperature depending on outdoor temperature, as shown in Figure 3. Euroheat & Power [Euroheat & Power, 2008] suggests that the primary supply temperature produced by the centralized plant should be no less than 60 to 75°C, depending on local conditions. Because of the low water supply temperature used in Drake Landing community, specially designed air-handling units are required for adequate heat distribution [Sibbitt et al., 2007]. The system design and choice of primary supply temperature levels are strongly related to historical and traditional factors. New district heating networks are often built using water as a circulation medium with relatively low design temperatures. This is to reduce distribution losses and to provide the possibility to combine with CHP plants [Gustafsson, 2011].

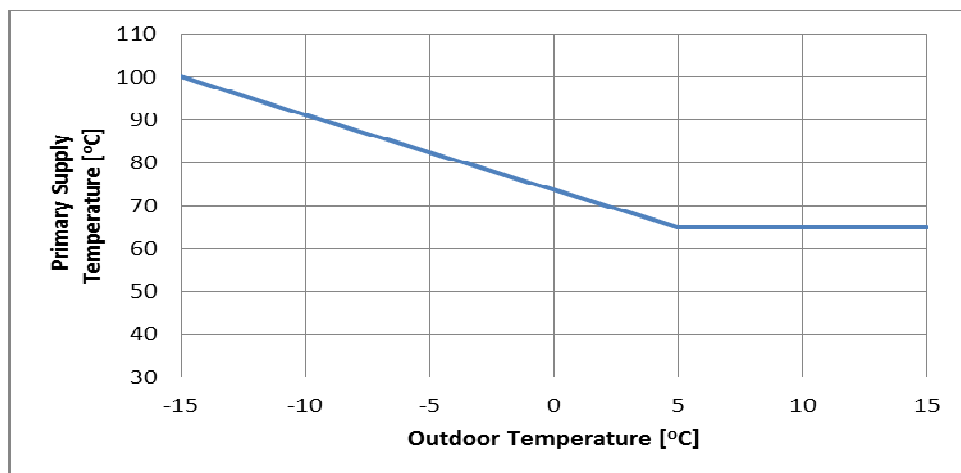


Figure 3: A primary supply temperature curve based on outdoor temperature [Euroheat & Power, 2008]

2.2.3 District Heating Substation and Building Heating System

A district heating substation is a system unit that transfers thermal energy from the distribution network to heating systems in buildings [Euroheat & Power, 2008]. The main components of a district heating substation include a terminal heat exchanger, a controller, a control valve, and an outdoor temperature compensator. For district heating systems, hydronic radiator systems are commonly employed to provide space heating, and the circulation loop that connects the terminal heat exchanger and the hot water radiators is called secondary loop. Therefore, the hot water that is supplied to the radiators is called secondary supply, and the water that is returned to the terminal heat exchanger is called the secondary return.

Figure 4 depicts a simplified system schematic of a district heating substation connected to a radiator. The terminal heat exchanger transfers heat from the distribution network to the heating system. It prevents hot water supplied from centralized production plant to be directly fed to the radiators in the building, thus allowing the substation to control the water temperature supplied to radiators and other terminal devices.

The controller regulates the primary flow rate into the heat exchanger via the control valve on the primary loop. By controlling the primary flow rate into the heat exchanger, the secondary supply temperature is maintained at a desired level. The set-point of the secondary supply temperature is determined by the controller via the outdoor temperature compensator. The outdoor temperature compensator measures the outdoor temperature and determines a secondary supply temperature set-point according to a temperature curve, as shown in Figure 5.

The hot water radiators are used to provide space heating within a building. Note that in practice, the hot water radiators within a building vary in sizes and numbers. A hot water radiator provides space heating via radiative and convective heat transfer. The amount of heat released from a radiator is controlled by a TRV (Thermostatic Radiator Valve). A TRV is a self-regulating valve that controls the indoor temperature by regulating the water flow rate across a radiator.

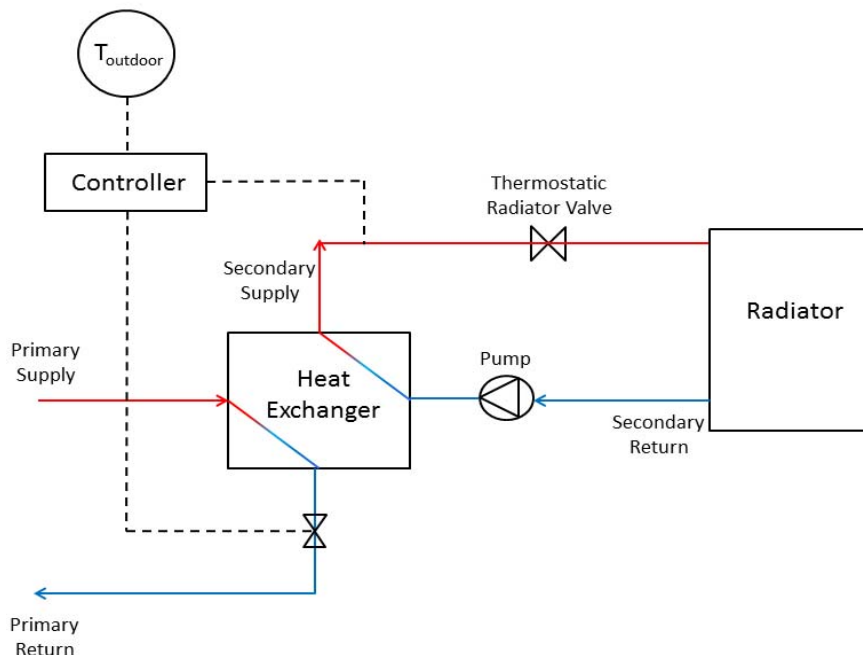


Figure 4: A simplified diagram of a district heating substation connected to a radiator

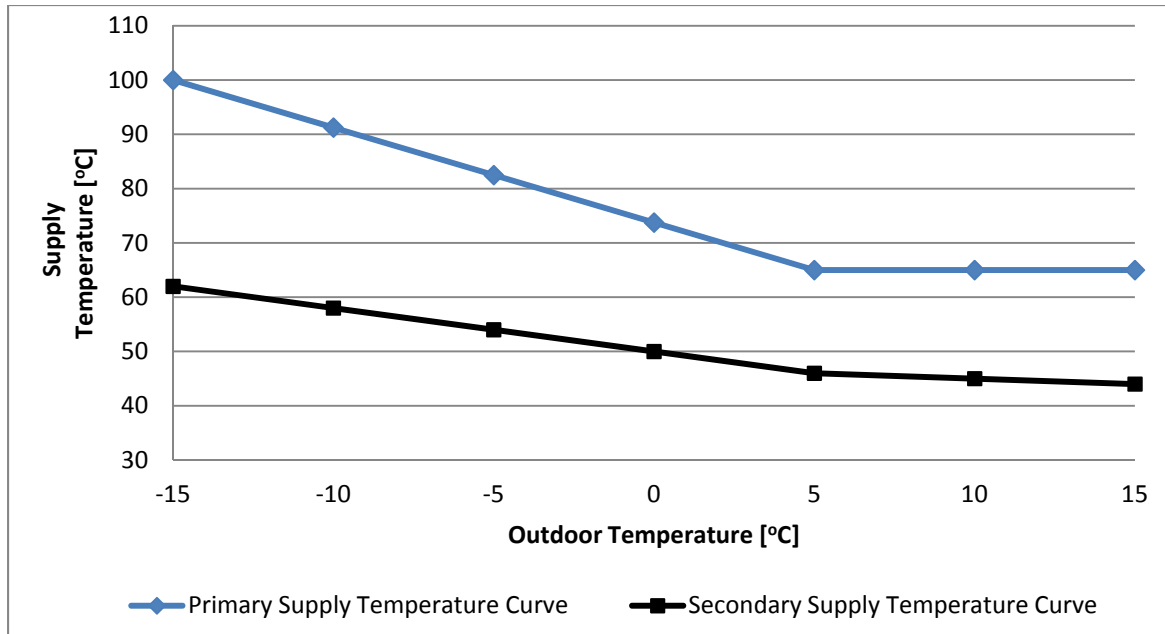


Figure 5: Primary and secondary supply temperature curve based on outdoor temperature [Euroheat & Power, 2008; Gustafsson et al., 2010]

It is important to note that some district heating systems do not employ terminal heat exchangers, and the circulation medium from the centralized plant is directly fed to the radiators within buildings for space heating. This is referred as a directly coupled district heating system. The usage of terminal heat exchangers is known as an indirectly coupled district heating system.

2.3 Potential Benefits of District Heating Systems

District heating can be more energy efficient than conventional heating system. Based on statistical data from 32 European Nations, it was reported that district heating system could obtain an average primary resource factor of 0.82, the lowest relative to other common on-site heating systems, see Figure 6 [Euroheat & Power, 2005]. The primary resource factor is defined as the ratio between the non-regenerative energy input and final energy use. Another

case study has also shown that fuel reduction ranging from 47% to 86% was achieved by adopting district heating systems in China [Hu, Zhou, Wang, & Neumaier, 2005].

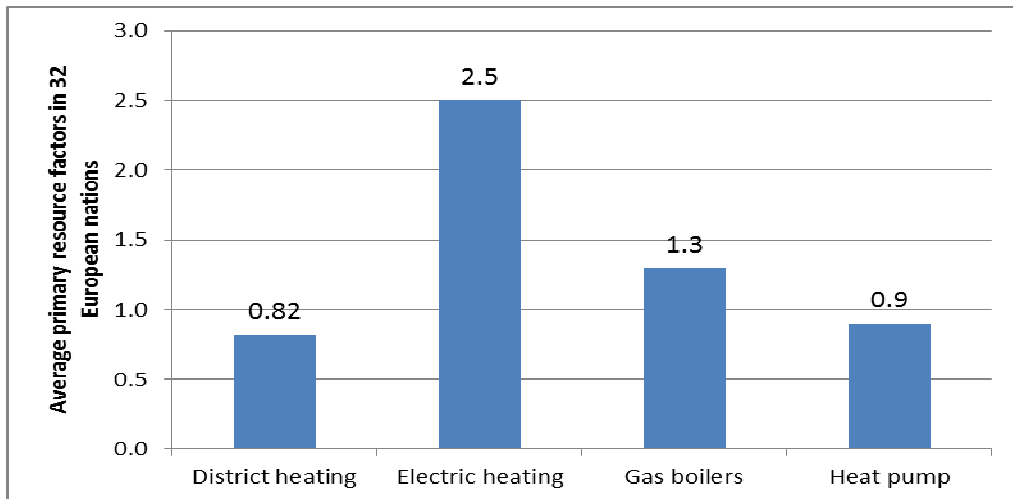


Figure 6: Average primary resource factors of heating systems based on data from 32 European nations

CHP district heating plant is substantially more energy efficient than separate generation of electricity and thermal energy, because heat that is normally wasted in conventional power generation is recovered. Conventional electricity-only power plant has a fuel efficiency ranged between 30 to 40%, whereas a CHP plant can reach fuel efficiency up to 90% [International Energy Agency (IEA), 1998; Euroheat & Power, 2005], resulting in overall fuel reduction. The generation of electricity also provides energy security on a community level. Following the Northeast Blackout in 2003, which left many communities in New York, New Jersey, Vermont, Connecticut, and most of Ontario without power, the idea for smart grid is propelled. CHP can help the power industry to shift towards a more decentralized electricity supply and bidirectional power flow.

International Energy Agency [IEA, 1998] has reported that existing district heating systems, including industrial CHP, had reduced CO₂ emissions from fuel combustion by approximately 3 to 4% annually. Adopting district heating systems has been recognized by Euroheat & Power (2008) as one of the main initiatives to help the European nations in reducing GHG emissions. In recent years, interests of district heating systems in Canada are growing and more district energy systems are being applied to small-size communities. For example, the Markham District Energy Inc. (MDEI) is a new district energy company that utilizes CHP to provide heating, cooling and electricity to Markham, Ontario, Canada. It is estimated that the system will reduce 50% of CO₂ emission and 78% of NO_x emission annually. Other communities that have recently adopted district energy systems include, but not limited to, Ouje-Bougoumou in Quebec, Dockside Green in British Columbia and Drake Landing in Alberta.

2.4 District Heating Systems in Canada

District heating systems have been used in Canada since the 1880s, primarily in the form of group systems serving university, hospital, and government complexes [Arkay & Blais, 1995]. A small list of current Canadian district heating systems is displayed in Table 1. While there are several successful district energy systems, Canada has been well behind many other countries in awareness and application of district energy technologies [Arkay & Blais, 1995]. In recent years, interest of district heating in Canada is growing and advanced district energy system is being applied to smaller communities.

The Drake Landing Solar Community Project in Okotoks, Calgary, Canada, is an example of an innovative district heating system that is applied to a small community [Sibbitt et al.,

2007]. Figure 7 depicts a simplified system schematic of the solar district heating. In spring and summer, solar energy is collected by solar collectors placed on garage roofs. The collected solar energy is stored in a field of insulated, underground boreholes. In winter, the thermal energy stored in the boreholes is extracted to provide space heating for buildings via a district heating loop. Data of preliminary operation indicated all major subsystems are operational, and a solar fraction of 90% will be achieved in 5 years from the initiation of system operation.

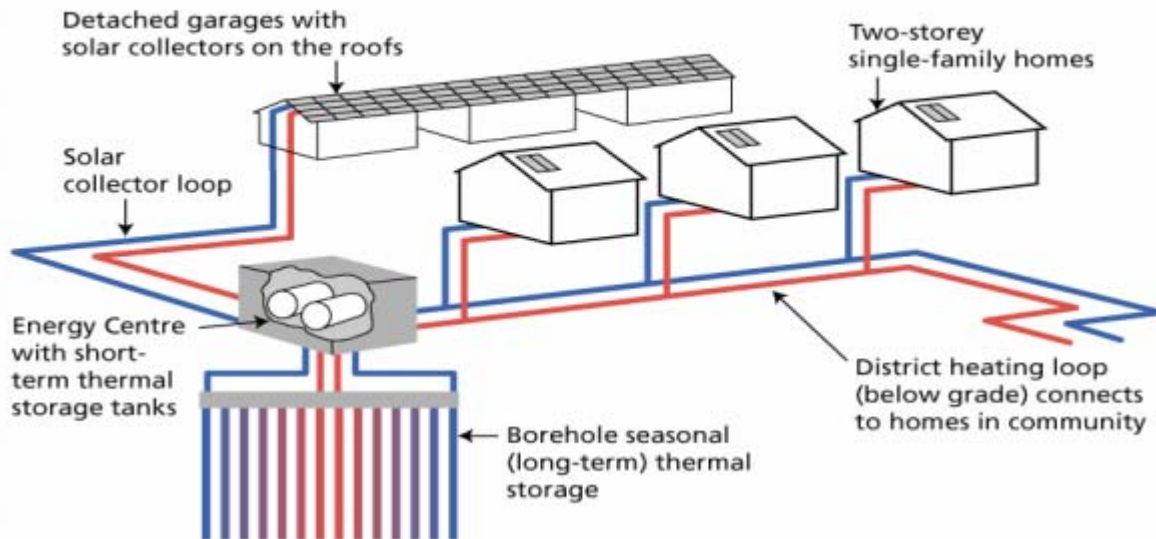


Figure 7: A simplified system schematic of the Drake Landing Solar Community Project [Sibbitt et al., 2007]

The community of Ouje-Bougoumou, Quebec is another example where district heating system is applied to a small-size community. The town of Ouje-Bougoumou has a population of approximately 500 people, and employs a district heating system that uses local renewable materials such as sawdust and other wood waste as fuel source, with oil as back-up. The district system services 122 houses and 19 public buildings, with a capacity of 3.7MW.

Table 1: Examples of existing district heating systems in Canada [Arkay & Blais, 1995]

Name of Organization	City	Age	Size
Tigen PEI	Charlottetown, PEI	1985	30 MW
CDH Cornwall District Heating	Cornwall, Ontario	1994	13 MW
North West Territories Power Corporation	Inuvik, N.W.T.	Mid 1950s	19 MW
Band Council of the Crees of Ouje-Bougoumou	Ouje-Bougoumou, Quebec	1991	3.7 MW
Tigen London	London, Ontario	1879	43 MW
Toronto District Heating Corp. (now Enwave Energy Corporation)	Toronto, Ontario	Early 1960s	276 MW (as of 1995)

2.5 Practical Problems

It is desirable to have a large primary temperature drop across the district heating substations in a district heating system, particularly for CHP operation. By having a higher temperature drop across the district heating network, more energy per unit volume of distributed water will be utilized, thus reducing the energy used in distribution pumps. Increasing the primary temperature drop also enhances the operational efficiency of the

centralized production plant. In a CHP plant, lower return water temperature increase the steam-condensation capabilities of the condenser to condense the hot steam return from the electricity producing turbines, resulting in a larger pressure drop across the turbine and thus increasing electricity production and efficiency. Study has suggested that an increase of primary temperature drop of 10°C in a district heating system can results in an approximately 55% reduction in required pumping power, and fuel savings up to 14% [Persson, 2005]. Similar study has also pointed out that a reduction of 1°C of return water temperature leads to an increase of the system primary resource factor between 0.007 and 0.02 [Henze & Floss, 2011]. The primary energy factor relates the number of fuel energy units required for every unit of delivered energy.

Reducing primary return temperature in a district heating system is a research problem addressed by many researches [Zsebik & Sitku, 2001; Gustafsson et al., 2010, Li & Zaheeruddin, 2007; Lauenburg & Wollerstrand, 2010]. Zsebik and Sitku (2001) analyzed different connection schemes of heat exchangers in a district heating substations and their effects on return water temperature. Gustafsson et al. (2010) proposed a new control strategy for district heating substation to minimize the primary return temperature. Li and Zaheeruddin (2007) proposed six different hybrid fuzzy logic control strategies to regulate primary supply water temperature in a direct-coupled district heating system. Lauenburg and Wollerstrand (2010) described how the control of a hydronic system connected to a district heating network can be optimised to provide the lowest possible primary return temperature.

A high primary return temperature is detrimental to the overall performance of the district heating system and is not favoured by both the district heating provider and end-user. It has been argued by professionals in the industry that the major causes of high primary return temperature are inappropriate sizing of the district heating substation. Based on literature review, no research was found that is related to the impact of sizing on the performance of district heating substation under the Canadian context. It is of interest to investigate the impact of design and operation parameters on the performance of a district heating substation, so that building designer and engineers can potentially better design and operate new and existing district heating systems.

2.6 Concluding Remarks

The application of district heating systems can provide a wide range of potential economic and environmental benefits. Case studies and statistical data have proved district heating as a sustainable and reliable method to provide space heating, and can effectively reduce fossil fuel consumption and greenhouse gas emissions. As concerns of a limited fossil fuel future and threats of global warming due to high CO₂ emissions continue to grow, district heating systems have an obvious place in the future energy systems.

To fully harness the economic and environmental benefits of district heating systems, achieving a high primary temperature drop is essential. However, low primary temperature drop is an existing problem in district heating industry today. A study on the design and operation parameters of district heating substation can help address this problem, and potentially generate new energy initiatives for district heating systems.

3. Development of a Dynamic Physical Model

3.1 Introduction

There are many different aspects to consider when developing a simulation model of a district heating system. Simulating the entire district heating system with a centralized production plant, transmission pipelines and pumps, heat exchange substations, and the heating equipment in a building is ideal, but the focus of this study is on the performance of district heating substations and primary temperature drop. For this reason, the boundary of the simulation scope is limited to the thermodynamic interaction between a district heating substation and a hydronic heating system.

3.2 Approach for Developing a Physical Model for a District Heating Substation

Commercial simulation packages for district heating exist, namely TERMIS and APROS, and have been used in the literature for performance optimization [Gabrielaitiene et al., 2007; Iversen, Ougaard, & Leppenthien, 2006; Li, Dalla Rosa, & Svendsen, 2010]. These simulation packages have the capability to simulate the temperature profile and pressure difference throughout an entire hydraulic network of a district energy system. This is particularly useful in the optimization of supply water temperature and plant production efficiency. These simulation packages, however, emphasize on the modelling of the entire hydraulic distribution network and the equipment in a centralized production plant, and are not best suited for the scope of this study. A simulation tool is needed to account for the thermodynamic behaviour of district heating substation in details, and provide flexibility on testing different control strategies.

Commercial thermal simulation programs such as EnergyPlus, DOE-2, TRNSYS, and DeST can be used to simulate the thermal performance of buildings connected to district heating system. However, Xu et al. (2011) argued that these existing commercial software focus heavily on the building's characteristics but do not take into account the details of the heating systems, e.g. TRV control processes, transport delay in radiators and heat exchangers, hydraulic interactions between consumers. These details are particularly important to analyze different control strategies such as response time, set-point overshoots and the degree of oscillation.

Many researches derived their own simulation models to account for the thermodynamic behaviours of buildings and their equipment [Xu, Fu, & Di, 2008; Liao & Dexter, 2004; Hong & Jiang, 1997; Li & Zaheeruddin, 2004; Gustafsson et al, 2008; Tahersima et al., 2010]. Hudson and Underwood (1999) outlined a simple building modelling procedure for a thermodynamic building for Matlab Simulink. Hong and Jiang (1997) outlined a state-space method to simulate the thermal behaviour of a room, and then used it to develop a multi-zone model. Liao and Dexter (2004) developed a simplified physical model for estimating the average air temperature in multi-zone heating systems for use in an inferential boiler control scheme. Li and Zaheeruddin (2007) developed a simplified physical model to evaluate six different hybrid fuzzy logic control strategies that regulate primary supply water temperature in a directly coupled district heating system. Xu et al. (2008) developed a simulation model to study the control effectiveness of thermostatic radiator valves (TRVs) in directly coupled district heating systems. Gustafsson et al. (2010) developed a simulation model to evaluate the efficiency improvement of a new control strategy for district heating substation. Most of the literature mentioned utilized Matlab Simulink to implement their simulation models.

Statistical method is an alternative approach to determine thermodynamic behaviours by using building performance data [Letherman, Pailing, & Park, 1982; Crawford & Woods, 1985; Andersen et al., 2002; Madsen & Holst, 1995; Braun & Chaturvedi, 2002; Wang and Xu, 2006]. Letherman et al. (1982) described a technique to measure room thermal responses using pseudo-random binary sequences. Crawford and Woods (1985) described a method for estimation of continuous-time models for the heat dynamics of buildings using discrete-time building performance data. Andersen et al. (2002) proposed a continuous time modelling of the heat dynamics of a building where statistical methods are used in parameter estimation and model validation, while physical knowledge is used in forming the model structure. Wang and Xu (2006) developed a genetic algorithm estimator to estimate the lumped internal thermal parameters of the building thermal network model using the operation data collected. The major drawback of developing statistical model is that it requires a significant amount of performance data, and may not be applicable to different buildings to reflect their physical behaviours. Statistical approach is also not recommended for the evaluation of control strategies [Wang & Xu, 2006].

Matlab Simulink is chosen as the computational platform for the implementation of the physical model. Matlab Simulink provides a graphical interface where the thermodynamic details and control process of a heating system can be freely designed, modelled and modified. Matlab Simulink is also a reliable computational platform, as many researches had implemented their physical models of district heating systems using Matlab Simulink [Xu, Fu, & Di, 2008; Liao & Dexter, 2004; Hong & Jiang, 1997; Li & Zaheeruddin, 2004; Gustafsson et al, 2008; Tahersima et al., 2010].

3.3 Physical Modelling of a Dynamic System using Lumped-Capacitance Method

This section presents the fundamental heat transfer equations used for the physical modelling of a heat exchanger, a radiator and a thermodynamic building. The lumped-capacitance model is applied to reduce the thermal system to a number of discrete nodes. The temperature is assumed to be uniform within each node, but may change over time. This approximation is useful to simplify complex partial differential heat equations to ordinary differential equations. The application of the lumped-capacitance model to simulate the thermodynamics of buildings were explained by Hudson and Underwood (1999), and had been applied to the simulation of buildings and control systems [Kulkarni and Hong, 2004; Tahersima F. et al., 2010; Gustafsson et al., 2010]. The fundamentals of heat transfer presented in this thesis are based on heat transfer textbooks [Holman, 2002; Welty et al, 2001; Bejan & Kraus, 2003]. Three basic types of heat transfer are described: conductive, convective, and radiative.

For one-dimensional heat conduction, Fourier's law can be applied as in Equation 1. Assuming temperature difference across the thickness of the material and thermal conductivity is constant, Equation 1 can be rewritten as 2, which is analogous with Ohm's law, where $\frac{L}{kA}$ is analogous to electrical resistance.

$$q = -kA \frac{dT}{dx} \quad (1)$$

$$q_{cd} = -kA \frac{\Delta T}{L} = -\frac{\Delta T}{\left(\frac{L}{kA}\right)} \quad (2)$$

where,

q_{cd} is the thermal conduction transfer rate (W),

k is the thermal conductivity ($\frac{W}{m \cdot K}$),

A is the cross-section area (m^2),

T is temperature (K),

L is the thickness of conductive material (m).

Thermal convection between a solid surface and a fluid (liquid or gas) can be described using

Newton's Law of Cooling as in Equation 3 [Holman, 2002]

$$q_{cv} = -h_c A(T_s - T_\infty) \quad (3)$$

where,

q_{cv} is the thermal convective transfer rate (W),

h_c is the convective heat transfer coefficient ($\frac{W}{m^2 \cdot K}$)

A is the cross-section area (m^2),

T_s is surface temperature (K),

T_∞ is temperature of fluid at a distance far enough from the surface not to be affected

by its temperature (K).

The radiation between two surfaces or between a surface and its surroundings can be

described by the Stefan-Boltzmann equation as Equation 4 [Holman, 2002]. For small

temperature difference, the radiation heat transfer can be rewritten to Equation 5, and the

total heat transfer by both convection and radiation can be put together on a common basis in

Equation 6 [Bejan & Kraus, 2003].

$$q_r = \epsilon\sigma(T_1^4 - T_2^4) \quad (4)$$

$$q_r = h_r A(T_1 - T_2) \quad (5)$$

$$q = (h_r + h_c) \cdot A \cdot (T_1 - T_\infty) \quad (6)$$

where,

q_r is the radiative transfer rate (W),

ϵ is the thermal emittance,

σ is the Stefan-Boltzmann constant at $5.67 \times 10^{-8} \left(\frac{W}{m^2 \cdot K}\right)$,

h_r is the radiative heat transfer constant ($\frac{W}{m^2 \cdot K}$).

3.3.1 Physical Modelling of a Dynamic System – Heat Transfer across Building

Envelope

The envelope of a building consists of multiple layers of different size and construction materials. The temperature distribution across each layer can be calculated analogously as an electrical circuit with heat current as electrical current and each wall layer as an electrical resistor. To calculate the surface temperature of the inner first layer of the wall envelope, a heat balancing can be performed on the inner half of the first layer of wall envelope. Assuming a wall envelope with N number of layer, the heat balance equation of the first layer (indoor) of the wall envelope ($i = 1$) can be described, using the lumped-capacitance model, in Equation 7a. Equation 7a can be simplified and rewritten as Equation 7b.

$$Cp_1\rho_1A_1 \frac{L_1}{2} \frac{dT_1}{dt} = h_r A_1(T_{in} - T_1) + h_c A_1(T_{in} - T_1) - \frac{k_1 A_1}{L_1} (T_1 - T_2) \quad (7a)$$

$$\frac{dT_1}{dt} = \frac{(h_r + h_c)(T_{in} - T_1) - \frac{2k_1}{L_1}(T_1 - T_2)}{Cp_1\rho_1\frac{L}{2}} \quad (7b)$$

where,

T_{in} is the indoor temperature (K),

T_i is the surface temperature of wall layer i (K)

Cp is the heat capacity (J/ kg·K),

ρ is the density (kg/m³)

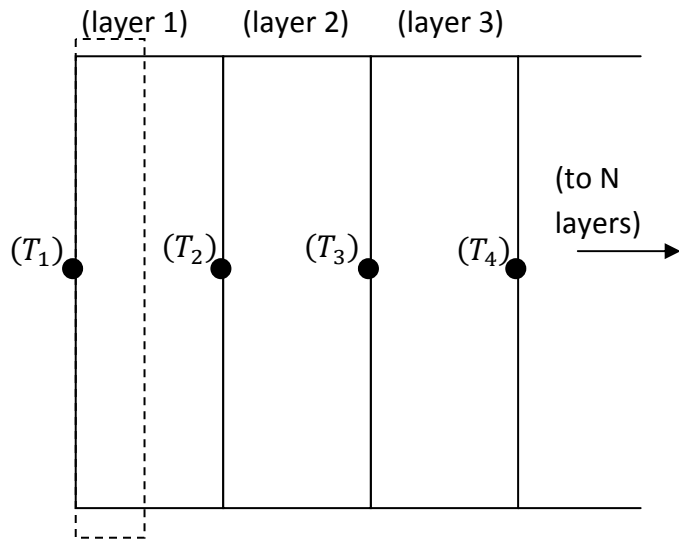


Figure 8: Heat balancing on the first half of the inner layer of a wall envelope

The surface temperature between layer 1 and 2, can be expressed as Equation 8a, which can be simplified and written as Equation 8b. Thus, for a wall assembly with n number of layers, the temperature of interior layer can be generally expressed as Equation 9.

$$(Cp_1\rho_1A_1\frac{L_1}{2} + Cp_2\rho_2A_2\frac{L_2}{2})\frac{dT_2}{dt} = \frac{k_1A_1}{L_1}(T_1 - T_2) - \frac{k_2A_2}{L_2}(T_2 - T_3) \quad (8a)$$

$$\frac{dT_2}{dt} = \frac{\frac{k_1}{L_1}(T_1 - T_2) - \frac{k_2}{L_2}(T_2 - T_3)}{(Cp_1\rho_1\frac{L_1}{2} + Cp_2\rho_2\frac{L_2}{2})} \quad (8b)$$

$$\frac{dT_i}{dt} = \frac{\frac{k_{i-1}}{L_{i-1}}(T_{i-1} - T_i) - \frac{k_i}{L_i}(T_i - T_{i+1})}{(Cp_{i-1}\rho_{i-1}\frac{L_{i-1}}{2} + Cp_i\rho_i\frac{L_i}{2})} \quad (9)$$

where $i = 2, 3 \dots N$

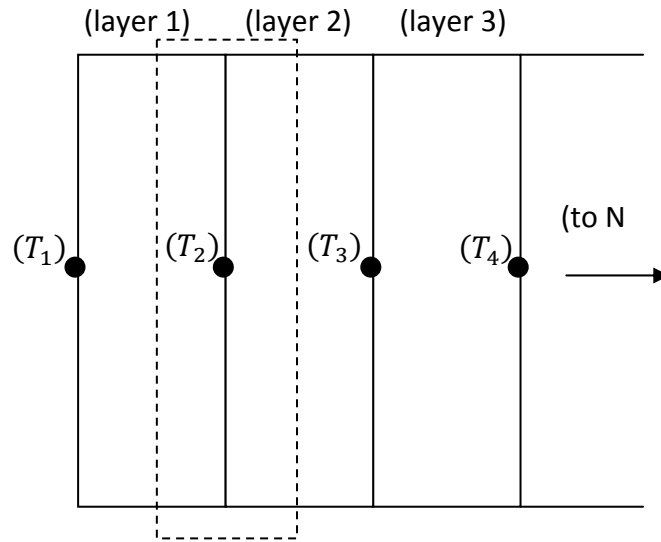


Figure 9: Heat balancing on the second inner node of a wall envelope

Finally, the outer surface temperature (T_{N+1}) of a wall envelope with N layers can be expressed similar to Equation 7b.

$$\frac{dT_{N+1}}{dt} = \frac{\frac{k_n}{L_n}(T_N - T_{N+1}) - (h_r + h_c)(T_{N+1} - T_{outdoor})}{Cp_N\rho_N\frac{L}{2}} \quad (10)$$

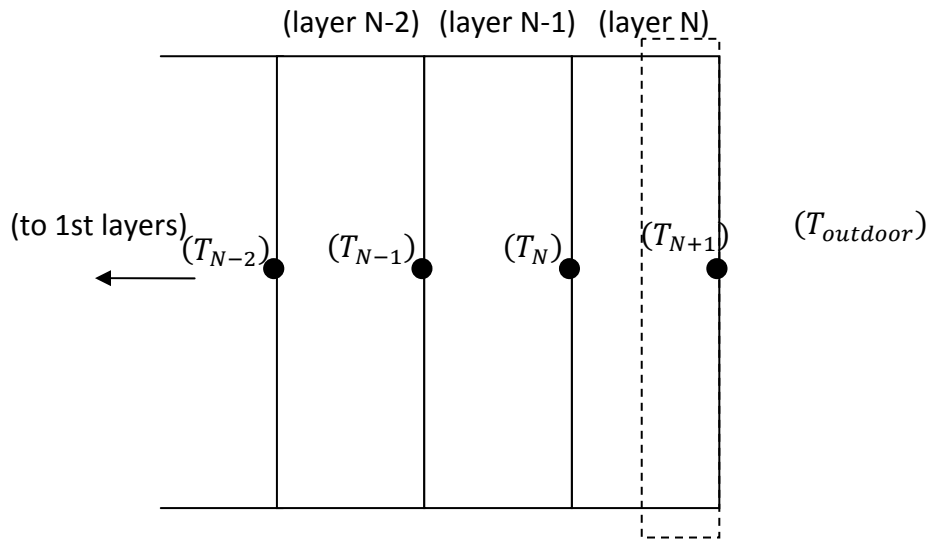


Figure 10: Heat balancing on the outer node of a wall envelope

A four-layer wall model with five temperature nodes is implemented in Matlab Simulink.

The simulation parameters used are described in Section 2.4. Figure 11 shows the interconnections between each temperature node. The wall model takes the input of indoor temperature and outdoor temperature and calculates the instantaneous heat transfer from the room to the wall. The indoor temperature is calculated by the room model, and the outdoor temperature is obtained from climatic data from Canadian Weather for Energy Calculations (CWEC) [Environment Canada, 2005].

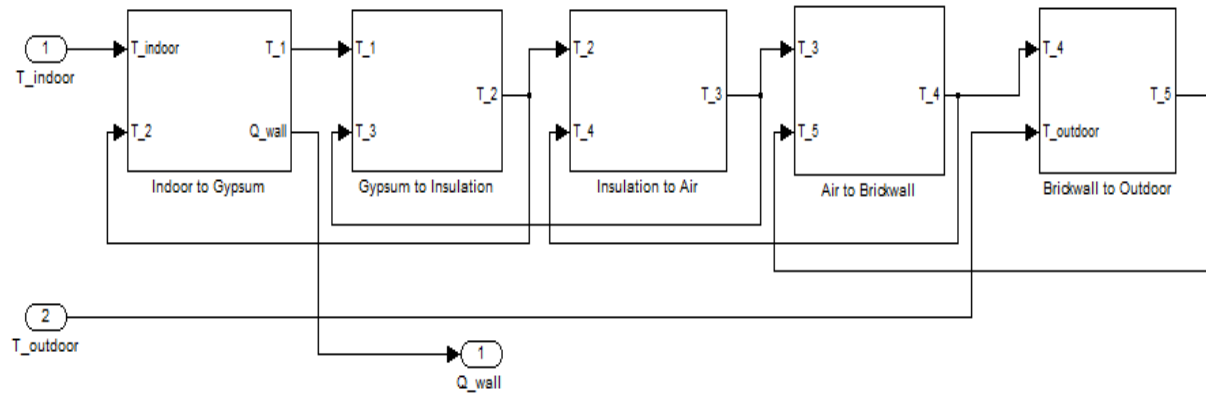


Figure 11: The wall model developed in Matlab Simulink showing the inter-connections between temperature nodes

3.3.2 Physical Modelling of a Dynamic System – Hot Water Radiator

The thermodynamic behaviour of a hot water radiator cannot be simply described by Equation 5 because the hot water temperature across the radiator is not uniform. One could take an arithmetic average of the inlet and outlet water temperature, but literature suggests a more accurate method by applying the Logarithmic Mean Temperature Difference (θ_{LMTD}) [Bejan & Karus, 2003] as expressed in Equation 11. Note that this Logarithmic Mean Temperature Difference is similar, but not identical to the ones commonly used in the heat transfer calculations of heat exchangers. The heat transfer rate of a radiator can be expressed as Equation 12. Note that F is a correction factor for pressure, capacity rate ratio and flow arrangement, and can be expressed as an approximate radiator constant n. For most applications, the radiator constant is commonly set at 1.3 [Tashersima et al., 2010; Gustaffson et al., 2008].

A heat balance can be performed on the outlet of the radiator, as expressed in Equation 14. The thermal energy supplied by the inlet water is expressed by Equation 13 and the outlet water temperature of radiator can be calculated by Equation 15.

$$\theta_L = \frac{T_{rad,out} - T_{rad,in}}{\ln \left(\frac{T_{rad,in} - T_{indoor}}{T_{rad,out} - T_{indoor}} \right)} \quad (11)$$

$$q_{transfer} = UAF\theta_L = UA\theta_L^n \quad (12)$$

$$q_{water} = Cp_w \cdot \dot{m}_s (T_{rad,in} - T_{rad,out}) \quad (13)$$

$$q_{accumulation} = q_{water} - q_{transfer} = Cp_w \cdot m \cdot \frac{dT_{rad,out}}{dt} \quad (14)$$

$$\frac{dT_{rad,out}}{dt} = \frac{Cp_w \cdot \dot{m}(T_{rad,in} - T_{rad,out}) - UA\theta_L^n}{Cp_w \cdot m} \quad (15)$$

where,

$T_{rad,in}$ is the water temperature entering the radiator (K),

$T_{rad,out}$ is the water temperature exiting the radiator (K),

θ_L is the logarithmic mean temperature difference for radiator (K),

\dot{m}_s is the secondary water flow rate (kg/s),

U is the overall heat transfer coefficient ($\text{W}/\text{m}^2\text{K}$),

$q_{transfer}$ is the heat transfer rate from the water to the indoor environment (J/s),

q_{water} is the net heat transfer rate from water flowing in and out of the radiator (J/s),

$q_{accumulation}$ is the accumulation rate of heat in the radiator (J/s).

Figure 12 shows the radiator model implemented in Matlab Simulink using the thermal relationships described from Equation 11 to 15. The radiator model takes the secondary supply temperature, secondary mass flow rate, and indoor temperature as inputs and calculates the secondary return temperature.

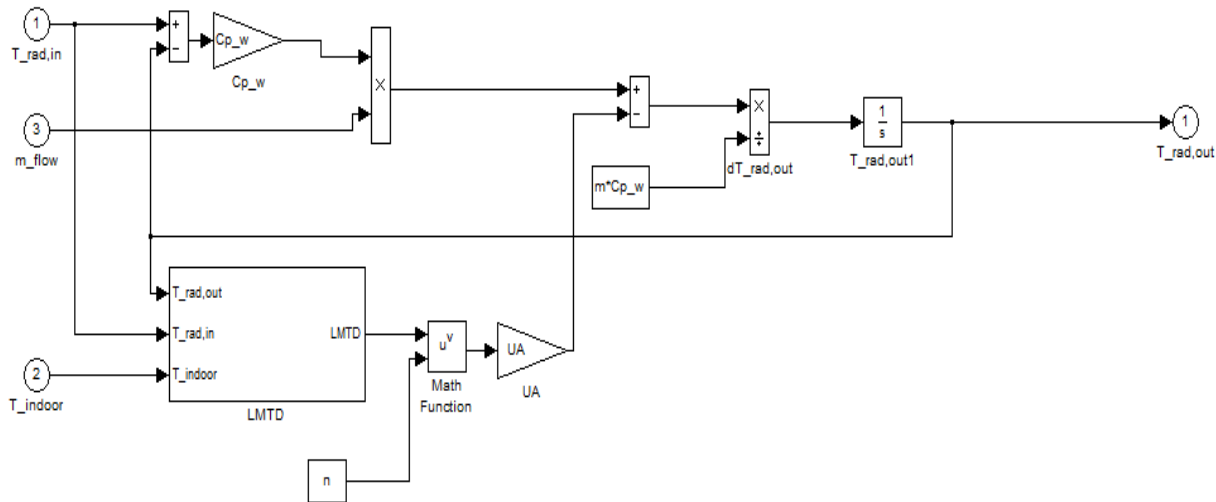


Figure 12: The radiator model created in Matlab Simulink environment

3.3.3 Physical Modelling of a Dynamic System – Heat Exchanger

The thermodynamic behaviour of a heat exchanger is similar to that of a hot water radiator. One can treat the hot side and cold side outlets of a heat exchanger as nodes using the lumped-capacitance method, as shown in Equation 16 and 17. But the log mean temperature difference includes both the hot side and the cold side outlet temperature, making Equation 16 and 17 nonlinear differential equations. The complication of non-linearity can be resolved by adding a node to the heat exchange wall between the hot and cold fluid [Gabrielaitiene et al., 2006, Gustafsson et al, 2008]. As a result, the heat transfer between the two fluids becomes convective heat transfer between a fluid and the heat exchanger wall.

Thus, the log mean temperature difference is split into linear Equations, as shown in Equations 19 to 21.

$$Cp_w \cdot m_h \frac{dT_{h,out}}{dt} = Cp_w \cdot \dot{m}_h (T_{h,in} - T_{h,out}) - UA\theta_{LMTD} \quad (16)$$

$$Cp_w \cdot m_c \frac{dT_{c,out}}{dt} = Cp_w \cdot \dot{m}_c (T_{c,in} - T_{c,out}) + UA\theta_{LMTD} \quad (17)$$

$$\theta_{LMTD} = \frac{(T_{h,in} - T_{c,out}) - (T_{h,out} - T_{c,in})}{\ln \frac{(T_{h,in} - T_{c,out})}{(T_{h,out} - T_{c,in})}} \quad (18)$$

$$Cp_w \cdot m_h \frac{dT_{h,out}}{dt} = Cp_w \cdot \dot{m}_h (T_{h,in} - T_{h,out}) - h_h A_h \left(\frac{T_{h,in} + T_{h,out}}{2} - T_w \right) \quad (19)$$

$$Cp_w \cdot m_c \frac{dT_{c,out}}{dt} = Cp_w \cdot \dot{m}_c (T_{c,in} - T_{c,out}) + h_c A_c (T_w - \frac{T_{c,in} + T_{c,out}}{2}) \quad (20)$$

$$Cp_{wall} \cdot m_{wall} \frac{dT_{wall}}{dt} = h_h A_h \left(\frac{T_{h,in} + T_{h,out}}{2} - T_w \right) - h_c A_c (T_w - \frac{T_{c,in} + T_{c,out}}{2}) \quad (21)$$

where,

$T_{h,in}$ is the water temperature entering the heat exchanger from the primary loop (K),

$T_{h,out}$ is the water temperature exiting the heat exchanger to the primary loop (K),

\dot{m}_h is the mass flow rate of water at the primary loop (kg/s),

θ_{LMTD} is the log mean temperature difference of the heat exchanger (K),

$T_{c,in}$ is the water temperature entering the heat exchanger from the secondary loop (K),

$T_{c,out}$ is the water temperature exiting the heat exchanger to the secondary loop (K),

\dot{m}_c is the mass flow rate of water at the secondary loop (kg/s),

T_w is the heat transfer wall surface temperature of heat exchanger (K),

h_h is the heat transfer coefficient of water from the primary loop ($\text{W}/\text{m}^2\text{K}$),

h_c is the heat transfer coefficient of water from the secondary loop ($\text{W}/\text{m}^2\text{K}$).

The heat transfer rate is not uniform across the heat transfer surface of a heat exchanger [Bejan & Kraus, 2003]. To better model the distribution of temperature across the heat transfer surface, the heat exchanger is divided into a finite number of discrete stages or nodes, as shown in Figure 13. The accuracy in calculating the physical temperature distribution across a heat exchanger is proportional to the number of discrete stages, but simulation time gets more intensive as the number of discrete stages increases. Gustafsson et al. (2008) used three discrete stages in series for the modelling of heat exchangers in a district heating substation. An example of the mathematical setup of a heat exchanger with three discrete stages is shown in Equations 22 to 30.

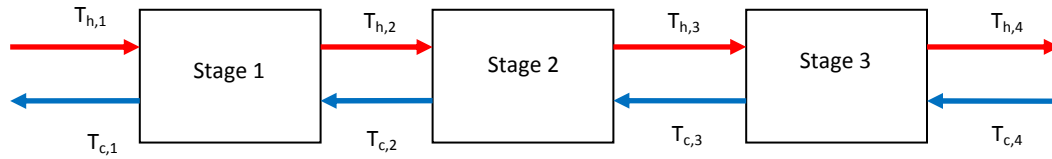


Figure 13: A graphical representation of a multi-stage heat exchangers

$$\frac{dT_{h,2}}{dt} = \frac{Cp_w \cdot \dot{m}_h (T_{h,1} - T_{h,2}) - h_h A_h \left(\frac{T_{h,1} + T_{h,2}}{2} - T_w \right)}{Cp_w \cdot \dot{m}_h} \quad (22)$$

$$\frac{dT_{h,3}}{dt} = \frac{Cp_w \cdot \dot{m}_h (T_{h,2} - T_{h,3}) - h_h A_h (\frac{T_{h,2} + T_{h,3}}{2} - T_{w,2})}{Cp_w \cdot m_h} \quad (23)$$

$$\frac{dT_{h,4}}{dt} = \frac{Cp_w \cdot \dot{m}_h (T_{h,3} - T_{h,4}) - h_h A_h (\frac{T_{h,3} + T_{h,4}}{2} - T_{w,3})}{Cp_w \cdot m_h} \quad (24)$$

$$\frac{dT_{c,1}}{dt} = \frac{Cp_w \cdot \dot{m}_c (T_2 - T_1) + h_c A_c (T_{w,1} - \frac{T_{c,2} + T_{c,1}}{2})}{Cp_w \cdot m_c} \quad (25)$$

$$\frac{dT_{c,2}}{dt} = \frac{Cp_w \cdot \dot{m}_c (T_3 - T_2) + h_c A_c (T_{w,2} - \frac{T_{c,3} + T_{c,2}}{2})}{Cp_w \cdot m_c} \quad (26)$$

$$\frac{dT_{c,3}}{dt} = \frac{Cp_w \cdot \dot{m}_c (T_4 - T_3) + h_c A_c (T_{w,3} - \frac{T_{c,4} + T_{c,3}}{2})}{Cp_w \cdot m_c} \quad (27)$$

$$\begin{aligned} & Cp_{wall} \cdot m_{wall,1} \frac{dT_{wall,1}}{dt} \\ &= h_h A_h \left(\frac{T_{h,1} + T_{h,2}}{2} - T_{w,1} \right) - h_c A_c \left(T_{w,1} - \frac{T_{c,1} + T_{c,2}}{2} \right) \end{aligned} \quad (28)$$

$$\begin{aligned} & Cp_{wall} \cdot m_{wall,2} \frac{dT_{wall,2}}{dt} \\ &= h_h A_h \left(\frac{T_{h,2} + T_{h,3}}{2} - T_{w,2} \right) - h_c A_c \left(T_{w,2} - \frac{T_{c,2} + T_{c,3}}{2} \right) \end{aligned} \quad (29)$$

$$\begin{aligned} & Cp_{wall} \cdot m_{wall,3} \frac{dT_{wall,3}}{dt} \\ &= h_h A_h \left(\frac{T_{h,3} + T_{h,4}}{2} - T_{w,3} \right) - h_c A_c \left(T_{w,3} - \frac{T_{c,3} + T_{c,4}}{2} \right) \end{aligned} \quad (30)$$

The heat exchanger model takes the primary flow rate, secondary flow rate, primary supply temperature and secondary return temperature as inputs, and calculates the primary return temperature and secondary supply temperature. The heat exchanger model is

developed by Gustafsson et al. (2008). Figure 14 shows the Simulink implementation of the heat exchanger model.

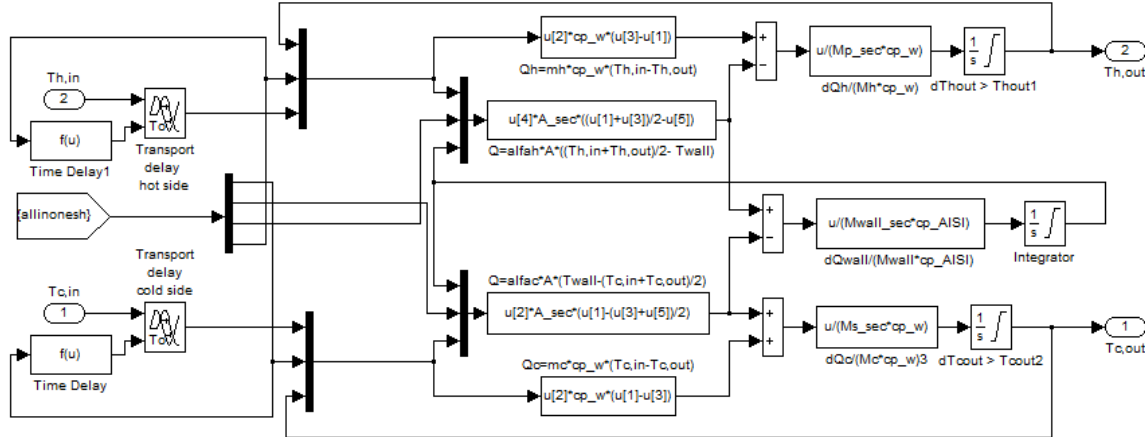


Figure 14: Heat exchanger model in Matlab Simulink environment [Gustafsson et al., 2008]

3.3.4 Physical Modelling of a Dynamic System – Interior Room

The thermal indoor environment can be described by the room air temperature using the lumped-capacitance model. Assuming temperature distribution is uniform within a zone of a building, the room air temperature of a single zone can be calculated by summing all the heat transfer rates as shown in Equation 31. Figure 15 illustrates the heat transfer processes within a zone of a building.

$$\begin{aligned}
 q_{\text{accumulation}} &= C_p_{\text{air}} \cdot \rho_{\text{air}} \cdot V_{\text{room}} \frac{dT_{\text{room}}}{dt} \\
 &= q_{\text{wall}} + q_{\text{window}} + q_{\text{floor}} + q_{\text{ceiling}} + q_{\text{radiator}} + q_{\text{ACH}} \\
 &\quad + q_{\text{solar}} + q_{\text{internal gain}}
 \end{aligned} \tag{31}$$

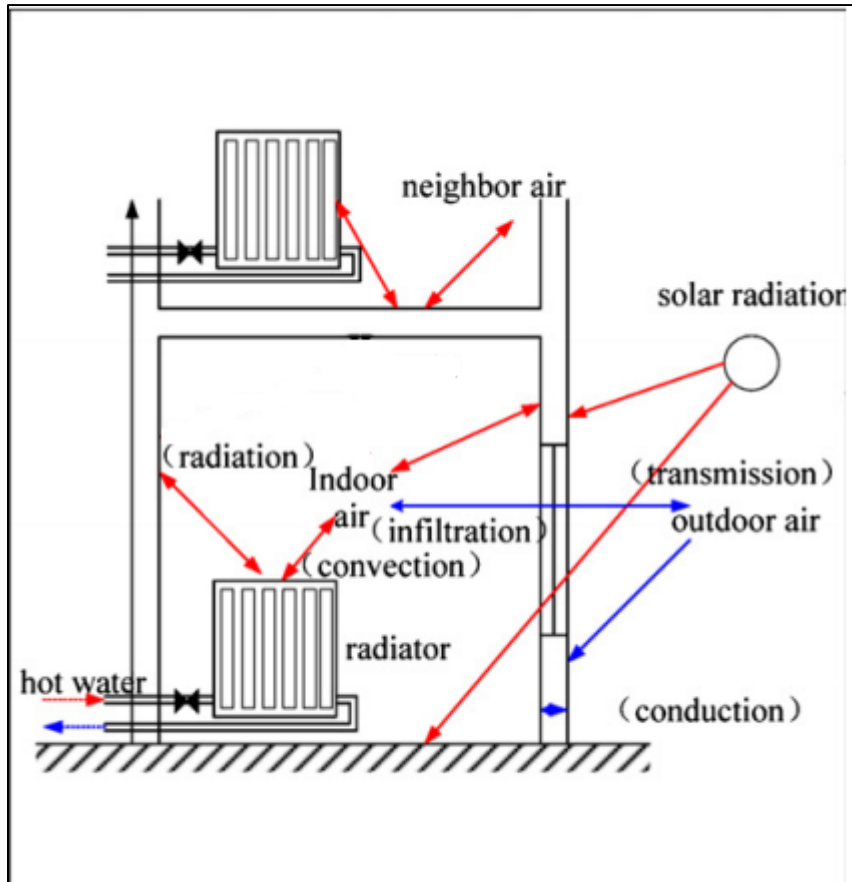


Figure 15: A sketch of heat transfer dynamics within a zone [Xu et al., 2008]

The heat transfer process in a room includes:

- Heat transfer from the hot water to the radiator shell through convection
- Heat exchange between the air and the inner layer of the envelope (wall, ground and roof) with thermal inertia
- Solar radiation
- Heat transfer through glazing without thermal inertia
- Heat transfer via air infiltration through crack and openings
- Heat transfer between neighbouring zone

Multiple zones can be setup by an additional term in Equation 31. The heat transfer rate between zones via internal partition can be calculated using Equation 7 to 10. The heat transfer rate between inter-connected zones must be added to the heat balance equation of each zone as shown in Equation 32. Figure 16 shows the interior room model developed in Matlab Simulink environment.

$$\begin{aligned}
 q_{\text{accumulation}} &= C p_{\text{air}} \cdot \rho_{\text{air}} \cdot V_{\text{room}} \frac{dT_{\text{room}}}{dt} \\
 &= q_{\text{wall}} + q_{\text{window}} + q_{\text{floor}} + q_{\text{ceiling}} + q_{\text{radiator}} + q_{\text{ACH}} \\
 &\quad + q_{\text{solar}} + q_{\text{internal gain}} + \sum_i^n q_{\text{partition},i}
 \end{aligned} \tag{32}$$

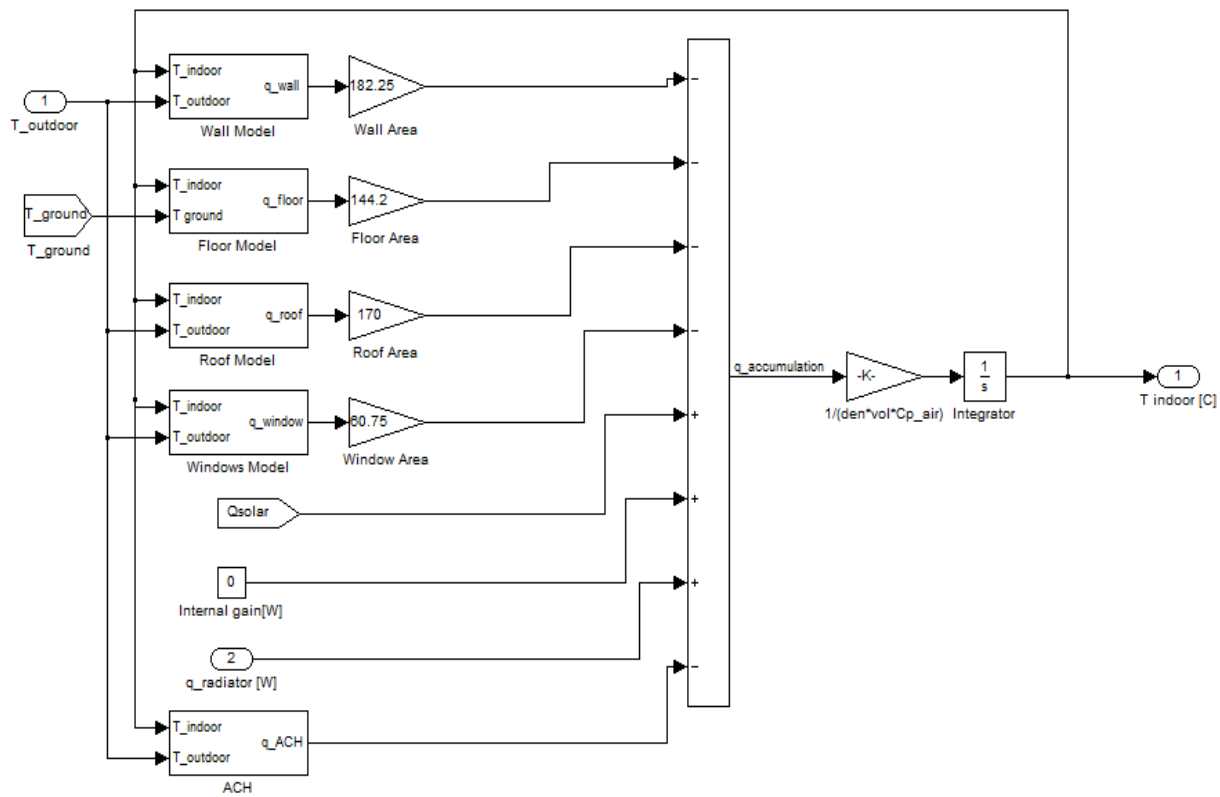


Figure 16: The interior room model developed in Matlab Simulink environment

3.3.5 Thermostatic Radiator Valve

A thermostatic radiator valve (TRV) controls the hot water flow rate across a radiator by sensing the indoor temperature. The sensor contains an actuator that passively adjusts the valve opening based on the temperature in the room. Control equations of the flow rate across TRV can be set up based on the works of Gustafsson et al. (2010). Equation 33 describes the control behaviour of the TRV. Figure 17 presents the thermostatic radiator valve model in Matlab Simulink environment.

$$\dot{m}_s = f(\Delta T_{sen-room}) \frac{K_{vs} \sqrt{\Delta P} \rho}{3600} \quad (33)$$

where,

\dot{m}_s is the water flow rate in the secondary loop (kg/s),

$\Delta T_{sen-room}$ is the difference between the measured room temperature and the room temperature set-point (K),

ΔP is the pressure drop across the valve (Pa),

K_{vs} is the valve characteristic coefficient (m^3/h),

ρ is the water density, and is considered as a function of temperature (kg/m^3)

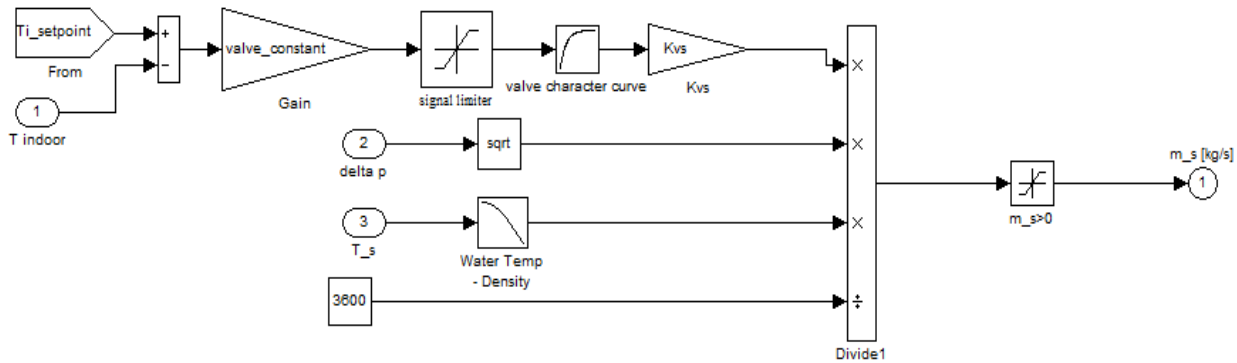


Figure 17: Thermostatic radiator valve model in Matlab Simulink environment

3.3.6 Controller at a District Heating Substation

Traditionally, the temperature set-point for hot water flowing across a radiator is fixed year-round. In the past decade, temperature compensators are commonly available and they can be used in district heating substations to adjust the secondary water supply temperature set-point according to outside temperature. This reduces the possibility of having excessively hot supply water flowing to radiators during intermediate seasons, and allows the TRV to compensate as little as possible even at large outdoor temperature change. This is expected to remediate a lot of overheating phenomena in direct-coupled district heating system described in literature [Xu et al., 2008].

The controller defines the secondary supply temperature set-point based on the secondary temperature curve in Figure 5. It measures the error in the secondary supply temperature and regulates the control valve located on the primary loop on the outlet of the heat exchanger. By adjusting the control valve, the water flow rate flowing into the heat

exchanger is regulated. A regular PI-controller is employed and the signal equation of the PI controller is described by Equation 34 [Liptak, 1995].

$$u(\Delta T_{sen-water}) = K_r \cdot \Delta T_{sen-water} + K_i \int \Delta T_{sen-water} dt \quad (34)$$

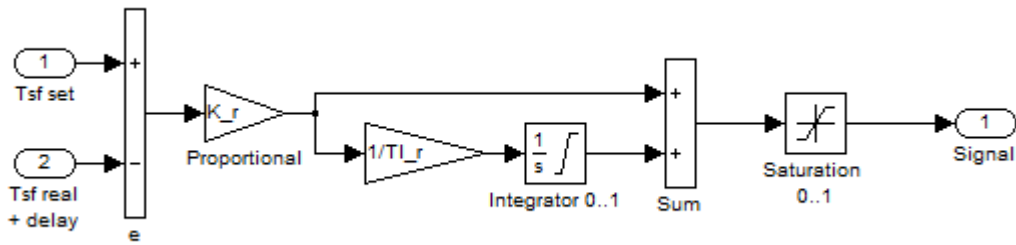


Figure 18: A PI-controller created in Matlab Simulink environment

3.4 Integrated Model

The physical models of different heating devices presented from Section 3.3.1 to 3.3.4 are combined together to form an integrated simulation model. Figure 19 presents the overall structure of the simulation model. It shows the inputs and outputs of each sub-processes and how they are inter-connected with each other. Overall, the integrated simulation model takes climatic data and primary supply temperature to simulate the primary return temperature and indoor temperature. The heat exchanger model and the heat exchanger controller model are considered part of the district heating substation, while the radiator model, TRV model, and the room model are considered part of the thermodynamic building.

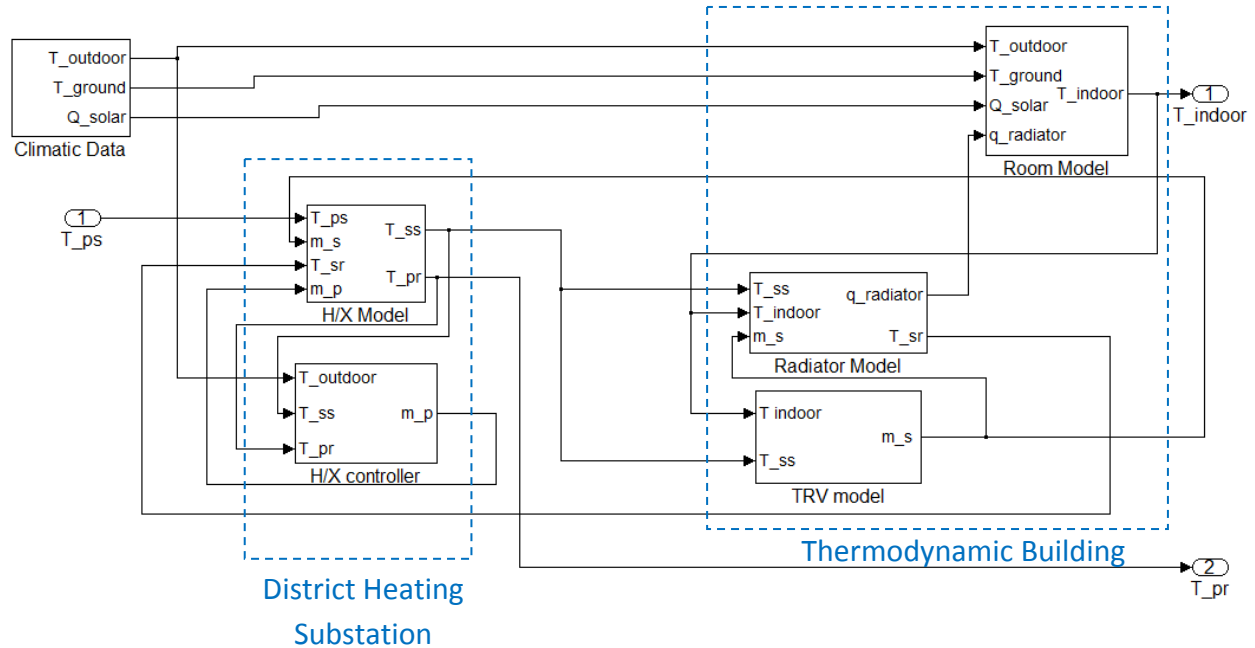


Figure 19: A diagram showing the overall structure of the integrated simulation model

3.5 Model Parameters

Based on the statistical data in 2008, single-detached houses made up of 56.5% of all residential types in Canada and this percentage remained consistent since 1990, see Table 2 and 3 [NRCan, 2008]. Single-detached houses also account for 74.4% of the total energy used for residential space heating in Canada in 2008 [NRCan, 2008]. Because of these factors, a single-detached residential house is chosen as the simulation subject, as they represent the most significant building type in terms of quantities and energy consumption.

The three provinces with the largest number of residential buildings are selected, which are Ontario, Quebec, and British Columbia. The three metropolitan cities selected are Toronto, Montreal, and Vancouver, as they contain the largest population in their respectively provinces [Statistics Canada, 2010].

Table 2: Residential building type by share in Canada [NRCan, 2008]

Share (%)	Canada	Ontario	Quebec	British Columbia
Single-detached	56.5	56.9	45.8	54.6
Single-attached	10.6	14.0	8.2	10.7
Apartments	31.0	28.7	44.9	30.6
Mobile Homes	1.9	0.4	1.1	4.1
	Atlantic Provinces	Alberta	Saskatchewan	Manitoba
Single-detached	70.9	64.7	74.5	68.3
Single-attached	6.3	10.8	5.5	5.4
Apartments	18.6	20.0	17.4	23.9
Mobile Homes	4.1	4.5	2.5	2.3

Table 3: Residential building type by quantities in Canada [NRCan, 2008]

Households by Building Type (thousands)	Canada	Ontario	Quebec	British Columbia
Single-detached	7,437	2773.9	1,533.70	970.9
Single-attached	1,399	682.6	274.6	189.30
Apartments	4,076	1,400.50	1,504.60	544.2
Mobile Homes	252	21.4	38.2	72.70
Total	13,164	4878.4	3351.1	1777.1
	Atlantic Provinces	Alberta	Saskatchewan	Manitoba
Single-detached	677.7	871.1	293.5	316.10
Single-attached	60.5	145.1	21.7	25
Apartments	178	269.9	68.6	110.70
Mobile Homes	39	60.5	9.9	10
Total	955.2	1346.6	393.7	461.8

District energy such as CHP to provide both space heating and cooling is common. In Canada, however, space heating is the predominate end use of energy, about 40 times more than cooling, see Table 4 [NRCan, 2008]. Thus, the scope of this study is limited to the heating season only. Heating season is considered to be from September to May.

Table 4: Residential single detached secondary energy use by end-use [NRCan, 2008]

Energy Use by End-Use (PJ)	1990	2004	2005	2006	2007	2008
Space Heating	581.4	651	634.2	597.9	673.9	685.3
Water Heating	149.5	155.5	155.1	154	158.3	156.9
Appliances	114.2	119.3	115.9	115.8	115.9	123.5
Lighting	39.1	48.5	46.4	46.1	45.3	47.7
Space Cooling	7.9	13.4	26.1	19.9	19.5	16.3

A typical house located in Toronto is selected and used as the subject for the simulation study. The geometry and building materials of the model house are presented in Table 5 and 6. The above-grade walls are constructed with a 100mm brick layer on the exterior face, followed by layers of 25 mm air cavity, 95mm extruded polystyrene insulation (EPS), and gypsum board on the inside. The below-grade wall consists of a layer of 200mm concrete, followed by layers of 25mm EPS insulation, plywood, and gypsum board on the inside. The roof is topped with a layer of roofing clay tile and is insulated with a layer of 145 mm EPS insulation. The windows are clear, double glazed units framed with polyvinylchloride (PVC) with a U-value of 2.27W/m²K. Example of the thermal properties of the building materials are presented in Table 6.

Table 5: Building dimension of the simulation model house

Component	Quantity
Ceiling [m²]	170
Floor [m²]	144.2
Windows [m²]	60.75
Walls [m²]	182.25
House height per floor [m]	2.5
House Width [m]	10.3
House Length[m]	14
Volume [m³]	721

Table 6: Properties of building materials

	Density [kg/m ³]	Thermal Conductivity [W/m·K]	Heat Capacity [W/kg·K]
Gypsum Plaster	900	0.25	1000
EPS Insulation	15	0.04	1400
Air Cavity	1.4	0.022	1005
Brick	1700	0.84	800

The distribution medium used in each district heating system is different. For example, district network at downtown Toronto uses steam as circulation medium and Cornwall, Ontario uses hot water [Arkay & Blais, 1995]. The advantages of using steam as a medium are that no pump is required at the distribution network, and steam can be used for winter humidification. However, using steam will result in higher distribution heat losses. The advantages of using hot water as a medium are that it is relatively safer and easier to satisfy operation codes than steam. It incurs a less heat losses during transmission and there are less expensive piping requirements. More importantly, hot water is more favoured over steam when a district heating system is in tandem with CHP, as discussed in Section 2.2.2. Therefore, hot water is used as the distribution medium for the simulation model.

The heating devices in the simulation model are sized according to ASHRAE guidelines [ASHRAE, 2009]. This is a method commonly used by engineers in the industry to size HVAC equipment. The Carrier System Design Manual also provides guidelines for design load calculation, and is commonly used by HVAC designers. Details of the calculations on design load are presented in the Appendix.

Ratio of capacity-to-load (RCL) is used to associate the capacity of heating devices. It is defined as the actual capacity over design load of a heating device, as shown in Equation 35. In the simulation study, five arbitrary RCL of 0.7, 0.9, 1.0, 1.1, and 1.3 will be used to mimic over- and under-sized heating equipment. The associated design flow rate and heat transfer area of the terminal heat exchanger at district heating substation are presented in Table 7. The hydronic radiator that regulates indoor temperature is essentially a heat exchanger, and is sized similarly to the sizing of the terminal heat exchanger, with the same value of power output.

$$RCL = \frac{\text{actual capacity of heating equipment}}{\text{design load of heating equipment}} \quad (35)$$

Table 7: Heat exchanger design specifications for Toronto, Montreal and Vancouver

Parameters	Value				
Incoming primary temperature [°C]	100				
Returning primary temperature [°C]	50				
Incoming secondary temperature [°C]	45				
Returning secondary temperature [°C]	60				
Log mean temperature difference [°C]	16.8				
Overall heat transfer coefficient [W/m ² ·K]	1300				
Design Heating Load, Toronto [W]	18141				
Ratio of Capacity-to-Load	0.7	0.9	1	1.1	1.3
Power [W]	12699	16327	18141	19955	23583
Secondary flow rate [kg/s]	0.20	0.26	0.29	0.32	0.38
Heat Transfer Area [m ²]	0.58	0.75	0.83	0.91	1.08
Design Heating Load, Montreal [W]	20916				
Ratio of Capacity-to-Load	0.7	0.9	1	1.1	1.3
Power [W]	14641	18824	20916	23007	27191
Secondary flow rate [kg/s]	0.24	0.30	0.34	0.37	0.44
Heat Transfer Area [m ²]	0.67	0.86	0.96	1.05	1.24
Design Heating Load, Vancouver [W]	11888				
Ratio of Capacity-to-Load	0.7	0.9	1	1.1	1.3
Power [W]	8322	10699	11888	13077	15455
Secondary flow rate [kg/s]	0.13	0.17	0.19	0.21	0.25
Heat Transfer Area [m ²]	0.38	0.49	0.54	0.60	0.71

3.6 Concluding Remarks

In this chapter, different approaches for developing a physical model for a district heating substation and heating equipment are investigated. Many existing commercial software are available to perform dynamic building simulations, but they usually do not take into account the details of the heating system or do not provide the flexible for users to readily

assess and modify the underlying mathematical algorithms. This is particularly important in analyzing control strategies. As a result, a physical model is specifically developed via basic fundamental principles in the Matlab Simulink environment.

A method to develop a physical model for a district heating substation and a thermodynamic building is presented in this chapter. Model parameters are specified according to literature and standard design guidelines. The physical models of different heating devices are connected together to create an integrated model in Matlab Simulink. The simulation model is now available to compute the performance of a residential single-detached home connected to district heating. In the next chapter, different design and operation parameters are used in the simulation to evaluate the impact of these variables on the building's performance.

4. Simulation for a Canadian Residential House connected to District Heating

4.1 Introduction

In North America, oversizing is often mentioned as a common observed problem in heating system. Oversized heating equipment can lead to energy inefficient operations, create uncomfortable conditions and large temperature swings in the house [U.S. Department of Energy, 2011; Andersen et al., 2000; Humphreys & Nicol, 2002]. United States Department of Energy mentioned that heating systems have been found two or three times larger than is needed for a given structure [US Department of Energy, 2011]. Other publications have also mentioned that some heating contractors and designers use simplified rules of thumb to determine how large a heating system is needed [US Department of Energy, 2011, Taunton Press, 1999]. For example, a case was observed where contractors on the West Coast in the United States use $40 \text{ Btu/h}\cdot\text{ft}^2$ (126 W/m^2) as a basis for sizing heating equipment, where heat loss calculations show that $11 \text{ Btu/h}\cdot\text{ft}^2$ (35 W/m^2) should be used [Ali, 2009].

The thermodynamic interactions among heating devices connected to district heating are different from conventional on-site heating systems, and the impact of over- and under-sizing of heating devices on the performance and indoor thermal comfort is also different. Based on literature review, no research was found that investigated the impact of oversizing on the performance of district heating substations. As interests in district energy system proliferate in Canada, it would be valuable to determine the positive or negative impacts of over- and under-sizing on the performance of district heating substations.

In the previous chapter, an integrated simulation model for a district heating substation, a thermodynamic building and its associated heating equipment was developed. In this chapter, sensitivity analyses are performed using the simulation model to better understand the impacts of design and operation parameters on the performance of a district heating substation under the Canadian climate. Specifically, the sizing of heating equipment under different primary supply modes and building locations is investigated. Through this study, the capability of the simulation model developed can be displayed, and potential optimization strategies for the performance of district heating substations can be proposed.

The simulation is performed using three different hot water supply modes, at three different locations, with five different ratios of capacity-to-load (RCL) for heating equipment. Details of the simulation cases are presented in Table 8. This combines to a total number of 45 simulation cases. The three supply modes are chosen according to actual common practices by centralized plants [Gustasson et al., 2010]. The first supply mode (supply mode A) is a conventional supply temperature scheme, where primary hot water supply temperature varies with outdoor temperature, as shown in Figure 5. The second supply mode (supply mode B) uses a constant supply temperature at 100°C, which represents a constant high supply temperature. The third supply mode uses a constant supply temperature at 70°C (supply mode C), which represents a constant low supply temperature.

Table 8: Simulation case parameters

Primary Supply Mode	Location	Ratio of Capacity-to-load
A: $T_{ps} = f(T_{outdoor})$	Toronto	0.7
B: $T_{ps} = 100^{\circ}\text{C}$	Montreal	0.9
C: $T_{ps} = 70^{\circ}\text{C}$	Vancouver	1
		1.1
		1.3

It should be noted that there are district heating systems in which primary supply temperature is much lower than 70°C . District heating systems that utilized renewable energy sources are observed to use low primary supply temperature [Sibbitt et al., 2007; Ostergaard & Lund, 2011]. For these district heating systems, specialized air-handling unit or heat pumps are employed, and traditional radiator systems may not be suitable. Since the heating system subjected to study is a hydronic system in an indirectly coupled district heating system, a constant primary supply temperature of 70°C is considered low [Euroheat & Power, 2008].

4.2 Methods of Performance Evaluation

Unlike furnace and hot water boiler, residential houses on district heating network receive heat from the terminal heat exchangers at district heating substations. The classification for operation efficiency of such system is different and much more complicated than traditional heating systems. In terms of fuel efficiency, a holistic evaluation would include the electricity and steam production at the centralized plant, to pump power and transmission losses in the distribution network, to the heat transfer efficiency of heat exchangers at heat transfer terminals, to pump power required for hot water circulation in buildings. In terms of

cost for end-users, district heating users in Europe are commonly charged based on the amount of energy they extract from the district heating network, which is calculated by multiplying the primary mass flow rate across the heat exchanger and the primary temperature drop (ΔT). In downtown Toronto, customers are charged based on the only primary mass flow rate. In Beijing, district heating cost is based on the floor area of the building and not consumption pattern [Beijing International, 2003]. Charging schemes for end-users vary for each district energy system.

Thermal comfort and energy performance are two important factors when evaluating operation performance, for which the evaluation on thermal comfort is more abstract and subjective. Thermal comfort is defined by ASHRAE as the state of mind that expresses satisfaction with the surrounding environment [ASHRAE, 2009]. The most common method to address thermal comfort is the Fanger's model, which is a set of comprehensive heat-balance equations based on the various elements of energy exchange. The equations can be solved to predict thermal comfort for any combination of environmental conditions and variables outlined below:

- Air temperature
- Mean radiant temperature
- Air movement/velocity
- Relative humidity
- Human clothing
- Activity levels

Fanger (1970) devised a means of estimating a predicted mean vote (PMV) based on the six characteristics above. PMV is a rating of a positive and negative scale centered at zero as optimal thermal comfort. Using the PMV, the percentage of people dissatisfied (PPD) can be predicted. But the acceptable range of comfortable temperature can be different based on local climate, culture, race, living habits, sex, age, etc. The Fanger's model is based on experimental results obtained during winter from American college-age subjects under exposures of three hours to uniform condition [Fanger, 1970]. Because of this, many researches have been carried out in different countries with different climatic zones and geographical locations [De Dear et al., 1991; Chung and Tong, 1990; Tanabe & Kimura, 1994]. Although, the results show no significant difference between comfort requirements in different climatic zones, ages, sex, and body build.

Calculating variables such as indoor air velocity, relative humidity, human clothing and activity levels brings an extended degree of sophistication to physical modelling. Another study has pointed out that it can be considered acceptable when the width of comfort zone band is within $\pm 2^{\circ}\text{C}$ of temperature set-point under the condition of no cloth changing or behavioural adjusting [Humphreys & Nicol, 2002]. Assenting to this study, Xu et al. (2008) defined overheating degree (OHD) and insufficient heat degree (IHD) to evaluate the control effectiveness of heating equipment based on room temperature. The mathematical definition of OHD and IHD are described in Equation 36 and 37, respectively.

$$OHD ({}^{\circ}\text{C} \cdot h) = \int_{t_0}^t (T_{room}(t) - T_{setpt}) dt, \quad \text{when } T_{room}(t) > T_{setpt}(t)+2 \quad (36)$$

$$IHD ({}^{\circ}\text{C} \cdot h) = \int_{t_0}^t (T_{setpt} - T_{room}(t)) dt, \quad \text{when } T_{room}(t) < T_{setpt}(t)-2 \quad (37)$$

The definition of OHD and IHD provides a direct mean for a comparison study on the control effectiveness of heating equipment based on room temperature.

It is relatively more difficult to assess the energy performance for district heating substations than for conventional heating systems. For example, fuel efficiency of a heating system is defined as the thermal energy output per fuel consumed in joules, as shown in Equation 38. For conventional heating system, fuel is converted into thermal energy on-site, and fuel input and energy output can be directly measured to calculate fuel efficiency. For district heating system, the production and consumption of thermal energy is not at the same place. Fuel is converted into thermal energy at a centralized location, and the thermal energy is consumed by a group of buildings. As a result, there is no direct, quantitative method to measure the fuel efficiency of a district heating substation.

$$\text{Fuel efficiency} = \frac{\text{thermal energy output (J)}}{\text{fuel input (J)}} \times 100\% \quad (38)$$

Based upon previous researches, the energy performance assessment of district heating substations are based on the primary loop water temperature drop across the terminal heat exchanger [Gustafsson et al., 2010; Xu et al., 2011, Henze & Floss, 2011]. This parameter is also known as the degradation of temperature difference, which is defined as the reduction of temperature difference between supply and return flow in a district heating system [Henze & Floss, 2011].

Maximizing the primary water temperature drop across district heating substations is a crucial factor in district energy system and has been cited in literature [Zsebik & Sitku, 2001; Gustafsson et al., 2010, Li & Zaheeruddin, 2007; Lauenburg & Wollerstrand, 2010]. The reasons

why it is desirable to achieve large temperature drop across district heating substations was discussed in Section 2.5. To assess the energy performance of district heating substations, the following parameter, average primary temperature drop ($\Delta\bar{T}_p$) is defined.

$$\Delta\bar{T}_p = \int_{t_0}^t (\Delta T_p(t)) dt = \int_{t_0}^t (T_{ps}(t) - T_{pr}(t)) dt \quad (39)$$

where,

T_{ps} is the primary water supply temperature (K) and

T_{pr} is the primary water return temperature (K).

Pump power used to circulate water in the secondary loop can account for significant amount of energy in a large building. For residential hydronic heating systems in single-detached houses and townhouses, small in-line circulation pumps of 1/25 to 1/20 horsepower (30 to 37W) are typically employed. The performance evaluation for pumps is described in Chapter 12 of ASHRAE handbook – HVAC Systems and Equipment. Performance curves for the small in-line pumps can be obtained from manufacturers [Taco Inc., 2009; Grundfos Inc., 2001; Armstrong Ltd., 2009; Bell & Gossett Inc., 2008] but the efficiency curves are not listed due of their small power consumption. Because of their relatively small energy consumption, pump power on the secondary loop is not considered in this study.

4.3 Simulation Results and Discussions

According to the simulation parameters outlined in Table 8, simulations were performed to investigate the impact of ratio of design-to-load, primary water supply mode, and location on indoor temperature of the thermodynamic building and primary water temperature drop at the

heat exchange terminal. Using the climatic data from Canadian Weather for Energy Calculations (2005), simulation is performed for the period from 1st of January to the 31st of May, with January to March to represent high heating load period and April to May to represent low heating load period. The simulation time-step is 5 minutes, and the simulation data is repeated in a 30-minute interval. The OHD, IHD, and $\Delta\bar{T}_p$ are calculated from the simulated results and summarized in Table 9 and 10. Discussions of the simulation results are presented in the upcoming sections.

Table 9: Simulation results for high load period from January to April

High Load Period		Toronto			Montreal			Vancouver		
RCL	Supply mode	OHD	IHD	$\Delta\bar{T}_p$	OHD	IHD	$\Delta\bar{T}_p$	OHD	IHD	$\Delta\bar{T}_p$
0.7	A	0	0	22.9	0	0	28.8	0	2056	16.8
0.9	A	0	0	25.0	0	0	29.8	0	1256	17.5
1	A	0	0	26.3	0	0	31.2	0	0	17.7
1.1	A	0	0	27.4	0	0	32.5	0	0	18.1
1.3	A	0	0	29.4	0	0	34.7	0	0	19.4
0.7	B	0	0	42.5	0	0	40.0	0	2075	48.5
0.9	B	0	0	45.7	0	0	43.4	0	1255	49.6
1	B	0	0	47.3	0	0	45.6	0	0	50.2
1.1	B	0	0	48.8	0	0	47.0	0	0	51.2
1.3	B	0	0	51.3	0	0	49.7	0	0	53.4
0.7	C	0	381	13.0	0	713	11.9	0	2056	18.6
0.9	C	0	0	14.2	0	139	13.2	0	24	19.1
1	C	0	0	14.8	0	25	13.8	0	0	19.5
1.1	C	0	0	15.5	0	0	14.3	0	0	20.1
1.3	C	0	0	16.8	0	0	15.4	0	0	21.4

Table 10: Simulation results for low load period from April to May

Low Load Period		Toronto			Montreal			Vancouver		
RCL	Supply mode	OHD	IHD	$\Delta\bar{T}_{pr}$	OHD	IHD	$\Delta\bar{T}_{pr}$	OHD	IHD	$\Delta\bar{T}_{pr}$
0.7	A	11	0	24.0	33	0	25.1	0	3	19.8
0.9	A	16	0	26.2	38	0	27.4	0	0	21.8
1	A	16	0	27.1	39	0	28.3	0	0	22.7
1.1	A	19	0	28.0	42	0	29.1	0	0	23.5
1.3	A	25	0	29.4	49	0	30.4	0	0	25.0
0.7	B	11	0	60.5	33	0	62.3	0	1	56.5
0.9	B	16	0	63.5	38	0	65.3	0	0	59.9
1	B	16	0	64.8	39	0	66.4	0	0	61.4
1.1	B	20	0	65.7	42	0	67.3	0	0	62.5
1.3	B	25	0	67.5	49	0	68.8	0	0	64.6
0.7	C	11	0	27.2	33	0	28.6	0	1	24.7
0.9	C	16	0	29.4	38	0	30.9	0	0	26.9
1	C	16	0	30.5	39	0	31.8	0	0	28.0
1.1	C	19	0	31.3	42	0	32.6	0	0	28.9
1.3	C	25	0	32.7	49	0	34.0	0	0	30.5

4.3.1 Impact of Ratio of Capacity-to-Load

During low heating load period, larger heating equipment are observed to have a higher number of OHD. This is aligned to findings from literature. With a PI controller at the heat exchange terminal, the order of magnitude in OHD is in the range of 10 to 100 $^{\circ}\text{C} \cdot \text{h}$. This is

close to the simulation study performed by Xu et al. (2008) for hot water radiator with proper TRV controls. This level of OHD is quite acceptable for indoor temperature control, as it is difficult to completely eliminate overheating during intermediate seasons. According to their study, the order of magnitude of OHD in a direct-coupled system with no TRVs can reach up to more than $10000 \text{ } ^\circ\text{C} \cdot h$ within a heating season. During low load period, all simulation cases are able to maintain consistent indoor temperature profile, see Figure 20 to 22. Oversized heating equipment by 30% (RCL 1.3) increased the OHD by 56% and 25% for Toronto and Montreal, respectively.

Simulation results show acceptable indoor condition where ASHRAE guidelines were used to calculate the design load for the heating systems. With a RCL of 1.3, a heating system did not produce an unstable indoor temperature profile. Also, hot water radiators are usually directly-coupled in older district heating systems. With a substation and an outdoor temperature compensator attached to the substation, overly hot water fed to radiator is prevented. Excessive supply water temperature is a major cause for indoor overheating phenomena [Xu et al., 2011, Tahersima et al., 2010].

In high heating load period, indoor temperature profile deviates from temperature set-point as RCL decreases. From Figure 20 and 21, it is observed that by under-sizing heating equipment to a RCL of 0.7, indoor temperature can still be maintained consistently within $\pm 2^\circ\text{C}$ of indoor temperature set-point (22°C) for the case in Toronto and Montreal. For the case of Vancouver, however, indoor temperature begins to fall outside the $\pm 2^\circ\text{C}$ range of indoor temperature set-point at RCL of 0.9 (Figure 22). At RCL of 0.7, indoor temperature falls

completely out of the $\pm 2^{\circ}\text{C}$ range of indoor temperature set-point, and has an IHD up to more than $2000 \text{ }^{\circ}\text{C} \cdot h$. Figure 23 presents the instantaneous heat transfer rate of the heating systems. For Toronto and Montreal, the instantaneous heat transfer rate is almost identical for all cases of RCL, except during peak loads for RCL 0.7. For Vancouver, the instantaneous heat transfer rate is consistently lower with RCL of 0.7 and 0.9, showing the system is unable to provide heat as a rate as needed throughout the entire simulated period. An under-sized heating system creates a more significant impact on indoor temperature for a location with warmer climate. This is counterintuitive. The reason for this is investigated in the next section where the impact of location on indoor temperature is discussed.

Primary water temperature drop (ΔT_{pr}) is observed to increase with RCL based on all simulation cases performed at both high and low heating load periods. Figure 24 and 25 present the profiles of primary water temperature drop with different RCLs. The figures show consistent trends of higher RCL resulting in a higher primary water temperature drop. This is because with a larger heat transfer area, same amount of heat can be transferred with a lower flow rate. With a lower flow rate, heat transfer coefficient is also decreased, but water is allowed longer time inside the heat exchanger (or radiator), transferring more energy per unit of volume. As a result, a higher temperature drop is achieved. This does not mean equipping a bigger size heating system leads to better performance, because larger system increases overheating phenomena during intermediate seasons. The amount of increase in primary temperature drop is also bounded to diminish with larger size of heating system. The relationship of diminishing return between primary temperature drop and RCL can be further explored in future studies.

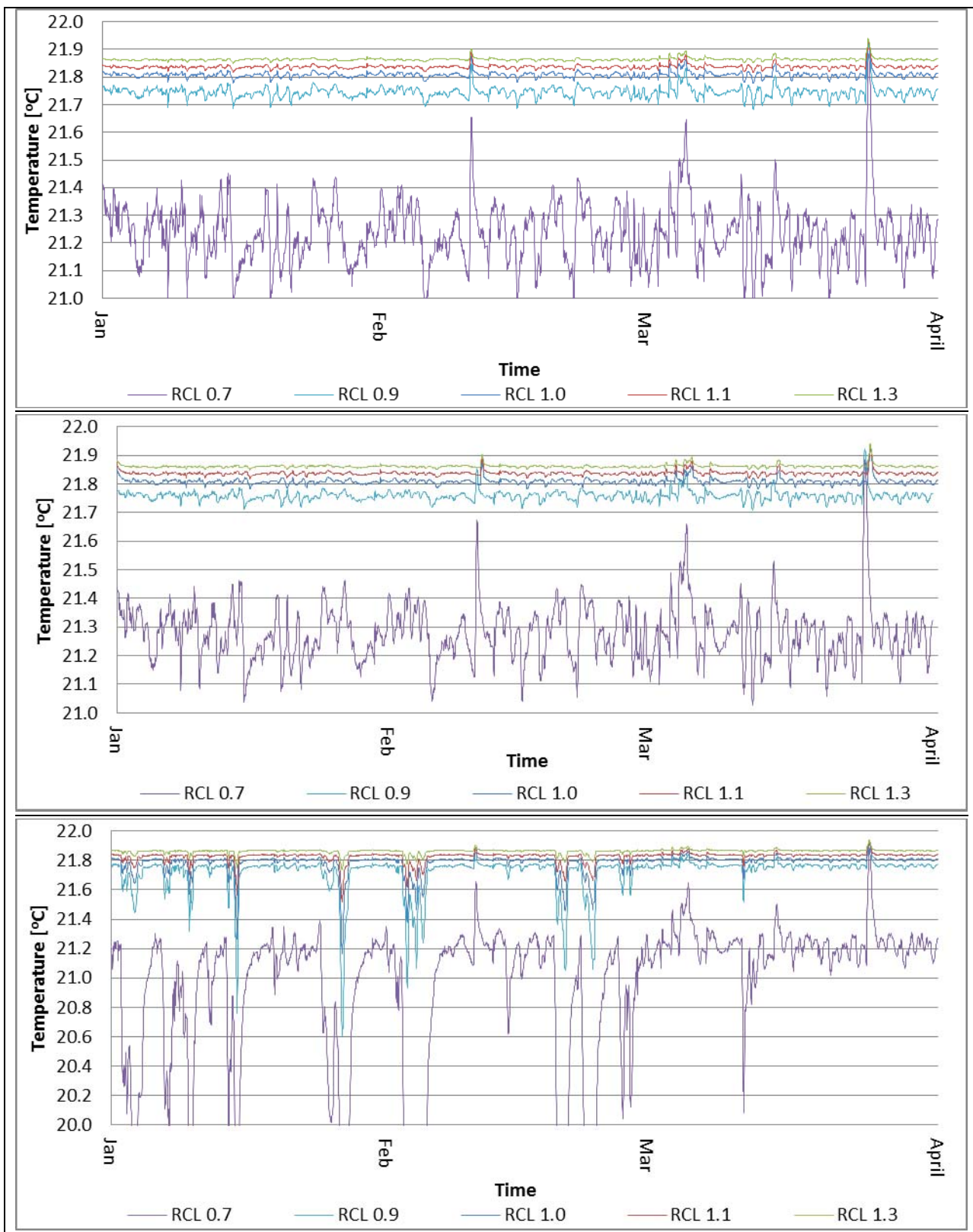


Figure 20: Simulated indoor temperature with different RCL for Toronto during high heating load period with primary supply mode A (top), primary supply mode B (middle) and primary supply mode C (bottom)

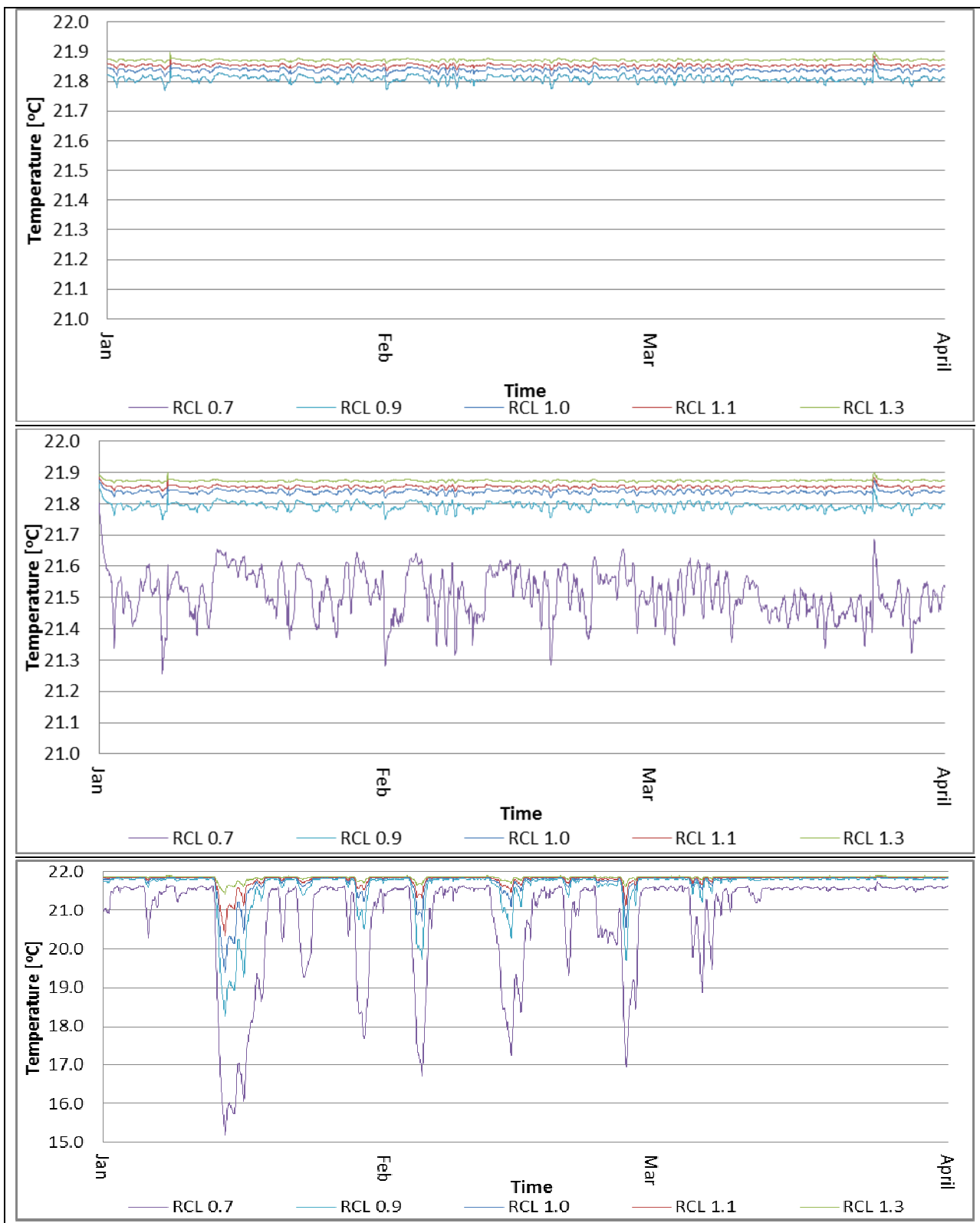


Figure 21: Simulated indoor temperature with different RCL for Montreal during high heating load period with primary supply mode A (top), primary supply mode B (middle) and primary supply mode C (bottom)

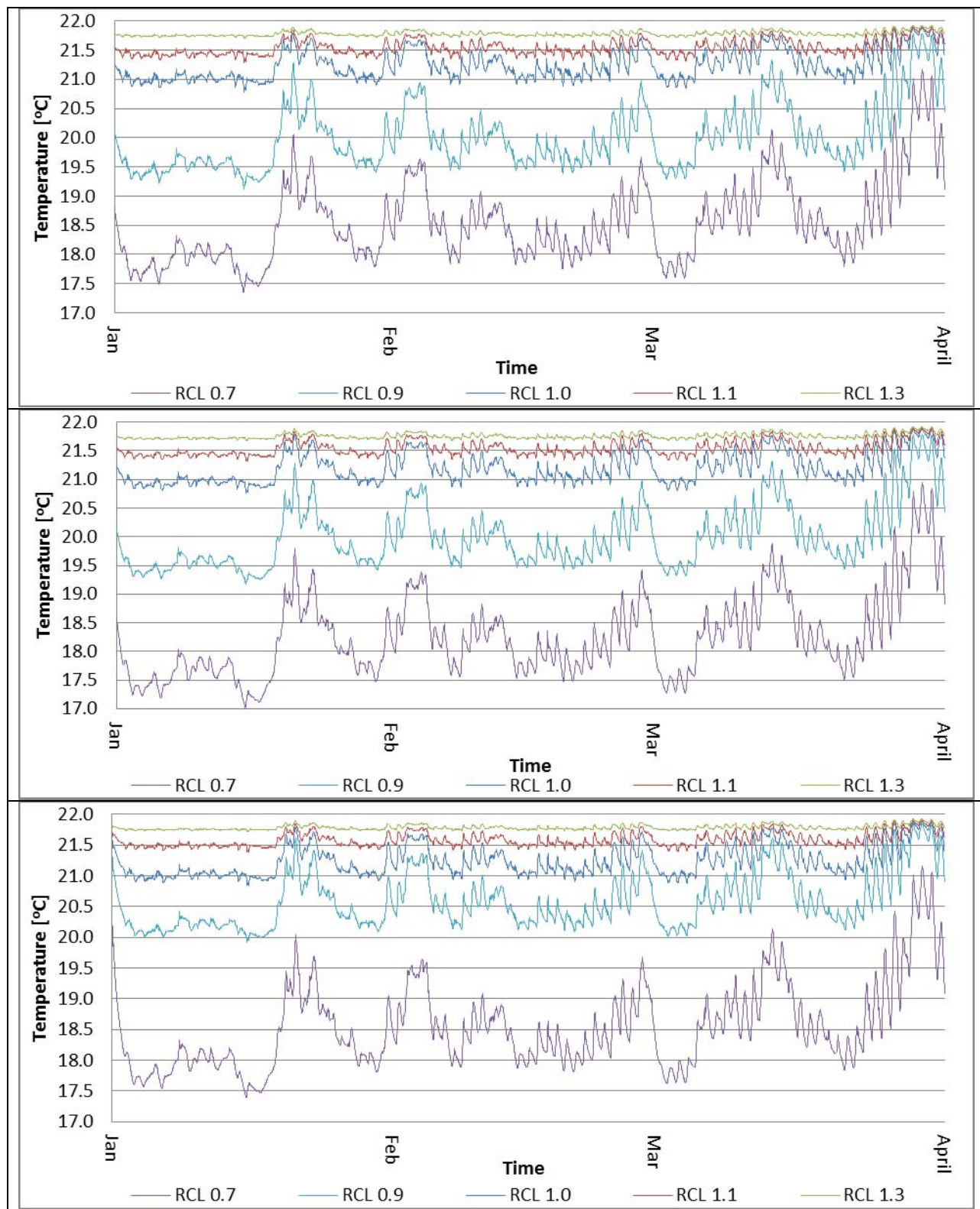


Figure 22: Simulated indoor temperature with different RCL for Vancouver during high heating load period with primary supply mode A (top), primary supply mode B (middle) and primary supply mode C (bottom)

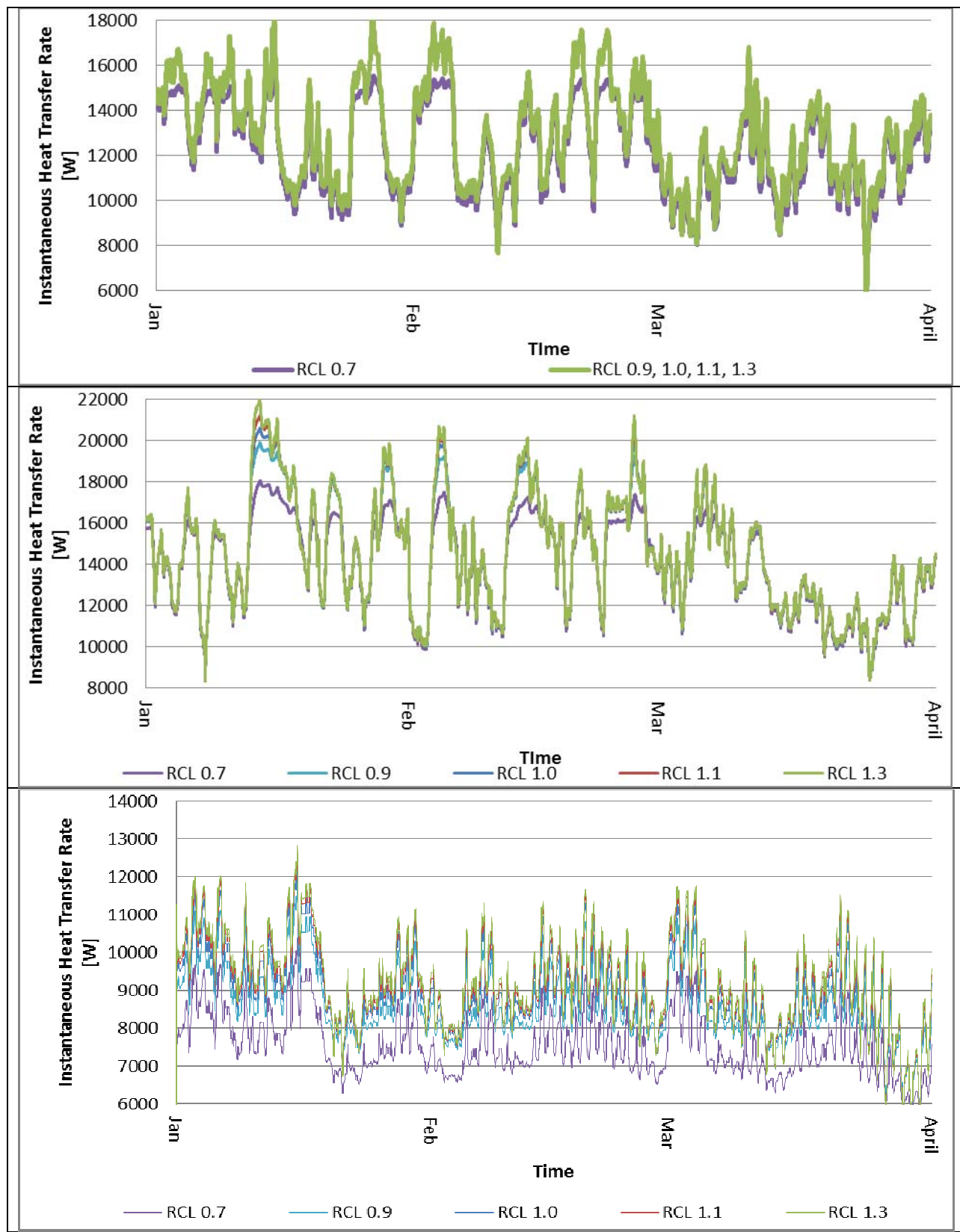


Figure 23: Simulated instantaneous heat transfer rate with different RCL during high heating load period with primary supply mode C for Toronto (top), Montreal (middle) and Vancouver (bottom)

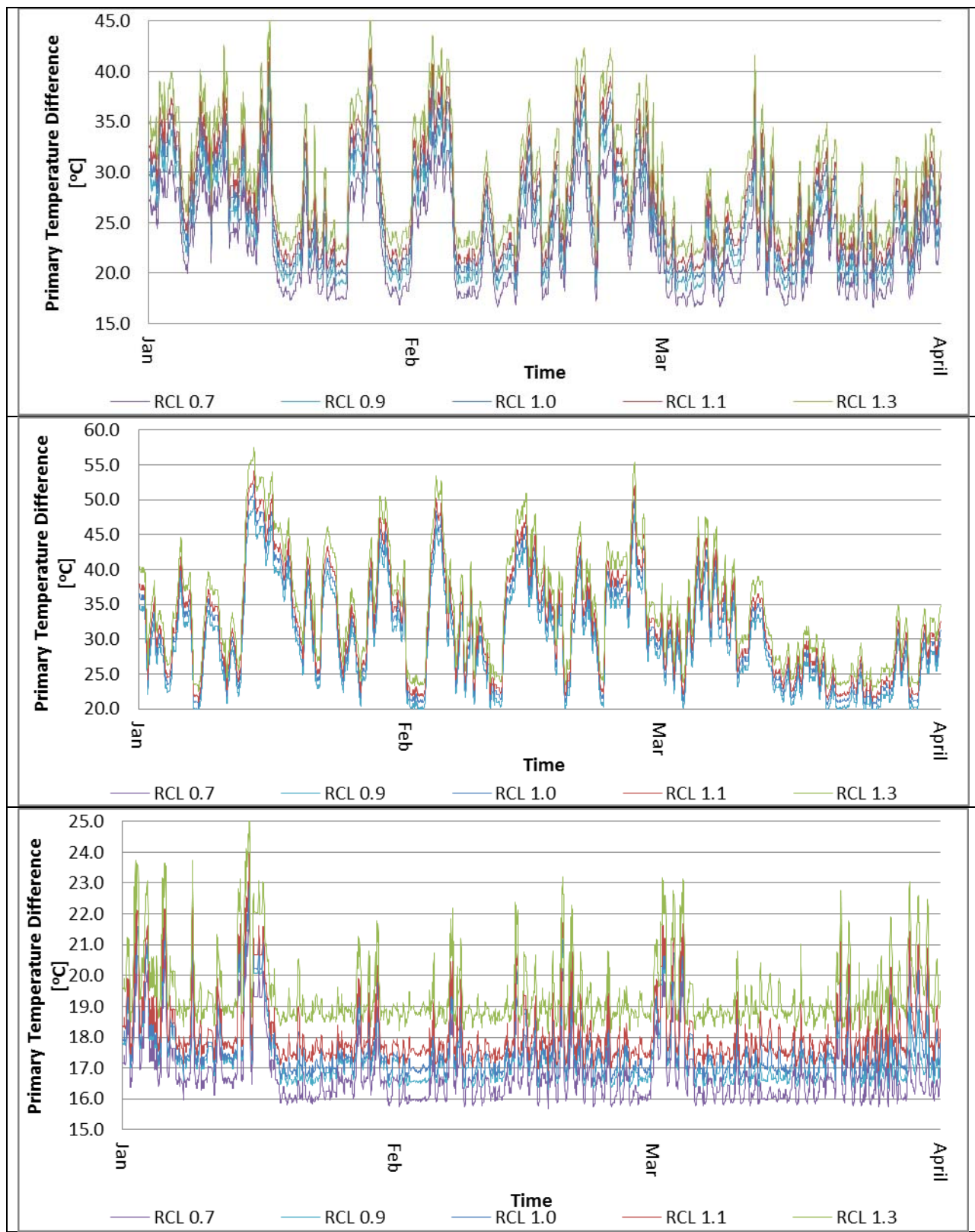


Figure 24: Simulated primary water temperature drop with different RCL during high heating load period with primary supply mode A for Toronto (top), Montreal (middle) and Vancouver (bottom)

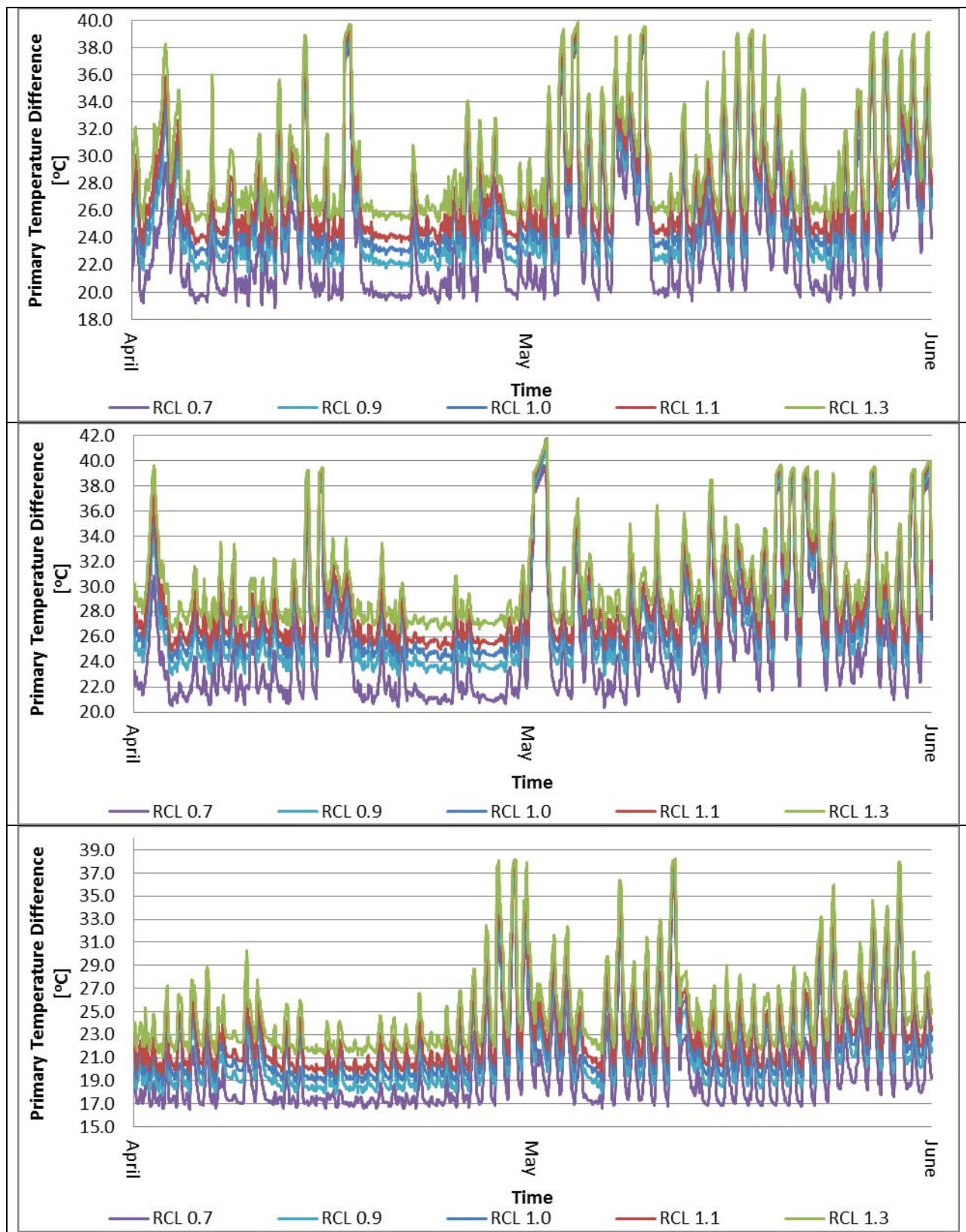


Figure 25: Simulated primary water temperature drop with different RCL during low heating load period with primary supply mode A for Toronto (top), Montreal (middle) and Vancouver (bottom)

4.3.2 Impact of Climatic Locations

Based on simulation results, heating system with a lower RCL has a stronger impact on operation performance in Vancouver than in Toronto and Montreal. Heating systems with RCL of 0.7 were able to provide sufficient heating in Toronto and Montreal except during peak load periods, but for Vancouver, it is unable to provide sufficient heating throughout the entire heating season. It is seemingly contrary that an under-sized heating system creates a more significant impact on indoor temperature for a location with warmer climate. This contradictory phenomenon is caused by the outdoor temperature compensator at the district heating substation.

Recall that the secondary supply temperature is controlled by the outdoor temperature compensator using the secondary supply temperature curve shown in Figure 5. Because of the warmer climate in Vancouver comparing to Toronto and Montreal, the outdoor temperature compensator has a lower temperature set-point for hot water supplied to radiator. Figure 26 and 27 are plots of outdoor temperature and the corresponding secondary supply temperature set-point for Toronto, Montreal and Vancouver. It is observed that the district heating substation supply a lower temperature to the secondary loop because of the higher outdoor temperature in Vancouver. The temperature difference between radiator supply temperature and indoor temperature is the driving force for heat transfer between the secondary loop and indoor environment. As a result, the control system attempts to meet the required heating load by increasing the secondary flow rate. However, the water flow rate can only be increased up to a limit in valves and pipes. As observed in Figure 28, the secondary flow rate increases as

RCL increases, but it is not able to increase its flow rate beyond the limit of the thermostatic radiator valve, at 0.42 kg/s.

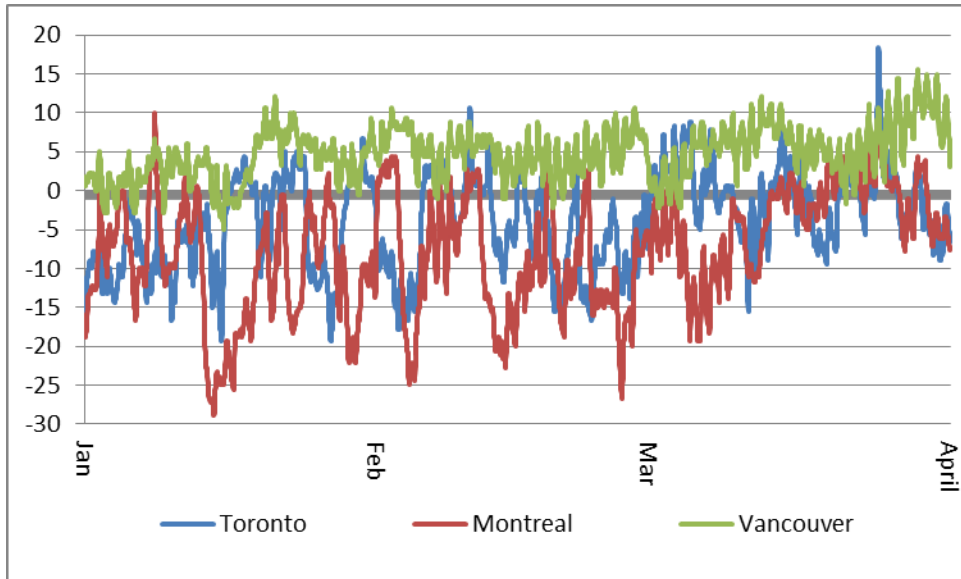


Figure 26: Plot of outdoor temperature for Toronto, Montreal and Vancouver

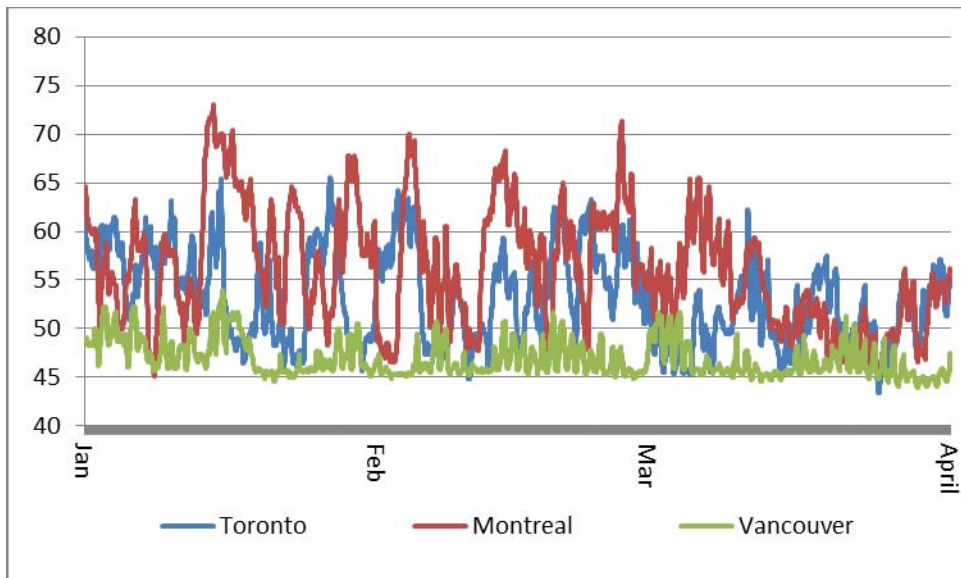


Figure 27: Plot of secondary temperature set-point for hot water radiator

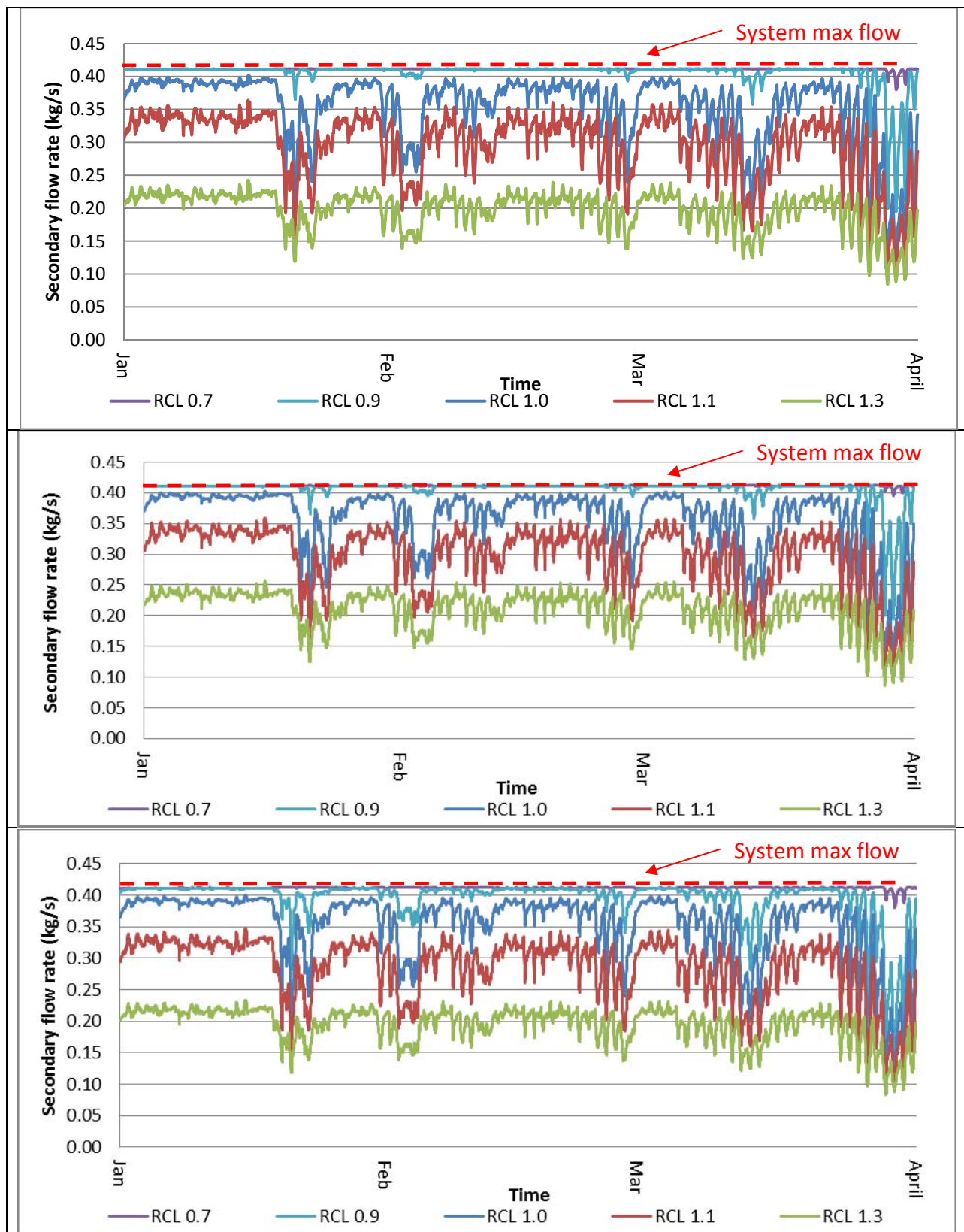


Figure 28: Simulated secondary flow rate at different RCL for Vancouver during high load period with primary supply mode A (top), primary supply mode B (middle), and primary supply mode C (bottom)

To overcome this design problem, one can employ larger sized pipelines and valve to allow higher flow. An alternative method is to skew the secondary supply temperature curve, for example, by 20% as shown in Figure 29. This will increase the temperature difference and thus, increase the heat transfer rate.

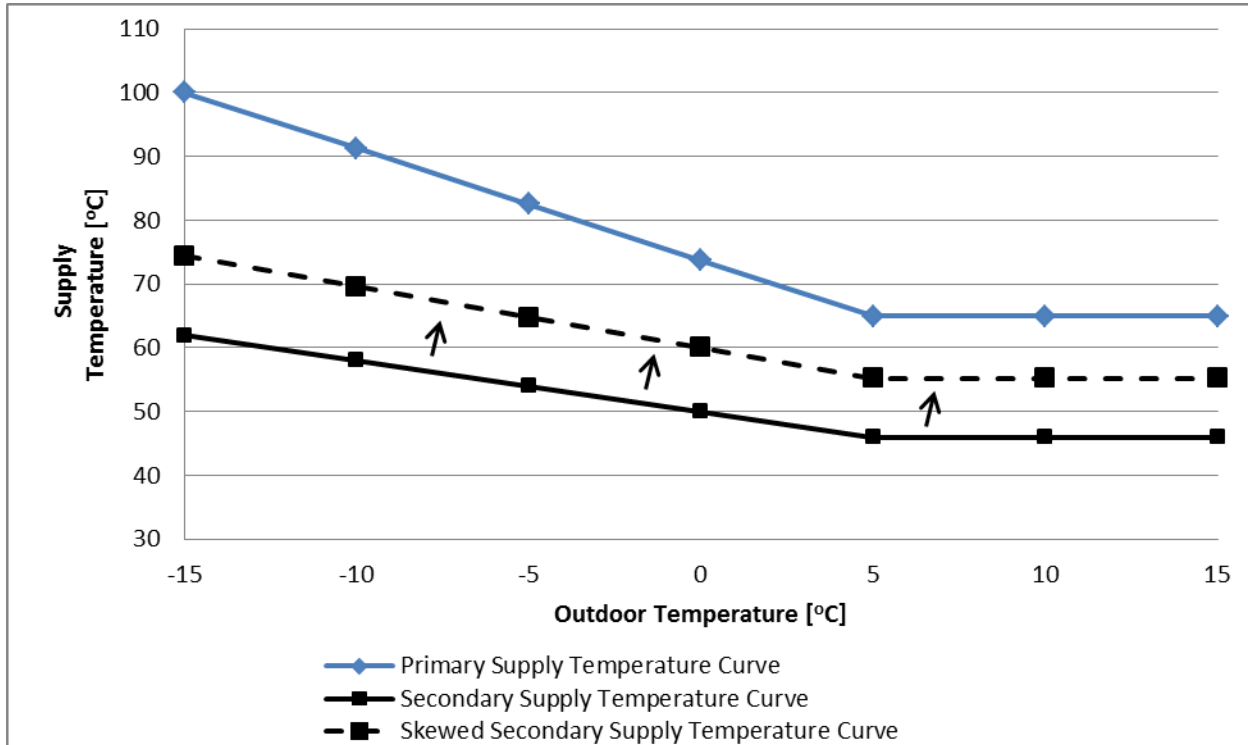


Figure 29: Radiator system control curve based on outdoor temperature

Simulation is performed to verify this solution, using a primary water supply temperature of 70°C in Vancouver with a RCL of 0.7 for the heating equipment. The results indicate that indoor temperature can be properly maintained, as shown in Figure 30. There are zero IHD throughout the entire simulated, high load period. The trade-off is a much higher primary flow rate and lower primary temperature drop, see Figure 31 and 32. The average decrease in primary water temperature drop is about 9°C. Recall that previous study has

suggested that a ΔT of 10°C in a district heating system can result in an approximately 55% difference in required pumping power, and a fuel efficiency difference up to 14% [Persson, 2005]. Higher primary flow rate and lower primary water temperature drop are obviously not desirable. It is more favourable to equip a heating system with an appropriate RCL at the design stage, or a system with high heat transfer area such as radiant floor heating.

This suggests that when designing heating systems connected district heating systems for different climate, appropriate sizing and secondary supply temperature curve are important to achieve desirable performance. It should also be noted that by carefully changing operation parameters, even an undersized heating system can still provide satisfactory indoor temperature.

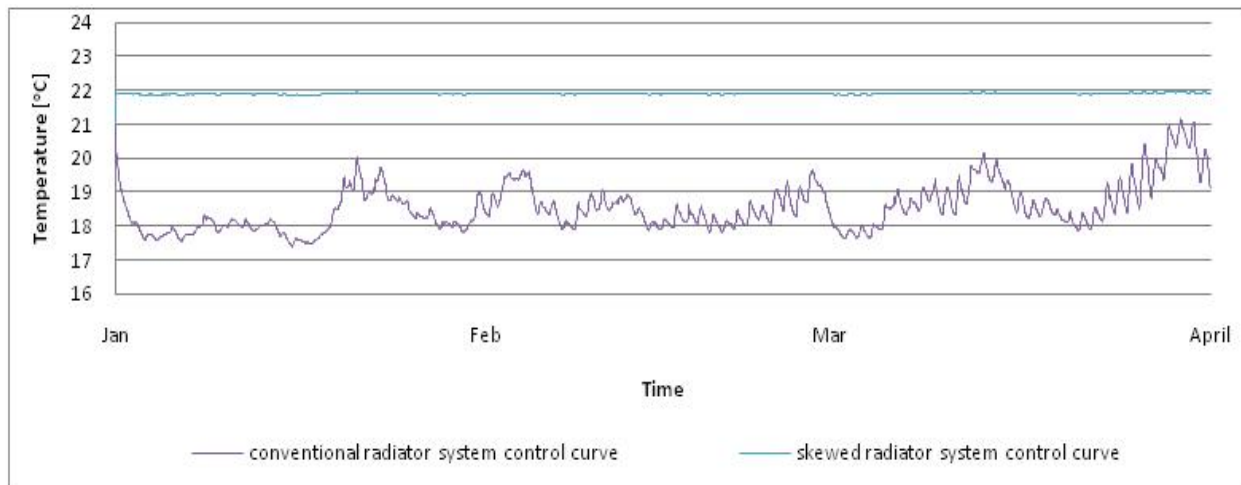


Figure 30: Simulation of indoor temperature for a heating system with a RCL of 0.7 in Vancouver

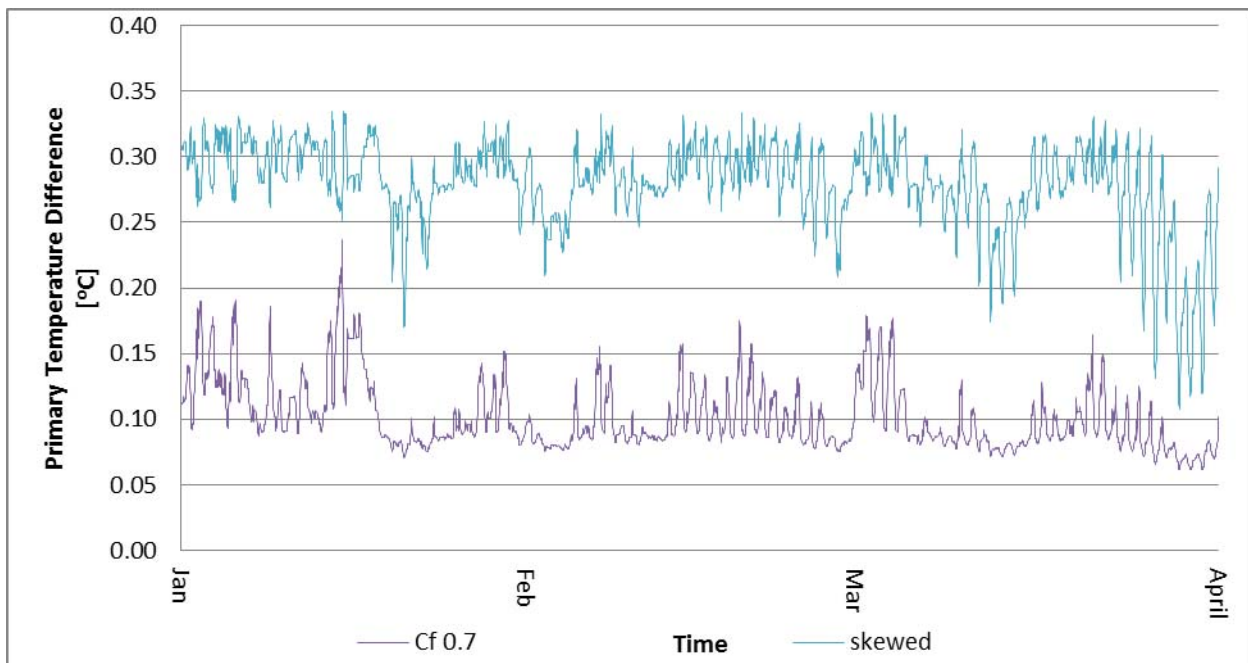


Figure 31: simulation of primary mass flow rate for a heating system with a RCL of 0.7 in Vancouver

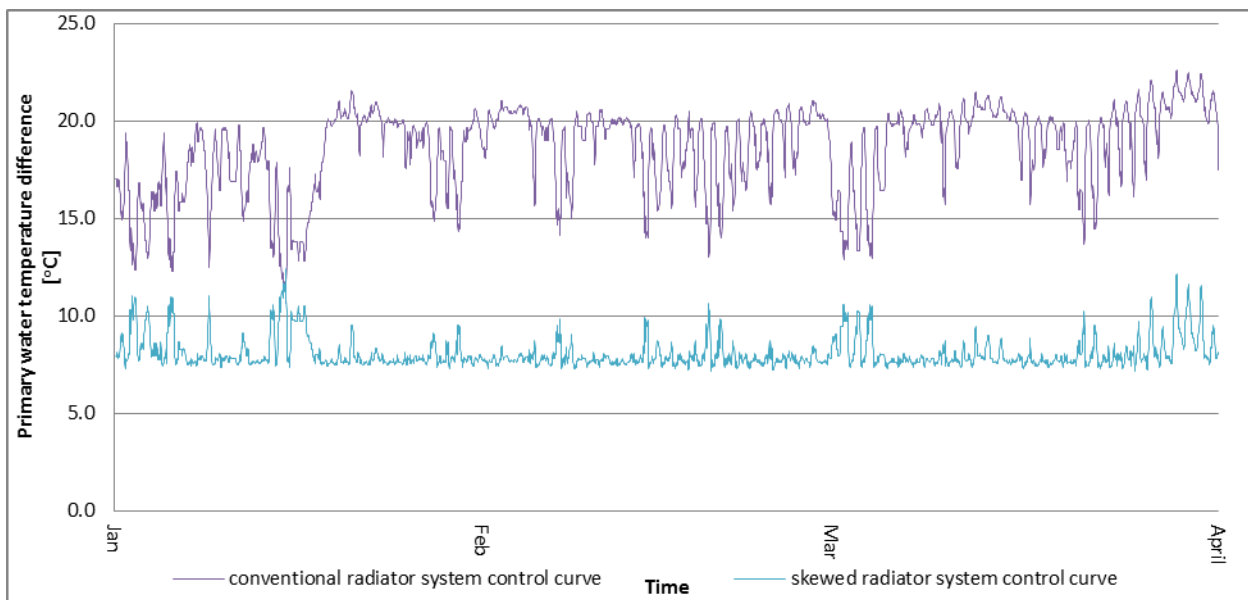


Figure 32: simulation of primary return temperature for a heating system with a RCL of 0.7 in Vancouver

4.3.3 Impact of Primary Water Supply Modes

In this section, the impact of three common primary water supply modes on the performance of a residential single-detached house is investigated. Note that the optimal

primary water supply mode is largely dependent on the operation mode of the centralized plant. Typically, centralized production plant supplies water at a temperature range that would yield the best production efficiency. As a result, this analysis is not meant to determine the optimal primary water supply mode for Canadian residential houses, but to obtain a better understanding on how district heating end-users in Canada would perform under different primary water supply modes.

Table 10 shows that heating systems with a RCL of 1.0 are able to maintain acceptable indoor conditions with all primary water supply modes, except for Montreal, where underheating is observed with a primary supply mode C. At RCL of 0.7, underheating was observed to at all locations with primary supply mode C. Based on the simulation results, comparisons of indoor temperature profiles with different primary water supply modes at RCL of 1.0 and 0.7 were generated and presented in Figure 33 and 34, respectively. From the figures, it was observed that primary supply mode A and B lead to similar indoor temperature profiles for Toronto and Montreal, while indoor temperature profiles are consistent regardless of primary supply temperature modes for Vancouver. With a RCL of 0.7, the temperature profile generated by primary supply mode C for Toronto and Montreal often falls outside the acceptable range of comfortable indoor temperature ($22\pm2^{\circ}\text{C}$).

Figure 35 shows the instantaneous heat transfer rate at the heat exchanger with RCL 1.0 and 0.7 with primary supply mode C for the model house in Toronto. It can be observed that even with an RCL of 1.0, primary supply mode C fails to meet heating demand. The same can be observed in Montreal as depicted in Figure 35. With a lower primary water supply

temperature, the temperature drop across the heat exchanger at the district heating substation is too low. Therefore, primary supply mode C is not suitable for Toronto's and Montreal's climate as it cannot provide sufficient heat transfer potentials at substations to meet heating load demand.

Table 9 indicates that primary supply mode C provided a higher average primary water temperature drop than primary mode A, which is not observed in the cases for Toronto and Montreal. This is because primary supply mode A adjusts the primary water supply temperature according to outdoor temperature. Figure 36 shows the primary water supply temperature profiles with primary supply mode A and C. It was observed that primary water supply temperature with primary supply mode A is frequently below the primary water supply temperature with primary supply mode C. Nonetheless, both primary modes are able to provide sufficient heating with heating systems at an RCL of 1.0. Looking at their respective primary flow rate in Figure 37, primary supply mode A provides a more stable profile throughout the entire simulated period. This may be more advantageous for pump operation because it can allow pumps to more frequently operate at a range with higher efficiency.

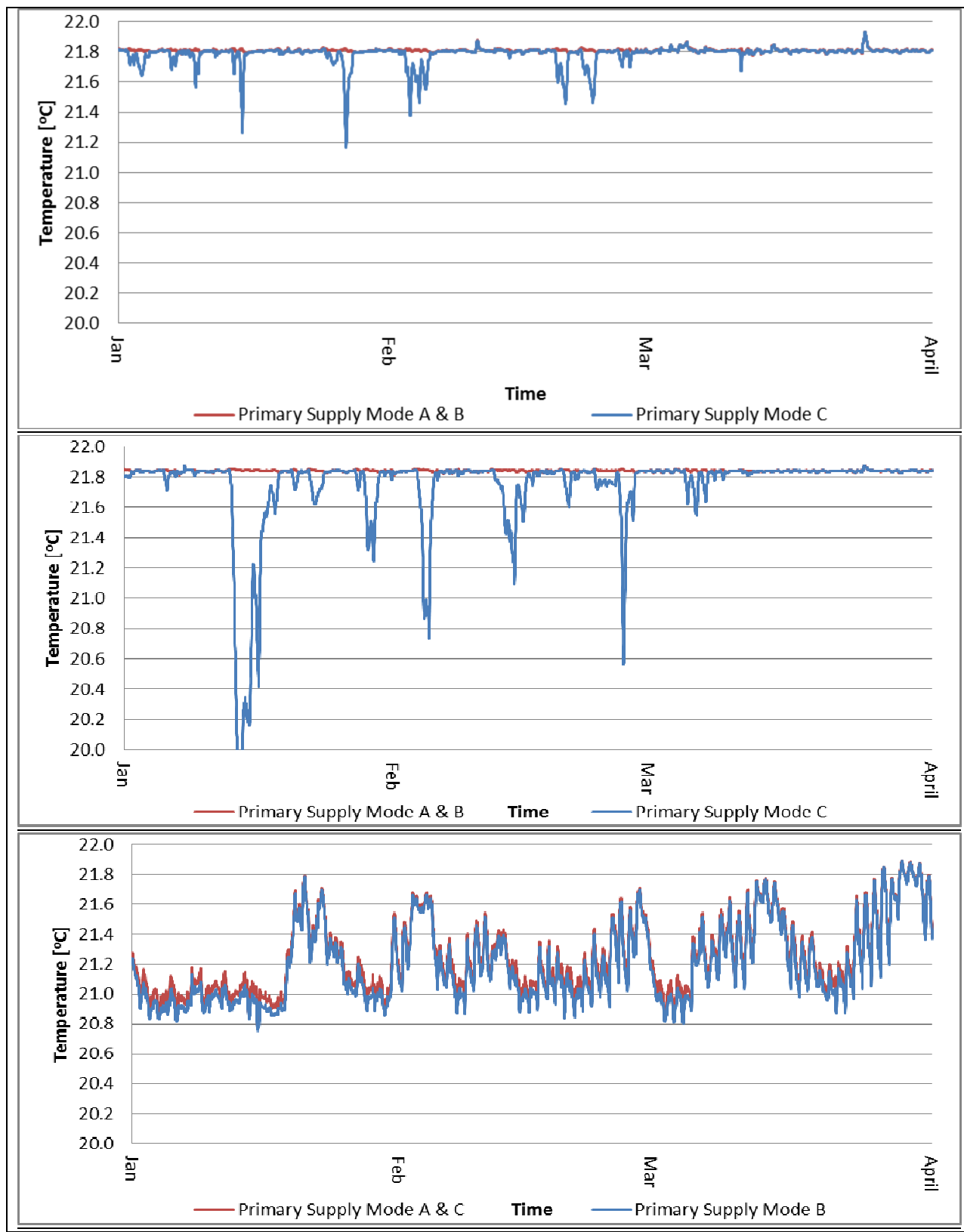


Figure 33: Simulated indoor temperature with different primary supply modes at RCL of 1.0 during high heating load period for Toronto (top), Montreal (middle) and Vancouver (bottom)

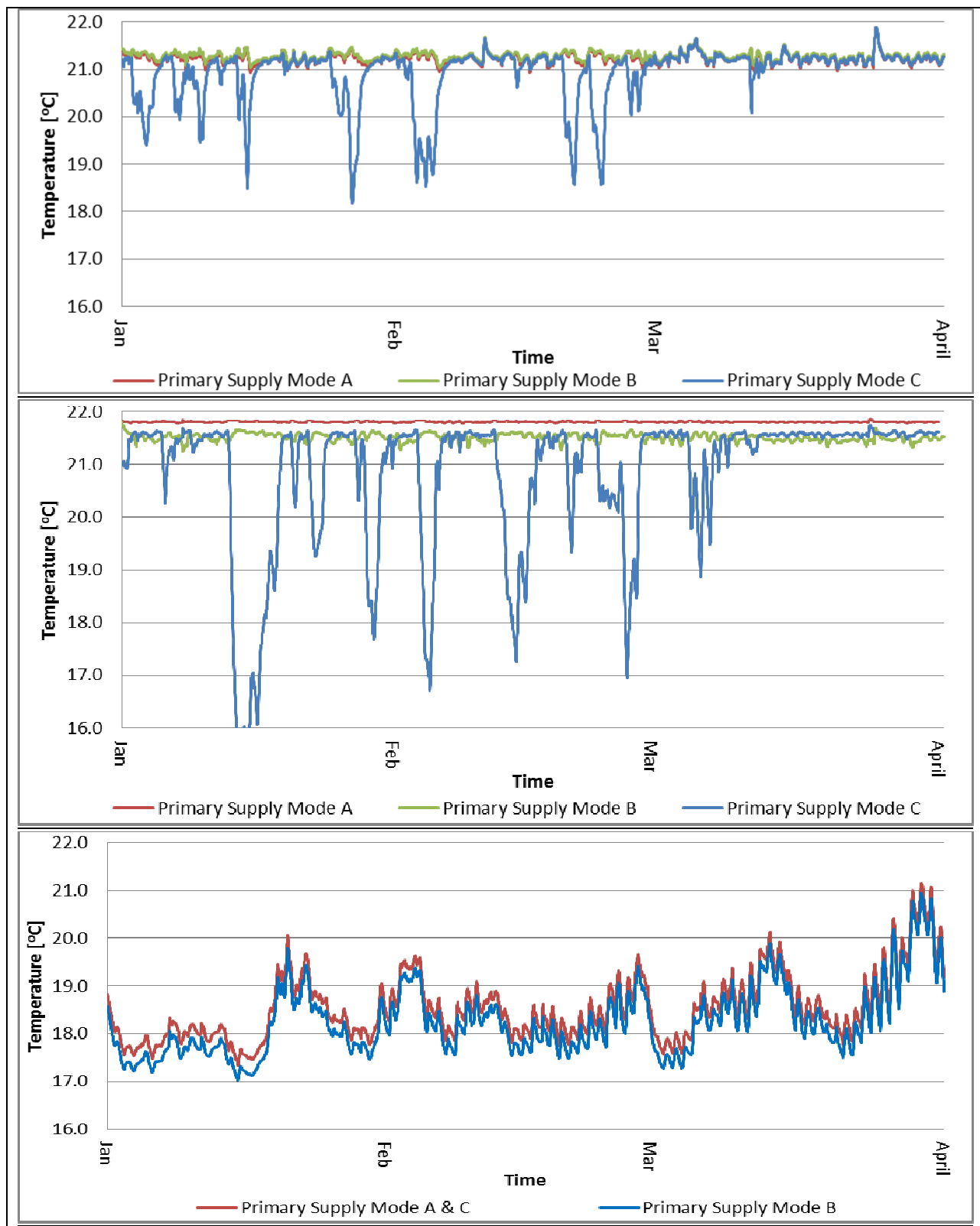


Figure 34: Simulated indoor temperature with different primary supply modes at RCL of 0.7 during high heating load period for Toronto (top), Montreal (middle) and Vancouver (bottom)

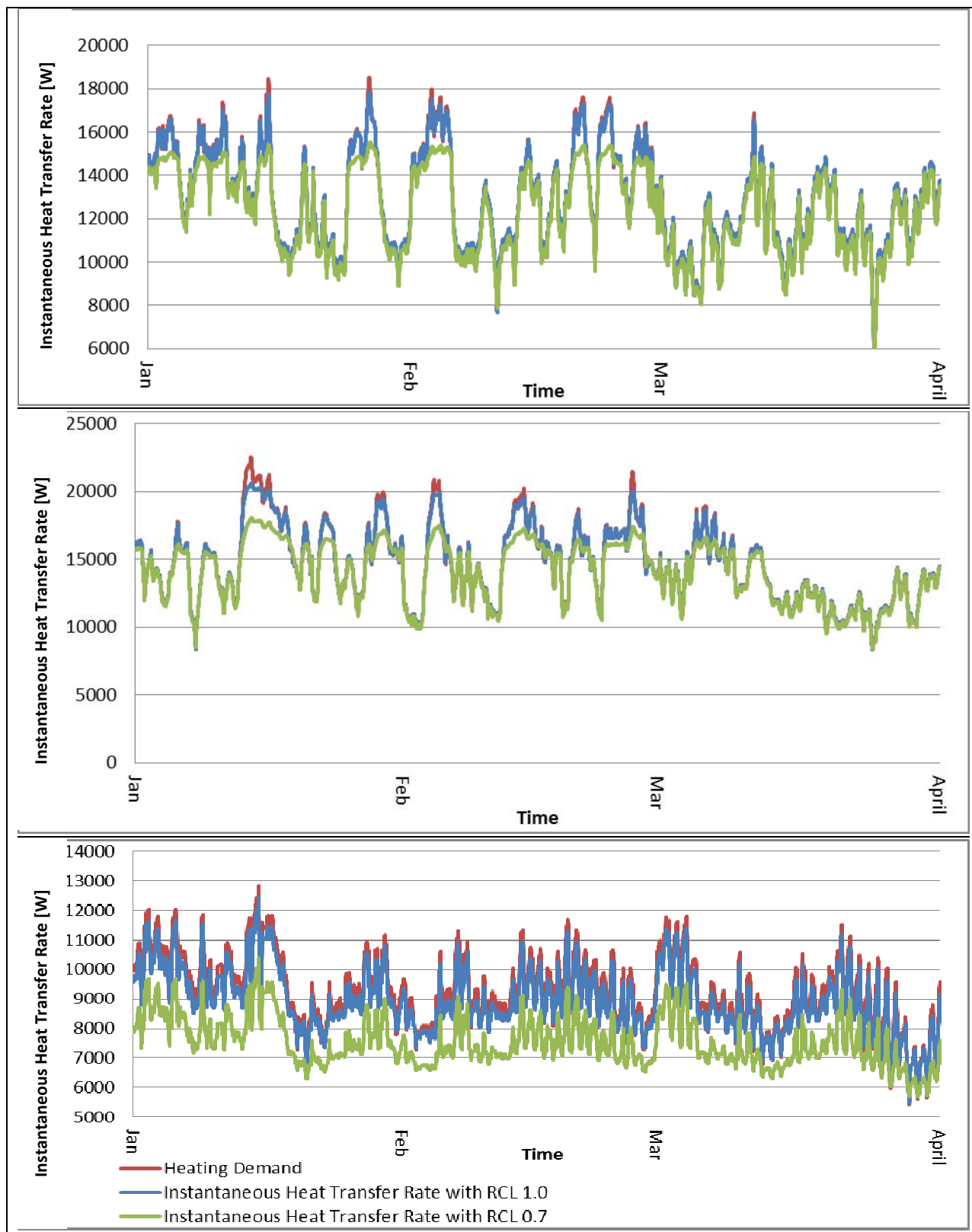


Figure 35: Simulated heating demand and instantaneous heat transfer rate with RCL of 1.0 and 0.7 with primary supply mode C for Toronto (top), Montreal (middle) and Vancouver (bottom)

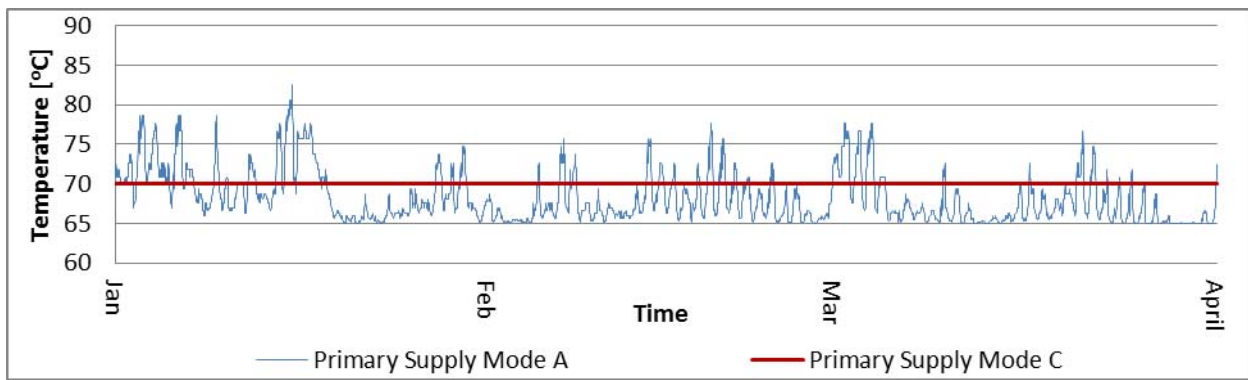


Figure 36: A plot of primary water supply temperature for Vancouver with supply mode A and C

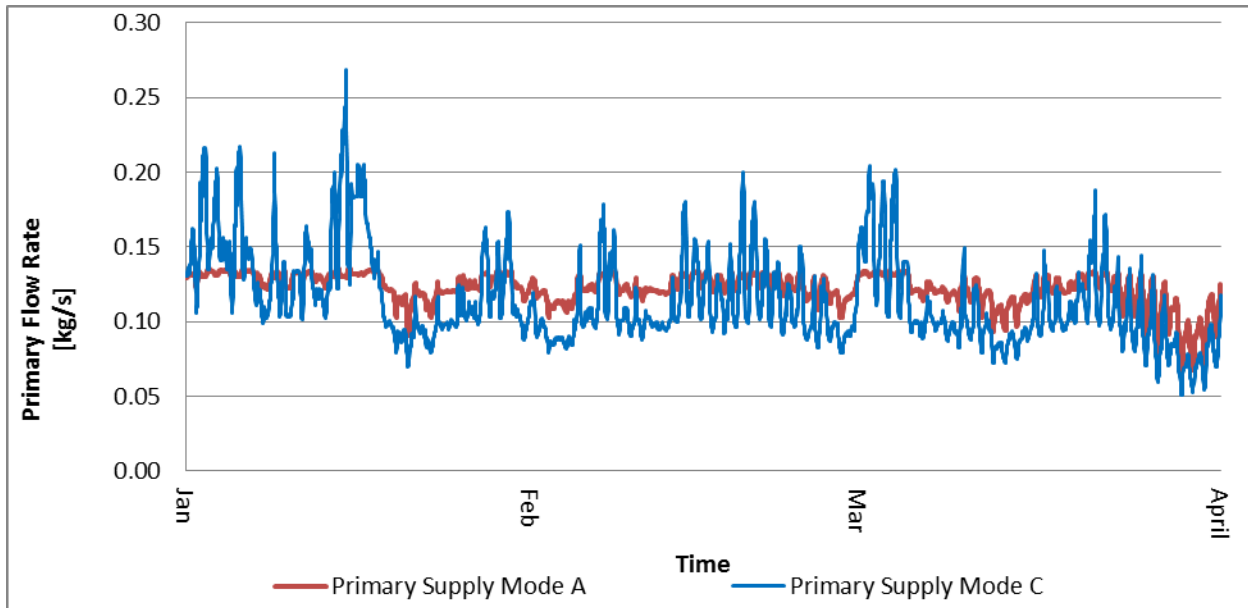


Figure 37: A plot of primary water flow rate for Vancouver with supply mode A and C

4.4 Concluding Remarks

In this chapter, the performance of a single-detached residential house is simulated at three different climatic locations, five different ratios of capacity-to-load, and three different primary supply schemes. Simulation results are presented to demonstrate the capability of the simulation model developed. The operation and thermodynamic behaviour of district heating substation, a residential single-detached house and its heating equipment are better

understood. A total number of 45 simulation cases are performed. The simulation results show that:

- A heating system with a larger RCL will result in a higher primary temperature drop, reducing primary and secondary flow rate, without creating unacceptable indoor temperature during high load period.
- With a 30% increase in the size of heating equipment, OHD is increased by 56% and 25% during intermediate season for Toronto and Montreal respectively.
- When designing heating systems connected district heating systems for different climate, suitable secondary supply temperature curve is important to achieve effective performance.
- Insufficient heating caused by an undersized heating system can be remediated by changing the control parameters, for example, by skewing the radiator supply control curve. The trade-off is a higher primary return temperature and higher primary and secondary flow rate. It is more desirable to accurately size heating system to maximize primary ΔT and reduce primary flow rate.
- Primary water supply mode C (constant supply temperature at 70°C) is not suitable for residential homes in Toronto and Montreal, which has a colder climate than Vancouver. With this primary supply mode, heating system with a RCL of 0.7 fails to provide satisfactory indoor temperature for all three climatic locations.
- Primary water supply mode A is able to provide a more stable profile of primary water flow rate. This may be advantageous for pump operation optimization.

- Having an oversized system may incur more OHD during low load period, but it can also induce a lower average primary return temperature.

The simulation model developed is a useful tool that can be used to evaluate different design parameters and control strategies for a heat exchange terminal in different climatic conditions, and with different size of buildings. In the next chapter, the simulation model will be used to evaluate a new control strategy on heat exchange terminal under the context of Canadian's climate.

5. Improving the Performance of District Heating Substation

5.1 Introduction

In the previous chapter, the performance of a district heating substation connected to residential single-detached house is simulated with different size of heating equipment and primary supply schemes. Through this work, the performance of a Canadian residential house connected to district heating under different design and operation parameters is better understood. In this chapter, a new control strategy is proposed to optimize the energy performance of district heating system. Using the simulation model, the proposed control strategy is compared with conventional control method. The objective is to quantitatively evaluate the performance improvement of the new control strategy.

5.2 Previous Researches

Throughout the past decades, there have been many researches that had proposed different approaches to optimize district energy system, for example, developing a mathematical model to select primary supply water temperature for minimal operational costs [Benonysson et al., 1995], using the thermal mass of the district heating system to adjust heat output in order to enhance plant operation efficiency [Lin & Yi, 2000], energy optimization of distribution pump operation [Indenbirken et al., 1995], improving the accuracy of predicting primary loop transport delay [Zhao et al., 1995; Li & Zaheeruddin, 2004], using alternative fuel type [Bahadorani et al., 2009; Nijjar et al., 2009] and using exergetic analysis [Ertesvag, 2007; Snoek & Kluiters, 2010]. Many of these researches, however, used a perspective of the centralized production plant, and used groups of large buildings as their study subjects.

Li and Zaheeruddin (2007) had proposed the use of six different hybrid fuzzy logic control strategies to regulate primary supply water temperature in a direct-coupled district heating system. Simulation results indicated that, with the proposed hybrid fuzzy logic control strategies, better zone temperature control in buildings is attained, distribution pumping cost is decreased and up to 17% of energy saving can be achieved.

Xu et al. (2008) developed a simulation model using Matlab Simulink to extensively study the control effectiveness of thermostatic radiator valves (TRVs) in direct-coupled district heating systems. The simulation includes a hydraulic model that considers the hydraulic coupling between consumers. Results showed that TRVs can significantly reduce overheating phenomena caused by an excessive supply water temperature and radiator area. However, it could not eliminate the phenomena of overheating entirely. It was suggested that low system flow rate can easily leads to control difficulties of TRVs. Control strategies of hourly and daily adjustment on supply water temperature were proposed and simulated. The idea is that the change in system flow rate can be a good representation of changes in room temperature and heating load. This means that taking the change in system flow rate as feedback and adjusting the supply water temperature can better accommodate the changes in the system head demand and thus can keep the system flow rate within appropriate range. Simulated results shows that the proposed control strategies can reduce overheating degree, reduce pump power consumption, and control the fluctuation range of the system flow rate within 50 to 100% of design flow rate, but it did not result in any evident difference in TRV control effectiveness. It is concluded that it is not necessary to adjust the primary supply water temperature too precisely because of the inertia influence of the DHS and buildings.

Performance improvement includes better controls of indoor environment. Literature had reported that it is common to observe unstable oscillation of indoor temperature at part load conditions for homes using hydronic radiators [Tahersima et al., 2010, Andersen et al., 2000]. To overcome this problem, an adaptive control that utilizes a controller gain scheduling can be employed [Tahersima et al., 2010] or using an advanced pump control that estimates the position of thermostatic radiator valve (TRV) so that it operates in a suitable area [Andersen et al., 2000]. These studies, however, focused only on the elimination of temperature oscillation and did not account for the energy consumption or return water temperature.

Many studies investigated the performance optimization of district heating substations by focusing on minimizing primary return water temperature. Zsebik and Sitku (2001) analyzed different connection schemes of heat exchangers in a district heating substations and their effects on return water temperature. Gustafsson et al. (2010) proposed a new control strategy to adjust the temperature set-point of hot water supply to radiator based on primary supply temperature. Based upon simulation results, the proposed control strategy is able to achieve up to 10% increase in primary water temperature drop. When applied to all residential homes, the proposed control strategy can achieved significant amount of collective savings.

The guidelines from Euroheat & Power (2008) stated that lower return temperature can be obtained by varying system flow according to system loading. Frederiksen and Wollerstrand (1987) analyzed three different types of operation modes for district heating substations, and discussed the idea of lowering radiator supply temperature and reducing water flow rate in the secondary loop. By reducing flow rate in the secondary loop, primary return temperature is

affected differently at low, medium and high heat load conditions. At low heat load, primary return temperature increases from reduced secondary flow rate. At high heat loads, the reduction in primary return temperature is depended strongly on the size of heat exchanger. With an ordinarily-sized heat exchanger, a secondary flow reduction is detrimental to the primary return temperature. In other literature, control of secondary flow rate by using variable speed pump was proposed but was claimed to be difficult to predict and control with varying pressure difference [Langendries, 1988; Petitjean, 1995].

Lauenburg and Wollerstrand (2010) presented a method of adaptive control of the radiator system to obtain a lowest possible return temperature. This idea originated from heat exchangers and radiator systems are often oversized due to safety margins. This fact renders it possible to reduce return water temperature. Lower return water temperature is achieved by operating with an optimal combination of radiator circuit supply temperature and circulation flow rate. When determining the optimal combination of operation parameters, however, the existing control system is not considered. In other words, the constraints of the system on controllable variables are not considered in determining the optimal operation parameters.

5.3 Theory

With the current control system, hot water temperature supplied to radiator is regulated by the controller at district heating substation according to outdoor temperature. With a terminal heat exchanger, there is regulation on the water temperature supplied to radiator. This results in less frequent secondary flow rate fluctuation and a more stable indoor temperature when comparing to a directly-coupled district heating system.

Literature have suggested that choosing an appropriate combination of flow rate and supply water temperature can lead to better operation performance of a district heating system [Euroheat & Power, 2008; Lauenburg & Wollerstrand, 2010]. Figure 38 displays the relationship between secondary supply temperature and secondary flow rate for a given system under different outdoor temperature. The curves show that a lower secondary supply temperature can be used to satisfy a given heating demand with a higher secondary flow, and vice versa.

Conventionally, the controller at the district heating substation does not control the secondary flow rate. The secondary flow is self-regulated by the TRV to maintain comfortable indoor temperature. Actively controlling both the secondary flow rate using a variable speed pump and secondary supply temperature was shown to be difficult and added a great deal of complexity to the control algorithm [Langendries, 1988; Petitjean, 1995]. From the simulation study in the previous chapter, it was observed that the control curve of secondary supply temperature can be adaptively adjusted to meet a given heat demand, and results with a different secondary flow rate. In other words, the secondary flow rate can be indirectly manipulated by adjusting the secondary supply temperature control curve.

For a given heating demand, it may be more advantageous to operate with a higher secondary flow rate and a lower secondary supply temperature. Because a lower radiator supply temperature can induce a larger temperature difference between primary supply temperature and secondary supply temperature at the substation's heat exchanger, resulting in a lower primary return temperature. The hypothesis is that by adaptively adjusting the control

curve of secondary supply temperature according to secondary flow rate, a lower primary water return temperature can be achieved. The underlying assumption is that the system has the potentials for secondary flow rate to be increased. This assumption is generally valid because heating systems are designed for extreme climate conditions and should operate frequently at conditions lower than their design conditions. Based on the simulation results, it was observed that the secondary flow rate is frequently operating at a value much lower than the design value, shown in Figure 39.

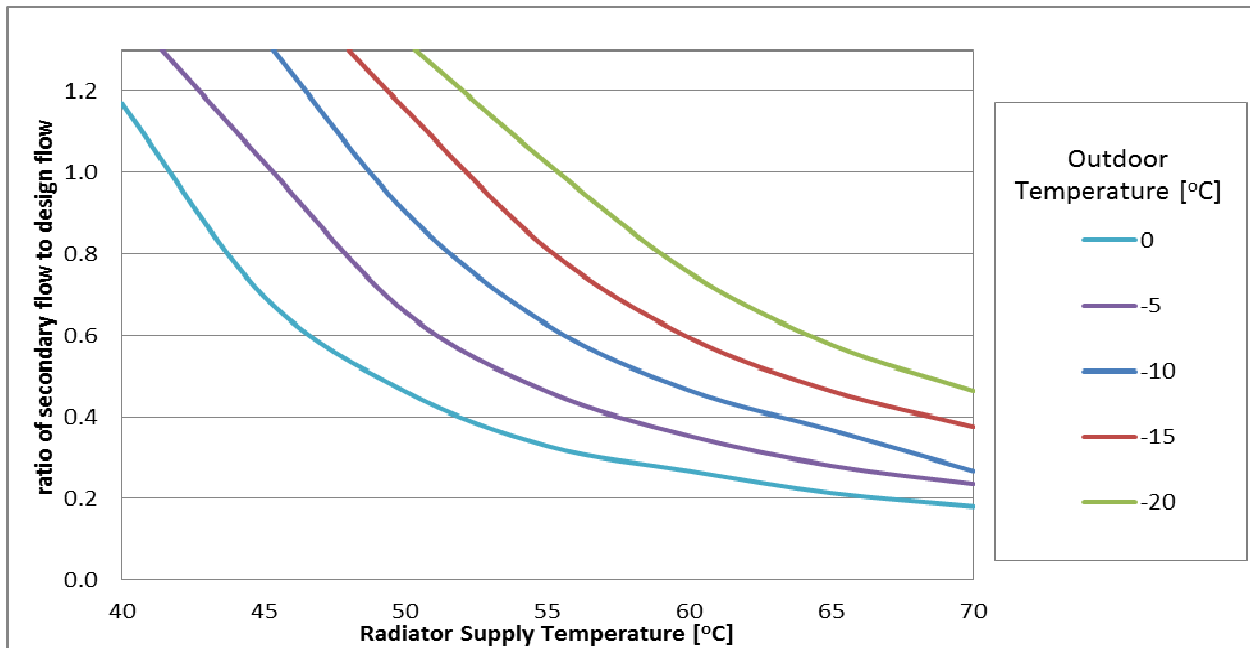


Figure 38: Operation curves of the secondary loop – hydronic radiator system

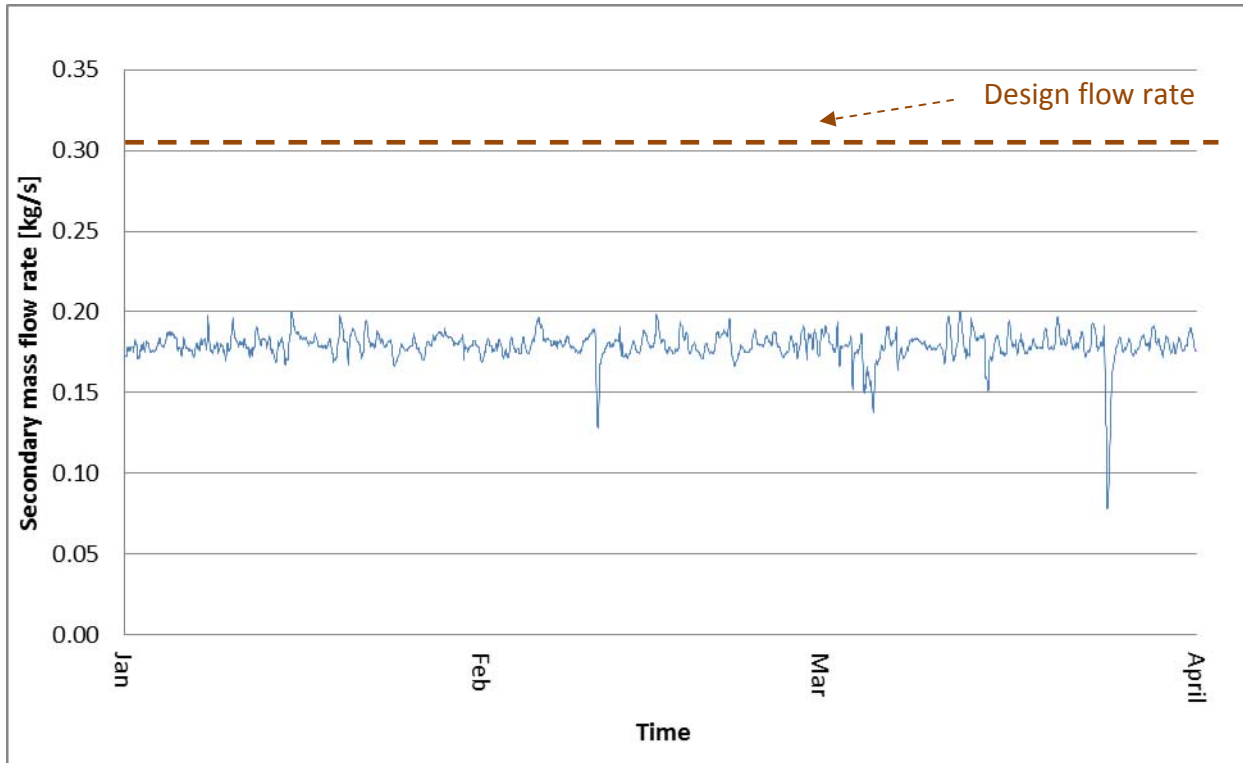


Figure 39: Simulated secondary flow rate and design secondary flow rate for a residential house connected to district heating in Toronto

5.4 Proposed Control Scheme

In a conventional control scheme, the controller at the district heating substation regulates secondary supply temperature based on outdoor temperature. Figure 40 depicts the conventional control scheme for the district heating substation. The conventional control scheme ensures that sufficient heating can be provided by the system when there is a sudden increase in heating load due to a sudden decrease in outdoor temperature. However, it does not necessarily operate at a condition that maximizes primary water temperature drop.

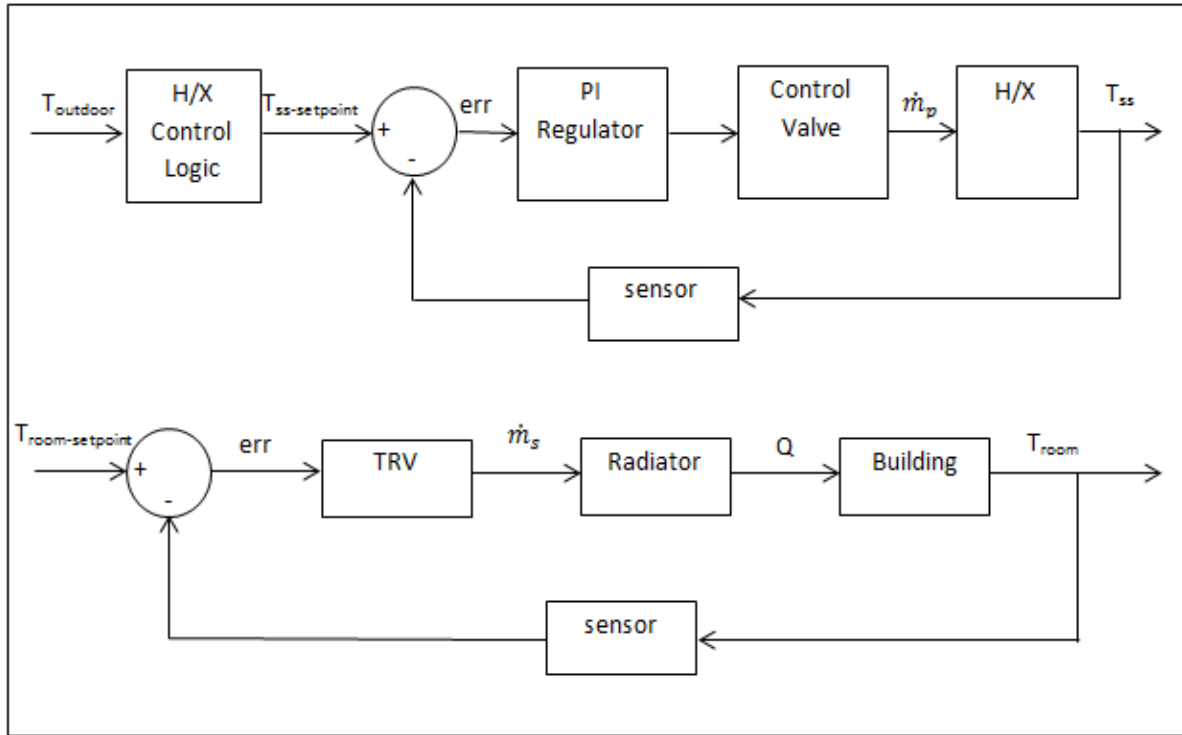


Figure 40: Conventional control scheme of district heating substation and secondary loop

It was hypothesized that by operating at a lower radiator supply temperature and a higher secondary flow rate for a given heating demand, a lower primary return water temperature can be achieved. Therefore, the goal of the proposed control method is to measure the secondary flow rate, and then to adaptively adjust the control curve of secondary water supply temperature. A control diagram of the proposed control method is displayed in Figure 41.

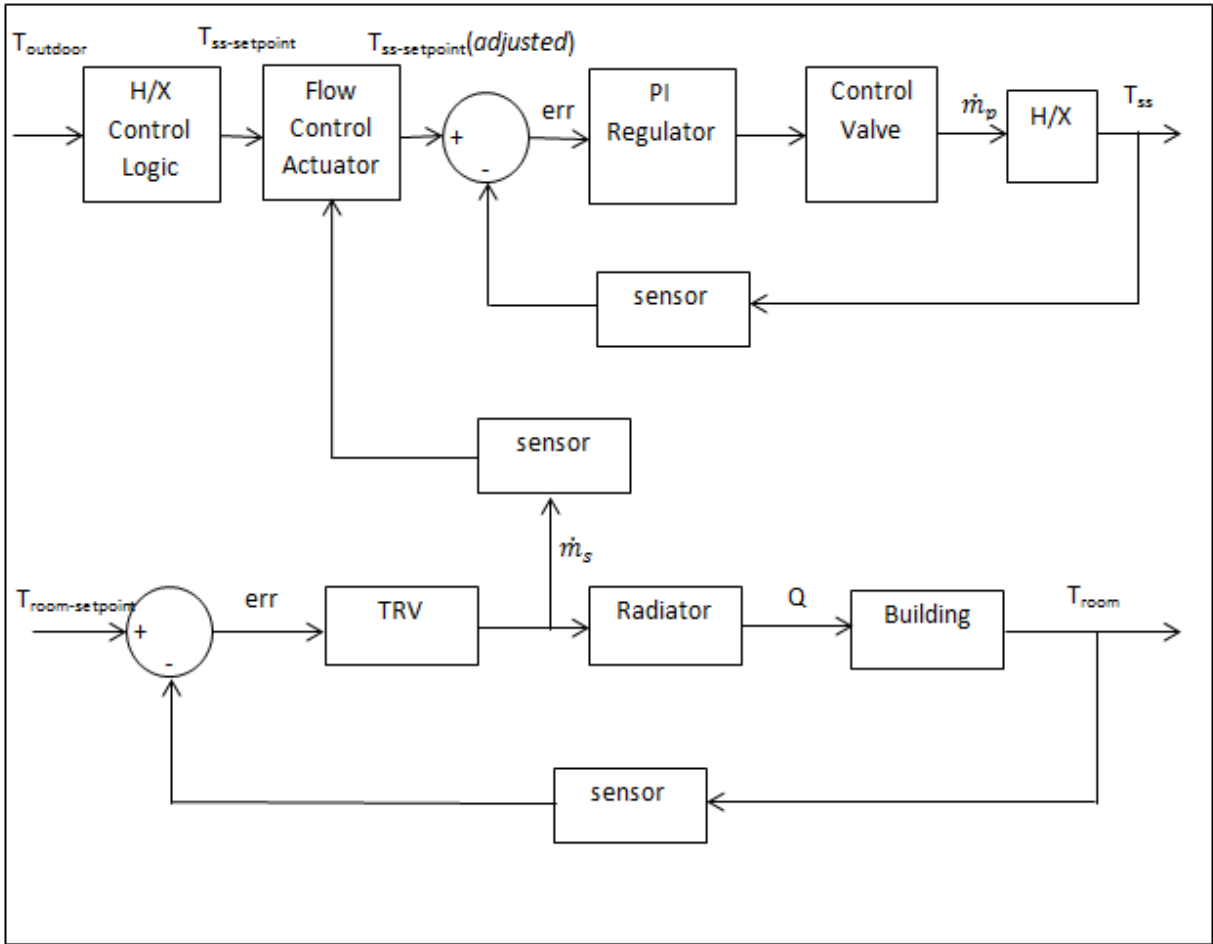


Figure 41: Diagram of the new proposed control scheme

The flow control actuator adjusts the control curve of secondary supply temperature until a certain secondary flow rate is reached. Based on a study by Xu et al. (2010), TRV works within a comfortable range when the flow rate is 50 to 100% of its design value. Therefore, the secondary design flow rate is chosen to be the target value of the secondary flow rate used in the flow control actuator.

Note that this does not mean that the system is operating at design conditions for extreme climate. When the system is operating at design conditions, both the secondary flow rate and the secondary supply temperature operate at design values.

The control behaviour of the flow control actuator is described by Equation 40 and displayed in Figure 42. The constant K is set at 10 so that the maximum temperature adjustment by the flow control actuator is 10°C.

$$T_{ss_adjusted} = T_{ss} - f\left(1 - \frac{m_{s_measured}}{m_{s_design}}\right) \cdot K \quad (40)$$

where $0 < f\left(1 - \frac{m_{s_measured}}{m_{s_design}}\right) < 1$

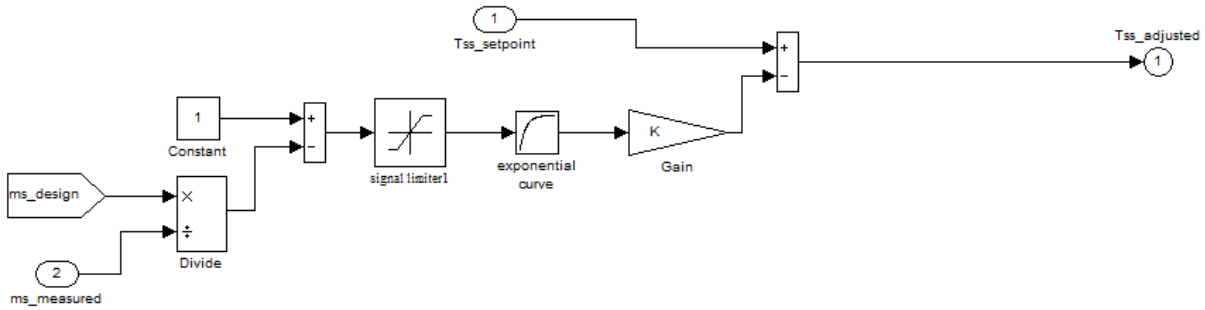


Figure 42: Control logic of the flow control actuator

5.5 Simulation Results and Discussion

To evaluate the new control strategy, simulation was performed with various primary supply temperature schemes to compare its performance against the conventional control method. Similar to the previous chapter, the first supply mode (supply mode A) is the conventional supply temperature scheme, where primary hot water supply temperature varies with the outdoor temperature, as shown in Figure 5. The second supply mode (supply mode B) uses a constant supply temperature at 100°C, which represents a constant high supply temperature. The third supply mode uses a constant supply temperature at 70°C (supply mode C), which represents a constant low supply temperature. Heating equipment are sized with a

RCL of 1.0, and climatic weather data of Toronto obtained from Canadian Weather for Energy Calculations (CWEC) was used. The simulations were run for the high load period.

Simulation results of primary temperature drop, secondary flow rate and indoor temperature are presented in Figure 43 to 45, and the mean values are presented in Table 11. Based on the simulated results, the new control scheme clearly shows that it increased the primary $\Delta\bar{T}$ and lowered the primary return water temperature, in all primary supply modes considered. The indoor temperature remained stable with the new control scheme and is consistent to the conventional control method. The primary mass flow is also lowered by using the new control strategy. This means that more energy per unit volume of distributed water is utilized, and distribution pump power can be reduced.

Table 11: Mean primary temperature drop, primary return temperature, primary and secondary flow rate during high load period with different primary supply modes

	Primary Supply Mode A		Primary Supply Mode B		Primary Supply Mode C	
	Conventional	New	Conventional	New	Conventional	New
Primary $\Delta\bar{T}$	26.27	28.68	46.86	49.28	14.84	17.21
\bar{T}_{pr}	54.59	52.18	53.14	50.72	55.16	52.79
\bar{m}_s	0.179	0.270	0.190	0.285	0.193	0.274
\bar{m}_p	0.119	0.110	0.070	0.066	0.249	0.211

An optimal heat transfer conditions requires a good combination of supply temperature and flow. The conventional control strategy operates with its only constraint being radiator supply temperature. As a result, flow condition is not optimized and results with energy waste in primary return water. The proposed control strategy devises a new algorithm that controls

the secondary flow by adaptively adjusting control curve of radiator supply temperature. Using the dynamic simulation model developed with real-world weather data, the new control method shows that it can effectively satisfy heating demand with a lower secondary supply temperature and a higher secondary flow rate. The benefit of the new control method is that it can decrease the primary return temperature meanwhile still maintaining stable indoor temperature. If this method is applied on a large scale throughout a district heating community, the environmental and financial gains would be substantial.

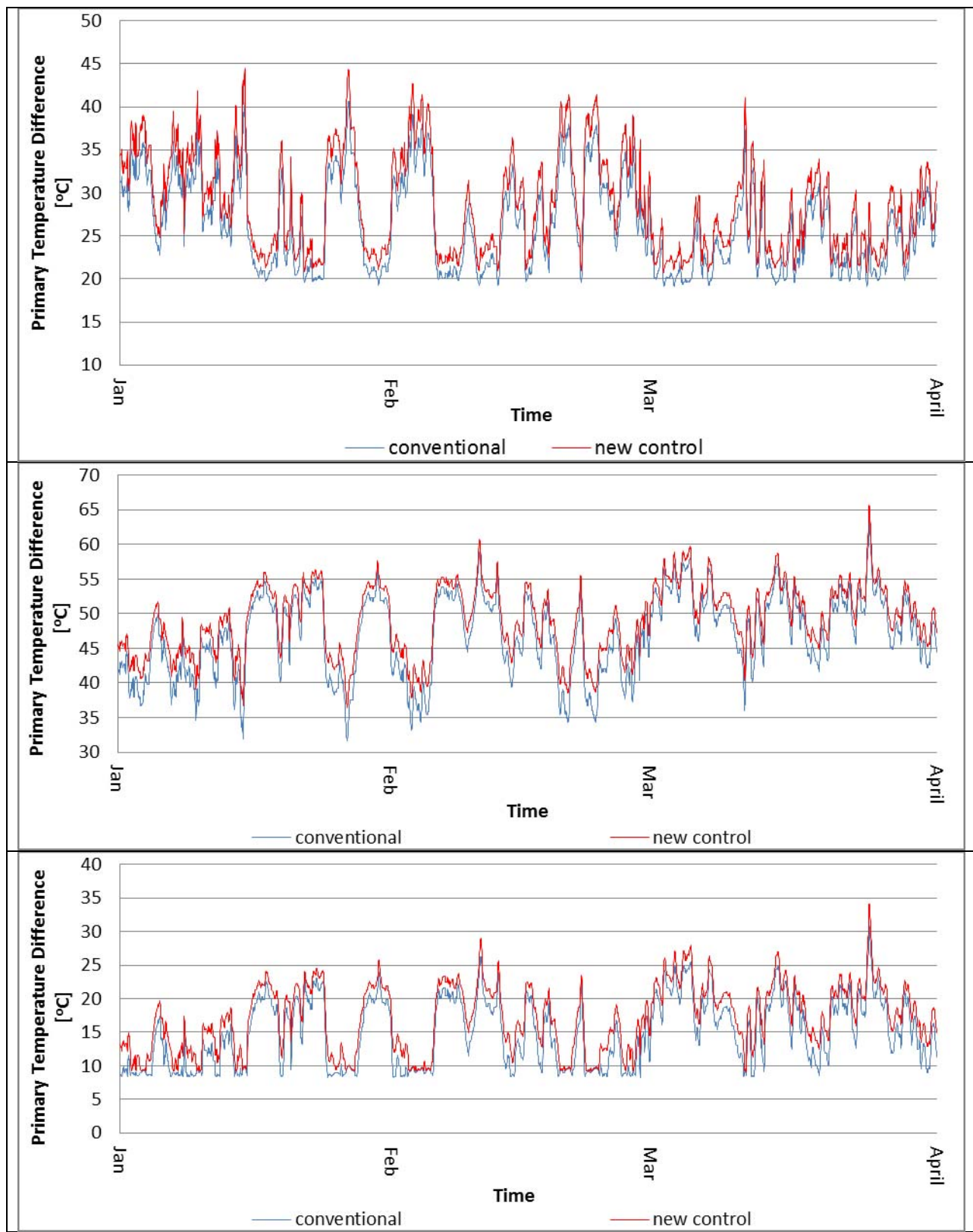


Figure 43: Simulated Primary Temperature Drop with Conventional and New Control Scheme with Primary Supply Mode A (top), Primary Supply Mode B (middle) and Primary Supply Mode C (bottom)

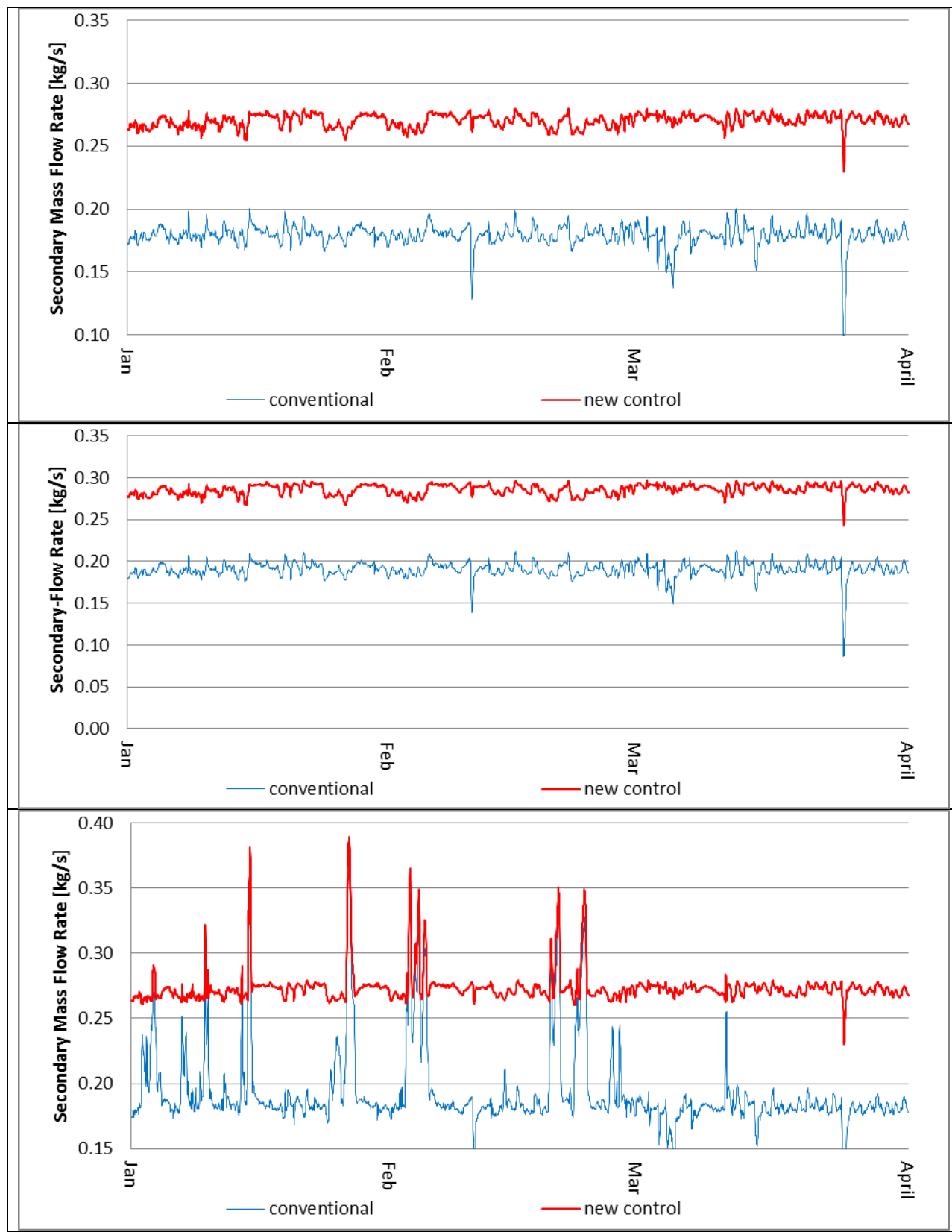


Figure 44: Simulated Secondary Flow Rate with Conventional and New Control Scheme with Primary Supply Mode A (top), Primary Supply Mode B (middle) and Primary Supply Mode C (bottom)

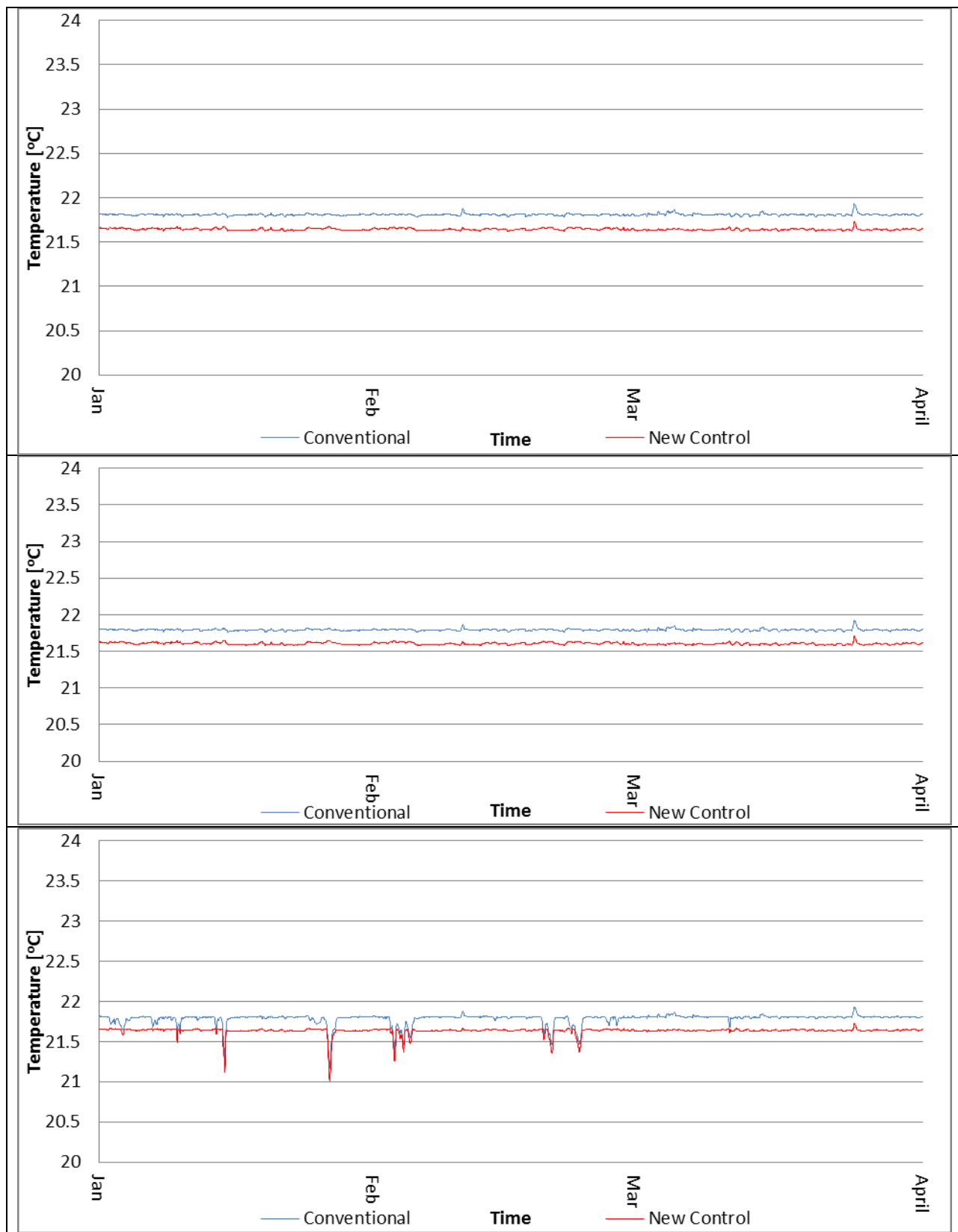


Figure 45: Simulated Indoor Temperature with Conventional and New Control Scheme with Primary Supply Mode A (top), Primary Supply Mode B (middle) and Primary Supply Mode C (bottom)

5.6 Limitations

Most traditional radiator control systems utilized constant speed centrifugal pumps.

Very often, the secondary flow rate is not measured. Adding a new flow sensor would be both expensive and time-consuming, especially considering that the new control method must be applied in most substations across the district heating network to result in a collective difference. Most substation and radiator control systems are equipped with manometers to monitor the system pressure. When a constant speed centrifugal pump is employed, the measured system pressure can be converted into flow rate, given that the system head curve is known. For variable or adjustable speed pumps, system pressure conversion is still possible, but more complicated.

It is important to note that the current simulation model is a single zone model. This assumption is not ideal because practically there are often multiple radiators equipped in a residential house. For a multi-zone model, hydraulic balancing should be considered in order to account for the hydraulic pressure difference between different zones. The physical modelling of a hydraulic network is outlined by Xu et al. (2008). Liao and Dexter (2004) had proposed a simplified physical model for estimating the average air temperature in multi-zone heating systems for control systems. The performance of proposed control method should be evaluated using a multi-zone model in future studies.

5.7 Concluding Remarks

A new control strategy for district heating substation is devised in order to reduce the primary return water temperature. Conventional control strategy operates with its only constraint being radiator supply temperature. The new control scheme operates the system at a more optimal combination of flow and supply temperature. This is done by measuring the secondary flow rate and then adaptively adjusts the control curve of the radiator supply temperature. Simulation results show that, by using the new control scheme, primary return water temperature is lowered compared to the conventional control method, in all primary supply modes considered. The new control strategy can effectively regulate the secondary flow rate so that it is closer to its design value during operation. There is no detrimental effect observed on indoor temperature with the new control method. Collective saving can be significant when the new control method applied to a community across the district heating network.

6. Conclusions and Future Studies

6.1 Conclusions

A physical model was developed in Matlab Simulink to simulate the thermodynamic behaviour of a district heating substation, a thermodynamic building and its heating equipment. The simulation model provides a computational platform to evaluate design and operation parameters, as well as control strategies for a district heating substation connected to a hydronic heating system.

Using the simulation model, the performance of a district heating substation is simulated at different capacity of heating devices, with different primary supply schemes, at different climatic locations. Simulation results show that oversized heating devices increased overheating degrees during part-load periods. At the same time, oversized heating devices also induced a larger primary water temperature drop. This does not mean equipping a bigger size heating system leads to better performance, because it increases overheating phenomena. The amount of increase in primary temperature drop is also bounded to diminish with larger size of heating system.

Simulation results show that under-sizing heating devices can lead to insufficient heating phenomena, and this effect is much more severe for Vancouver's than for Toronto's and Montreal's. This is caused by the inappropriate secondary supply temperature curve of the outdoor temperature compensator. By modifying the secondary supply temperature curve, indoor temperature can be properly maintained throughout the simulated period with under-sized heating devices. The trade-offs are higher primary flow rate and a lower primary

temperature drop. When designing heating devices for different climatic locations, it is important to use a suitable secondary supply temperature curve in order to achieve desirable performance of district heating substation.

Based upon the knowledge generated from the simulation study, a new control strategy is proposed by operating the system at a lower secondary supply temperature and a higher secondary flow rate. This is achieved by adaptively changing the secondary supply temperature curve based on secondary flow rate. The control strategy is evaluated using the simulation model. Simulation results show that a lower primary return temperature is obtained with all three primary supply schemes considered. By operating at a more optimal combination of radiator supply temperature and secondary flow rate, energy saving is realized without compromising indoor environmental conditions.

6.2 Future Studies

This thesis had focused on common and a limited amount of design and operation parameters. In reality, there exist infinite combinations of design and operation parameters. There are many different heating devices that are commonly used and can be setup with district heating, namely, forced air radiator, radiant floor system, heat pumps, etc. Evaluation of performance with different heating equipment can be remarkably beneficial and can generate useful information for design and operation guidelines and energy saving strategies. The physical modelling of new heating systems will require an extensive literature research and may require experimental measurement.

According to a survey study performed, building occupants in Canada commonly experience thermal discomfort due to their heating system being unable to maintain consistent temperature across different zones [Ng K.L.R., 2010]. Control strategies for a multi-zone system should be considered in future studies. Hydraulic balance should be considered to account for the hydraulic pressure difference between different zones. The physical modelling of a hydraulic network is outlined by Xu B. et al. After a physical model is developed, a control strategy is needed for the district heating substation to maintain the indoor conditions of multiple zones. Liao and Dexter (2004) had proposed a simplified physical model for estimating the average air temperature in multi-zone heating systems. The application of the model can be applied to control the operation of district heating substation.

Appendix – Calculating Design Load using ASHRAE guidelines

According to ASHRAE fundamentals - handbook, the calculation of design heating load can be divided in the following:

- Heat loss across exterior opaque surface
- Heat loss across exterior transparent surface
- Heat loss across the floor
- Heat loss from infiltration
- Heat load for ventilation
- Distribution loss

The design data for the model house are obtained from ASHRAE fundamentals - Handbook, and are tabulated in Table 12. The thermal resistance of different components of the building envelope are tabulated in Table 13. Using these values, the design heat loss across the exterior surface of the building can be calculated using a steady-state 1-dimensional heat balance equation:

$$q_{es} = UA\Delta T \quad \text{A-1}$$

where,

q_{es} is the heat loss across the exterior surface (W),

U is the overall heat transfer coefficient ($\text{W}/\text{m}^2 \text{ K}$),

A is the surface area (m^2), and

ΔT is the design temperature difference ($^\circ\text{C}$).

Studies have shown that heat loss from an unheated concrete slab floor is mostly through the perimeter rather than through the floor and into the ground. ASHRAE has outlined a simplified approach to estimate slab heat loss through slab perimeter.

$$q_{pe} = pF_p\Delta T$$

A-2

where,

q_{pe} = heat loss through perimeter (W),

F_p = heat loss coefficient per foot of perimeter (W/m·K), and

p = perimeter of floor (m).

The heat loss coefficient per foot of perimeter for an insulated brick facing wall is approximately 0.85. The design heat losses across different surfaces are tabulated in Table 14.

Table 12: Design data for the model house for three Canadian metropolitan cities

Item	Toronto	Montreal	Vancouver	Note
Latitude	43.5	45	49	
Elevation [m]	76	57	22	
Indoor Relative Humidity	N/A	N/A	N/A	
Design Outdoor temperature [°C]	-16.1	-21.1	-3.94	99% value
Wind speed [m/s]	6.7	6.7	6.7	ASHRAE default assumption
Annual Mean Air Temperature [°C]	8.28	6.89	10.39	
Ground Surface Temperature Amplitude [°C]	12	12	10	
Design Ground Surface Temperature [°C]	-3.72	-5.11	0.39	
Design ΔT	36.1	41.1	23.94	

Table 13: Thermal resistance of the building envelope

	R _{SI}	R _{IPERIAL}	U _{overall} (W/m ² K)
Above-grade Wall	3.01	17.1	0.33
Floor Stab	1.41	8.0	0.71
Roof	5.41	30.6	0.19
Windows	0.37	2.1	2.71

Table 14: Design heat losses (Q_{es}) across different building surfaces, in [W]

	Toronto	Montreal	Vancouver
Above-grade Wall	2184	2487	1449
Floor Perimeter	1437	1607	1178
Roof	1135	1293	753
Windows	5943	6766	3941
Sum	10699	12153	7321

The heat loss via air infiltration can be calculated by the sets of equations listed below.

The typical values of constants for solving the equations below are obtained in 2005 ASHRAE Handbook-Fundamentals, Chapter 27 and 28.

$$q_{\text{infiltration}} = C_s Q_i \Delta T \quad \text{A-3}$$

$$Q_i = ACH(V/3.6) \quad \text{A-4}$$

$$Q_i = A_L \text{IDF} \quad \text{A-5}$$

$$A_L = A_{es} A_{ul} \quad \text{A-6}$$

where,

C_s = air sensible heat factor (W/L·s·K) (equals to 1.23 at sea level),

Q_i = air volumetric flow rate via infiltration (L/s),

ACH = air exchange per hour (change/hr)

V = volume of the house (m^3)

A_L = building effective leakage area at reference pressure difference = 4Pa,

IDF = infiltration driving force (L/s·cm),

A_{es} = building exposed surface area (m^2), and

A_{ul} = unit leakage area (cm^2/m^2) (2.8 cm^2/m^2 for average typical current housing).

To calculate the ventilation air flow rate from mechanical systems, one should note that mechanical pressurization may modify the infiltration leakage rate. To assess this effect, overall supply and exhaust flow rates must be determined and then divided into “balanced” and “unbalanced” components:

$$Q_{bal} = \min(Q_{sup}, Q_{exh}) \quad A-7$$

$$Q_{unbal} = \max(Q_{sup}, Q_{exh}) - Q_{bal} \quad A-8$$

where,

Q_{bal} = balanced airflow rate (L/s),

Q_{sup} = total ventilation supply airflow rate (L/s),

Q_{exh} = total ventilation exhaust airflow rate (L/s), and

Q_{unbal} = unbalanced airflow rate (L/s).

The combined infiltration/ventilation flow rate is thus calculated as follows:

$$Q_{vi} = \max(Q_{unbal}, Q_i + 0.5Q_{unbal}) \quad A-9$$

Equipment like exhaust fans that operate intermittently via manual control are generally not included in load calculations. With no heat recovery unit or energy recovery unit, the design heat load for ventilation is calculated based on required minimum whole-building ventilation rate outlined in ASHRAE Standard 62.2-2004 as:

$$Q_v = 0.05A_{cf} + 3.5(N_{br} + 1) \quad A-10$$

where,

Q_v = required ventilation flow rate (L/s),

A_{cf} = building conditioned floor area (m^2), and

N_{br} = number of bedrooms (not less than 1).

Using $A_{cf} = 288.4 m^2$ and $N_{br} = 3$, the resulting required ventilation flow rate is calculated and presented in Table 15. For design purposes, assume that this requirement is met by a mechanical system with balanced supply and exhaust flow rates ($Q_{unbal} = 0$) [ASHRAE, 2009]. The resulting combined infiltration/ventilation flow rate and heat load are summarized in Table 15.

Table 15: The design infiltration and required ventilation flow rate, and the combined infiltration/ventilation design heat load for the model house

	Toronto	Montreal	Vancouver
Q_i [L/s]	95.4	100.6	83.4
$ACH_{infiltration}$ [change/hr]	0.48	0.50	0.42
Q_v [L/s]	28.4	28.4	28.4
Q_{vi} [L/s]	123.8	129.0	111.9
ACH_{total} [change/hr]	0.62	0.64	0.56
q_{vi} [W]	5213	6130	3284

Distribution losses are contributed by the duct work in the attic. The distribution loss factors are estimated from Table 6 of Chapter 29 of 2005 ASHRAE Fundamental-Handbook at 0.12. A summary of the model house total design heating loads is presented in Table 16.

Table 16: A summary of the model house total design heating load

	Toronto	Montreal	Vancouver
Envelope [W]	10699	12153	7321
Infiltration/Ventilation [W]	5498	6522	3294
Subtotal [W]	16197	18675	10614
Distribution loss [W]	1944	2241	1274
Total design load [W]	18141	20916	11888

The design heat transfer coefficient, and inlet and outlet temperature of heat exchangers are based on the previous researches on detached residential home on district heating by Gustafsson J. et al. The design heat transfer coefficient is verified to be within the range of a common water-to-water heat exchanger [Holman J.P., 2002]. The design specifications of heat exchangers are listed in Table 17. The design secondary flow rate is calculated by a 1-D steady-state heat balance:

$$\dot{m}_{design} = \frac{q_{design}}{Cp \cdot \Delta T_{sec}}$$

A-11

where,

\dot{m}_{design} = design secondary flow rate (kg/s),

q_{design} = design power of heat exchanger (W),

Cp = heat capacity of water (J/kg·K), and

ΔT_{sec} = temperature drop of the secondary loop (K).

The design heat transfer area of the heat exchanger is calculated by the heat transfer equation:

$$A_{design} = \frac{U\theta_{dLMTD}}{q_{design}}$$

A-12

where,

A_{design} = design heat transfer area of heat exchanger (m^2)

U = design heat transfer coefficient ($\text{W}/(\text{m}^2 \cdot \text{K})$), and

θ_{dLMTD} = design log mean temperature difference (K).

Based on the two equations above, the design heat transfer area and secondary flow rate for a single-detached residential home in Toronto are presented in Table 17.

Table 17: Heat exchanger design specifications for Toronto, Montreal and Vancouver

Parameters	Value				
Incoming primary temperature [°C]	100				
Returning primary temperature [°C]	50				
Incoming secondary temperature [°C]	45				
Returning secondary temperature [°C]	60				
Log mean temperature difference [°C]	16.8				
Overall heat transfer coefficient [W/m ² ·K]	1300				
Design Heating Load, Toronto [W]	18141				
Ratio of Capacity-to-Load	0.7	0.9	1	1.1	1.3
Power [W]	12699	16327	18141	19955	23583
Secondary flow rate [kg/s]	0.20	0.26	0.29	0.32	0.38
Heat Transfer Area [m ²]	0.58	0.75	0.83	0.91	1.08
Design Heating Load, Montreal [W]	20916				
Ratio of Capacity-to-Load	0.7	0.9	1	1.1	1.3
Power [W]	14641	18824	20916	23007	27191
Secondary flow rate [kg/s]	0.24	0.30	0.34	0.37	0.44
Heat Transfer Area [m ²]	0.67	0.86	0.96	1.05	1.24
Design Heating Load, Vancouver [W]	11888				
Ratio of Capacity-to-Load	0.7	0.9	1	1.1	1.3
Power [W]	8322	10699	11888	13077	15455
Secondary flow rate [kg/s]	0.13	0.17	0.19	0.21	0.25
Heat Transfer Area [m ²]	0.38	0.49	0.54	0.60	0.71

References

- Ali, I.H. (2009). Oversizing Equipments. ASHRAE Journal, Vol. 51, No. 5, pp. 14.
- Andersen, K.K., Madsen, H., Hansen, L. H. (2000). Modeling the heat dynamics of a building using stochastic differential equations. Energy and Buildings, Vol. 31, pp. 13-24.
- Andersen, P., Pedersen, T.S., Stoustrup, J., Svensen, J., Lovmand, B. (2000). Elimination of oscillations in a central heating system using pump control. Proceedings of the American Control Conference, Vol.1, pp. 135-139.
- Andersson, S. (1993). Influence of the net structure and operating strategy on the heat load of a district-heating network. Applied Energy, Vol. 46, pp. 171-179.
- Arkay, K.E., Blais, C. (1995). The district energy option in Canada. Natural Resources of Canada. ISBN 0662246470.
- Armstrong Ltd. (2009). Astro Circulators – Submittal Data Sheet. Retrieved January, 2011, from <http://www.armstrongpumps.com/>
- ASHRAE. (2009). ASHRAE Handbook – Fundamentals. American Society of Heating, Refrigeration and Air-conditioning Engineers. ISBN 1615831703.
- ASHRAE. (2008). ASHRAE Handbook – Heating, ventilating, and air-conditioning systems and equipment. American Society of Heating, Refrigeration and Air-conditioning Engineers. ISBN 1601197950.
- Bahadorani, P., Naterer, G.F., Nokleby, S.B. (2009). Optimization of heat exchangers for geothermal district heating. Transactions of the Canadian Society for Mechanical Engineering, Vol. 33, No. 2, pp. 79-96.
- Bell & Gossett Inc. (2008). Lead-free wet rotor circulators for hot water circulation. Retrieved January, 2011, from <http://completewatersystems.com/>

Barton, J.J., (1970). Domestic heating and hot water supply. London, United Kingdom: Applied Science Publishers Ltd.

Beijing International. (2003). Guide to heating, electricity, water, and gas - policies and procedures. Retrieved January, 2011, from
http://www.ebeijing.gov.cn/feature_2/GuideToHeatingElectricityWaterAndGas/PriceGuide/t1107664.htm

Bejan, A., Kraus, A.D. (2003). Heat transfer handbook. Hoboken, New Jersey: John Wiley and Sons Inc.

Benonysson, A., Bohm, B., Ravn, H.F. (1995). Operational optimization in a district heating system. Energy Conversion and Management, Vol. 36, No. 5, pp. 297-314.

Braun, J., Chaturvedi, N. (2002). An inverse gray-box model for transient building load prediction. HVAC and R Research, Vol. 8, pp. 73-99.

Brown, B. (1996). Klamath Falls geothermal district heating system evaluation. Geothermal Resources Council – Transactions, Vol.20, pp. 51-58.

Carrier Air Conditioning Company. (1972). System design manual 1: load estimating. Syracuse, New York: Carrier Air Conditioning Company.

Chung, T.M., Tong, W.C. (1990). Thermal comfort study of young Chinese people in Hong Kong. Building and Environment, Vol. 25, No.4, pp.317-328.

Crawford, R.R., Woods, J.E. (1985). A method for deriving a dynamic system model from actual building performance data. ASHRAE Transactions, Vol. 91, pp. 1859-1874.

Dagdas, A. (2007). Heat exchanger optimization for geothermal district heating systems: A fuel saving approach. Renewable Energy, Vol. 32, pp. 1020-1032.

Danfoss Global Group. Product specification sheet: VX Solo II, 2009. Retrieved January, 2011, from <http://heating.danfoss.com/>

De Dear, R., Leow, K., Amen, A. (1991). Thermal-comfort in the humid tropics – Part I, climate chamber experiment on temperature references in Singapore, ASHRAE Transactions 1991, pp. 874-879.

Dotzauer, E. (2002). Simple model for prediction of loads in district-heating systems. Applied Energy, v.73, p. 277-284.

EnergyPlus™. (2010). EnergyPlus engineering reference, U.S. Department of Energy. Retrieved October, 2010, from
<http://apps1.eere.energy.gov/buildings/energyplus/pdfs/engineeringreference.pdf>

Environment Canada. (2005). Canadian weather year for energy calculation (CWEC). Retrieved January, 2010, from <http://www.climate.weatheroffice.gc.ca/>

Ertesvag, I.S. (2007). Exergetic comparison of efficiency indicators for combined heat and power. Energy, Vol. 32, No. 11, pp. 2038-2050.

Euroheat & Power. (2005). Ecoheatcool: reducing Europe's consumption for fossil fuels for heating and cooling. Retrieved June, 2010 from
http://www.euroheat.org/files/filer/ecoheatcool/documents/Ecoheatcool_Results_Web.pdf

Euroheat & Power. (2008). Guidelines for District Heating Substations. Retrieved February, 2011, from <http://www.euroheat.org/Technical-guidelines-28.aspx>

Fanger, P.O. (1970). Thermal-comfort analysis and applications in environmental engineering. New York: McGraw-Hill.

Fraas, A.P. (1989). Heat Exchanger Design (2nd Ed.). Toronto, Ontario: John Wiley & Sons.

Frederiksen, S., Wollerstrand, J. (1987). Performance of district heating house station in altered operational modes. 23rd UNICHAL-Congress, Berlin.

Frunzulica, R. Damian, A. (2007). Energy consumptions analysis in a rehabilitated small-scale substation from a district heating system. Proceedings of the 3rd WSEAS/IASME International Conference on Energy, Environment Ecosystems and Sustainable Development, pp. 577-583.

Gabrielaitiene, I., Bohn, B., Sundén, B. (2007). Modelling temperature dynamics of a district heating system in Naestved, Denmark – A case study. *Energy Conversion and Management*, Vol. 48, No. 1, pp. 78-86.

Gabrielaitiene, I., Sundén, B., Wollerstrand, J. (2006). Heat transfer modelling in double pipes for domestic hot water systems. *WIT Transactions on Engineering Sciences*, Vol. 53, pp. 381-390.

Ghafghazi, S., Sowlati, T., Sokhansanj, S., Melin, S. (2010). A multicriteria approach to evaluate district heating system options. *Applied Energy*, Vol. 87, pp. 1134-1140.

Gilmour, B., Warren, J. (2008). The new district energy: building blocks for sustainable community development – online handbook. Retrieved August, 2010, from http://www.questcanada.org/documents/UES_Handbook_Final_21-01-081.pdf

Gorshkov, A.S., Sokolov, E.Y. (1984). Methods of increasing the efficiency of district heating and of centralised heat supply. *Thermal Engineering*, Vol. 31, No. 9, pp. 2-6

Grundfos Inc. (2001). Submittal data sheet – UP series circulator pumps. Retrieved January, 2011, from <http://www.grundfos.com/>

Gustafsson, J., Delsing, J., van Deventer, J. (2010). Improved district heating substation efficiency with a new control strategy. *Applied Energy*, Vol.87, pp.1996-2004.

Gustafsson, J. (2011). Wireless Sensor Network Architectures as a Foundation for Efficient District Heating. Ph.D. dissertation, Department of Computer Science, Electrical and Space Heating, Lund Institute of Technology, Lund University, Sweden, 2011.

Henze, G.P., Floss, A.G. (2011). Evaluation of temperature degradation in hydraulic flow networks. *Energy and Buildings*, Vol. 32, pp. 1820-1828.

Hepbasli, A. (2005). Thermodynamic analysis of a ground-source heat pump system for district heating. *International Journal of Energy Research*, Vol. 29, pp. 671-687.

Hong, T., Jiang, Y. (1997). A new multizone model for the simulation of building thermal performance. *Building and Environment*, Vol. 32, pp. 123-128.

Hu, N., Zhou, B., Wang, W., Neumaier, K. (2005). Energy and environmental conservation through district heating. *Energy Engineering*, Vol. 102, No. 1, pp. 10 – 20.

Hudson, G., Underwood, C.P. (1999). A simple building modelling procedure for MATLAB/SIMULINK. *Proceedings of the IBPSA Conference – Building Simulation '99*, Kyoto, pp. 776-778.

Humphreys, M.A., Nicol, J.F. (2002). Adaptive thermal comfort and sustainable thermal standards for buildings. *Energy and Buildings*, Vol. 34, pp. 563-572.

Indenbirken, M., Troster, L., Steiff, A. (1995). Economical optimization of pump operation in district heating networks with “Bofit”. *District Heating International*, Vol. 24, No. 1, pp. 28-38.

International District Energy Association. (2011). Combined Heat and Power: essential for a cost effective clean energy standard. Retrieved August, 2010, from
http://www1.eere.energy.gov/industry/distributedenergy/pdfs/chp_clean_energy_std.pdf

International Energy Association. (1998). Annex V: Promotion and recognition of DHC/CHP benefits in greenhouse gas policy and trading programs. Retrieved June, 2011, from
<http://www.iea-dhc.org/020306.html>

Iversen, S., Ougaard, P., Leppenthien, J. (2006). Dynamic temperature optimization – Providing instant results. *Journal of Euroheat and Power*, Vol.3, No.2, pp. 46-49.

Jagoda, K., Lonseth, R., Lonseth, A., Jackman, T. (2011). Development and commercialization of renewable energy technologies in Canada: An innovation system perspective. *Renewable Energy*, Vol. 36, pp. 1266 – 1271.

Jiang, Y. (1981). State-space method for the calculation of air-conditioning loads and the simulation of thermal behaviour of the room, *ASHRAE Transactions* Vol. 99, pp. 122-132.

Joelsson, A., Gustafsson, L. (2009). District heating and energy efficiency in detached houses of differing size and construction. *Applied Energy*, Vol.86, pp. 126-134.

Lauenburg, P., Wollerstrand, J. (2010). Adaptive control of radiator systems for a lowest possible return temperature. *12th International Symposium on District Heating and Cooling*, Tallinn, Estonia. pp. 206-214.

Letherman, K.M., Pailing, C.J., Park, P.M. (1982). The measurement of dynamic thermal response in rooms using pseudo random binary sequences. *Building and Environment*, Vol. 17, pp. 11-16.

Li, L., Zaheeruddin, M. (2004). A control strategy for energy optimal operation of a direct district heating system. *International Journal of Energy Research*, Vol. 28, No.7, pp. 597-612.

Li, L., Zaheeruddin, M. (2007). Hybrid fuzzy logic control strategies for hot water district heating systems. *Building Services Engineering Research and Technology*, Vol. 28, No.1, pp. 35-53.

Li, H., Dalla Rosa, A., Svendsen, S. (2010). Design of low temperature district heating network with supply water recirculation. *12th International Symposium on District Heating and Cooling*, pp. 73-80.

Liao, Z., Dexter, A.L. (2004). A simplified physical model for estimating the average air temperature in multi-zone heating system. *Building and Environment*, Vol. 39, pp. 1013-1022.

Liao, Z. (2004). An inferential control scheme for optimizing the control of boilers in multiple-zone heating systems. PhD thesis, Department of Engineering Science, St. Catherine's College, the University of Oxford, United Kingdom, 2004.

Lin, F., Yi, J. (2000). Optimal operation of a CHP plant for space heating as a peak load regulating plant. Energy, Vol. 25, No. 3, pp. 283-298.

Liu, L., Fu, L., Jiang, Y. (2009). A novel “wireless on-off control” technique for household heat adjusting and metering in district heating system. Proceedings of the ASME 3rd International Conference on Energy Sustainability 2009, pp. 135-143.

Liptak, B. (1995). Instrument engineers' handbook: process control (3rd Ed.). Radnor, Pennsylvania: Chilton Book Company.

Madsen, H., Holst, J. (1995). Estimation of continuous-time models for the heat dynamics of a building. Energy and Buildings, Vol. 22, pp. 67-79.

Math Works Inc. (2000). SIMULINK: Dynamic system simulation for MATLAB, The Math Works Inc. Retrieved July, 2010, from <http://www.mathworks.com/help/toolbox/simulink/>

Natural Resources Canada (NRCan). (2008). Comprehensive energy use database tables. Retrieved February, 2010, from
<http://oee.nrcan.gc.ca/corporate/statistics/neud/dpa/home.cfm>

Natural Resources Canada (NRCan). (2004). Community energy case studies: District Energy Capital Expansion Project – Markham Centre, ON. Retrieved August, 2010, from
<http://canmetenergy-canmetenergie.nrcan-rncan.gc.ca>

Ng, K.L.R. (2010). The role of thermal simulation in various phases of buildings' life-cycles in improving building performance. MSc. thesis, Program of Building Science, Department of Architectural Science, Ryerson University, Canada, 2010.

Nijjar, J.S., Fung, A.S., Hughes, L., Taherian, H. (2009). District Heating System Design for Rural Nova Scotian Communities Using Building Simulation and Energy Usage Databases. Transactions of the Canadian Society for Mechanical Engineering, Vol. 33, No.1, pp. 51-64.

Ostergaard, P.A., Lund, H. (2011). A renewable energy system in Frederikshavn using low-temperature geothermal energy for district heating. Applied Energy, Vol. 88, pp. 479-487.

Ozgener, L., Hepbasli, A., Dincer, I. (2007). A Key review on performance improvement aspects of geothermal district heating systems and applications. Renewable and Sustainable Energy Reviews, Vol.11, pp. 1675-1697.

Persson, T. (2005). District heating for residential areas with single-family housing – with special emphasis on domestic hot water comfort. PhD thesis, Lund University, Division of Energy Economics and Planning, Department of Heat and Power Technology, Lund Institute of Technology, Lund University, Sweden; June 2005.

Petitjean, R. (1995). Total Hydronic Balancing, Ljung, Sweden: Tour & Andersson Hydronics.

Rosen, M.A. Le, M.N., Dincer, I. (2005). Efficiency analysis of a cogeneration and district energy system. Applied Thermal Engineering, Vol.25, pp.147-159.

Sibbitt, B., Onno, T., McClenahan, D., Thornton, J., Brunger, A., Kokko, J., Wong, B. (2007). The Drake Landing solar community project – early results. Retrieved August, 2011, from <http://www.dlsc.ca/reports.htm>

Siegenthaler, J. (1995). Modern hydronic heating: for residential and light commercial buildings (2nd Ed.). Clifton Park, New York: Delmar Learning

Smith, J.N., Van Ness, H.C., Abbott, M.M. (2005) Introduction to Chemical Engineering Thermodynamics (7th Ed.). New York, NY: McGraw-Hill.

Snoek, C.W., Kluiters, S.C. (2010). Application of exergoeconomics to the optimization of building heating systems connected to district heating networks. 12th International Symposium on District Heating and Cooling, pp. 45-52.

Sokolov, E.Y. (1988). The presentday situation and the main problems facing district heating and centralised heat supply. Thermal Engineering, Vol. 35, No.3, pp. 129-133

Straube, J., Burnett, E. (2005). Building Science for Building Enclosures (2nd Ed.). Westford, MA: Building Science Press.

Taco Inc. (2009). Model 006 cartridge circulator – submittal data information. Retrieved January, 2011, from <http://www.taco-hvac.com/>

Tanabe, S.I., Kimura, K.I. (1994). Effects of air temperature, humidity, and air movement on thermal-comfort under hot humid conditions. ASHRAE Transactions, Vol. 100, No. 2, pp. 953-969.

Taunton Press. (1999). Energy-efficient building. Newtown, Connecticut: Taunton Press.

United States Department of Energy. (2000). Combined heat and power: a federal manager's resource guide (Final Report). Retrieved March, 2011, from http://www1.eere.energy.gov/industry/distributedenergy/pdfs/chp_femp.pdf

United States Department of Energy. (2011). Energy saver: sizing heating and cooling equipment. Retrieved August, 2010, from http://www.energysavers.gov/your_home/space_heating_cooling/index.cfm/mytopic=12340

Villarroel, D.E., Klein, M. (2006). High Efficiency Combined Heat and Power Solutions. 2006 IEEE EIC Climate Change Conference, pp. 11

Wang, S.W., Xu, X.H. (2006). Parameter estimation of internal thermal mass of building dynamic models using genetic algorithm. *Energy Conversion and Management*, Vol. 47, pp. 1927 - 1941.

Welty, J., Wicks, C.E., Wilson, R.E., Rorrer, G.L. (2001) Fundamentals of momentum, heat and mass transfer (4th Ed.). Singapore, Singapore: John Wiley & Sons Inc.

Wiggin, J.M. (1991). District heating in canada: where we are and where we going. *District heating international*, Vol. 20, No. 1-2, pp. 120-123.

Xu, B., Fu, L., Di, H. (2008). Dynamic simulation of space heating systems with radiators controlled by TRVs in buildings. *Energy and Buildings*, Vol. 40, pp. 1755-1764.

Xu, B., Fu, L., Di, H. (2009). Field investigation on consumer behaviour and hydraulic performance of a district heating system in Tianjin, China. *Building and Environment*, Vol. 44, pp. 249-259.

Xu, B., Huang, A., Fu, L., Di, H. (2011). Simulation and analysis on control effectiveness of TRVs in district heating systems. *Energy and Buildings*, Vol. 43, pp. 1169-1174.

Yao, D., Qui, L. (2010). Analysis of the impact of energy-saving factors on the heating system with distributed variable frequency pump. 2010 International Conference on Advances in Energy Engineering, pp. 239-242.

Yildirim, N., Gokcen, G. (2004). Modeling of low temperature geothermal district heating systems. *International Journal of Green Energy*, Vol. 1, No. 3, pp. 365 – 379.

Zhang, J., Sun, H., Zhang, J.T. (2008). Application of adaptive fuzzy sliding-mode controller for heat exchanger system in district heating. 2008 International Conference on Intelligent Computation Technology and Automation, pp. 850-854

Zhao, H., Bohn, B., Ravn, H.F. (1995). On optimum operation of a CHP type district heating system by mathematical modelling. Euroheat & Power Fernwaerme International, Vol. 24, No. 11, pp. 618-622.

Zsebik, A. Sitku, G. (2001). Heat Exchanger Connection in Substations – A Tool of Decreasing Return Temperature in District Heating Networks. Energy Engineering, Vol. 98, No. 5, pp. 20-31.